Physiol Rev 88: 173–210, 2008;
doi:10.1152/physrev.00044.2006.

Cochlear Outer Hair Cell Motility

JONATHAN ASHMORE

Department of Physiology and UCL Ear Institute, University College London, London, United Kingdom

Ashmore J. Cochlear Outer Hair Cell Motility. *Physiol Rev* 88: 173–210, 2008; doi:10.1152/physrev.00044.2006.—Normal hearing depends on sound amplification within the mammalian cochlea. The amplification, without which the auditory system is effectively deaf, can be traced to the correct functioning of a group of motile sensory hair cells, the outer hair cells of the cochlea. Acting like motor cells, outer hair cells produce forces that are driven by graded changes in membrane potential. The forces depend on the presence of a motor protein in the lateral membrane of the cells. This protein, known as prestin, is a member of a transporter superfamily SLC26. The functional and structural properties of prestin are described in this review. Whether outer hair cell motility might account for sound amplification at all frequencies is also a critical question and is reviewed here.

I. INTRODUCTION

In 1862, Helmholtz published the first edition of *Die Lehre von den Tonempfindungen*, ("On the Sensations of Tone"). By the time this volume had reached its fourth edition in 1877, the work included critical new evidence of the architecture of the inner ear and allowed Helmholtz to construct hypotheses about how the cochlea functioned (135). The evidence was derived from the work of Hensen, Corti, and other anatomists who, with a range of new tissue fixation techniques, were charting the richness of the cochlear structure. Helmholtz saw these contributions as part of what we would now call a multidisciplinary work that spanned two sciences, physiological acoustics on the one side and musical science on the other. It is, however, the way in which he developed models of the cochlea, integrating both physiological and mathematical models that have laid the foundations of inner ear physiology. In fact, Helmholtz's description was so magisterial that it may well have slowed discussion for several decades.

In this review I describe some of the recent developments in understanding how the mammalian inner ear amplifies sound using a mechanism associated with the outer hair cells of the cochlea. Discovered a little over two decades ago, outer hair cell motility has opened up hearing research in a way that has involved molecular, cellular, and systems physiology in a manner which Helmholtz would have recognized. We now know that the molecular basis of this phenomenon depends critically on a molecule named "prestin," which is expressed at high levels in the outer hair cell. The field has not yet reached a watershed; there is no attempt here to be magisterial.

II. AUDITORY PHYSIOLOGY AND COCHLEAR MECHANICS

The mammalian cochlea of the inner ear is a fluid-filled duct. It is coiled into a compartment within the temporal bone on either side of the head. In mammalian species, the structure varies less in size than does the mass of the animal, but the temporal bone itself may vary greatly in dimensions. Sound is funneled through outer ear and transmitted through the middle ear to the cochlear fluids where the final effect is to stimulate, appropriately, the sensory hair cells of the cochlea. As examples of the scale in two important experimental animals, the uncoiled length of the cochlea of a mouse is ~11 mm and that of a guinea pig 19 mm. For comparison, the uncoiled length of a human cochlea is ~34 mm.

In what we describe below, it is worth recalling that many auditory functions are best described using logarithmic scales. For frequency, it is appropriate to use an octave measure (where an octave is a doubling of frequency); for sound stimuli, it is appropriate to use a decibel (dB) scale so that each order of magnitude increase in sound pressure is a 20-dB step. By definition, auditory sensitivity is measured by a stimulus relative to an agreed threshold sound level. This agreed level is the amplitude of the pressure wave for a threshold sensation. It is referred to as 0 dB SPL and corresponds to a pressure wave with an amplitude of 20 μPa. Human hearing is designed to work optimally with sound levels between 0 and 80 dB SPL without excessive long-term damage. The human auditory frequency range covers about 8–9 octaves in a young healthy subject, from ~40 Hz to nearly 20 kHz. In the mouse, the range of hearing is ~4 octaves, although the range is displaced so that the upper limit of murine hearing extends 1.5 octaves above the human.

The coiled duct of the cochlea is divided down its length by a partition ("the cochlear partition") consisting of the basilar membrane and the innervated sensory epithelium, the organ of Corti (314). The basilar membrane itself is a macroscopic structure consisting of collagen fibers and an epithelium of supporting and sensory cells which vibrates when sound enters the cochlea. One of the three internal compartments of the cochlea, the scala media, also runs the length of the duct and provides a specialized ionic environment for the mechanotransducing membranes of the sensory hair cells. (For a review of the detailed anatomy, see, for example, the websites http://147.162.36.50/cochlea/; http://www.iurc.montp.inserm.fr/cric/audition.)

The mammalian cochlea contains two classes of hair cells arranged in rows along the organ of Corti. Hair cells are neuroepithelial cells, with the apical pole specialized for mechanotransduction and the basal pole specialized for the release of neurotransmitter. Inner hair cells (IHCs), of which there are ~3,500 in each human cochlea, are innervated by dendrites of the auditory nerve and are

considered to be the primary sensory hair cells of the cochlea. Outer hair cells (OHCs) number ~11,000 in each human cochlea and lie in 3 or 4 rows. They have a much less pronounced afferent innervation. The separation into two classes of hair cell is not confined to mammals, for two classes of morphologically distinct hair cells are found in archosaurs (birds and crocodilians), which also have a high sensitivity to sound and an extended frequency range (215). The cell bodies of the afferent fibers of both hair cell types form the spiral ganglion of the cochlea. Only ~5% of the dendrites of the auditory nerve are associated with OHCs. Such fibers, the so-called type II fibers as distinct from the type I fibers innervating the IHCs, have been recorded only infrequently (31, 275). For this reason, it is not possible to make a statement about the tuning of the OHC afferents as it is for the larger population of fibers innervating the IHCs except that, on anatomical grounds, the tuning is probably broader.

In contrast to their afferent innervation, OHCs, especially at the basal (high frequency) end of the cochlea, are the target of an efferent neural pathway. This pathway, the crossed olivo-cochlear bundle (COCB), is cholinergic (for a review of its development across species, see Ref. 311). IHCs are also a target for a descending pathway, but in this case, the efferent axons form a synapse on the postsynaptic (afferent) terminal and will not be considered further here.

A. The Cochlea as a Frequency Analyzer

The cochlea performs the decomposition of a sound into its component frequencies. It was Helmholtz who pointed out that the basilar membrane, the structure which bisects the cochlear duct and on which the organ of Corti is placed, is constructed of fibers which run radially and, by varying in length along the duct, could perform this function. The design confers radial flexibility across membrane, but with relatively little longitudinal coupling. The obvious parallel is to a piano, with the strings arranged from treble to bass as one progresses from the basal end of the cochlea (near the middle ear) to the apical end of cochlea (terminating with the helicotrema). Helmholtz developed a quantitative, but physically inspired, model to describe this system of fibers and suggested that they were free to resonate but with different resonant frequencies along the length of the duct (see Ref. 135., p. 146 and appendix X). In a more elaborated model, he let the fibers be of variable length. The mathematical solution to this system of resonators is analytically soluble. The complication, and one recognized by Helmholtz, was that the fluid itself in the cochlear duct would tend to damp out the resonant behavior of the partition.

The Helmholtz model can account for the observation that the cochlea is the organ that separates out different frequencies in a sound signal. In modern parlance, the cochlea acts like a spectrum analyzer. In his words, "The sensation of different pitch would consequently be a sensation in different nerve fibers. The sensation of a quality of tone would depend upon the power of a given compound tone to set in vibration not only those of Corti's arches which correspond to its prime tone, but also a series of other arches and hence to excite sensation in several groups of nerve fibers."

The hypothesis therefore meshed physics with the physiology of a place code. It also included the primitive idea of how population coding could be important. In attempting to go further, Helmholtz suggested that the rods of Corti (i.e., the microtubule-containing inner and outer pillar cells and elements of the organ of Corti) could form part of the apparatus which led to the excitation of the auditory nerve fibers. These structures clearly survived the tissue fixation better than the hair cells or other cells of organ of Corti. Sensory hair cells, although known to the late 19th century anatomists (134), remained to be described properly only with the advent of electron microscopy (83, 315, 337). For a modern description of cochlear structure, see Reference 314.

B. Cochlear Bandwidths and Models

The tuning mechanism in the Helmholtz model is an array of resonators. The idea was originally formulated as a hypothesis. If a physical system is tuned to a pure tone of frequency f_0, the quality factor (Q_{10dB}) describes the width of the response curve centered on f_0 at a point 10 dB down from the maximum, and the higher the quality factor, the sharper the tuning. Helmholtz reported, by (indirect) psychoacoustic experiments, $Q_{10dB} = 8.5$ for the tuning of the auditory system, not significantly different from modern values. Comparably high values of Q were also measured psychoacoustically by many other authors in the mid c 20 (e.g., Ref. 121). The physiological basis for cochlear excitation was taken up by Bekesy in pioneering work (23). Nevertheless, Bekesy's direct physiological measurements on the basilar membrane in a wide range of mammalian cochleas in work carried out in the 1930s and 1940s found bandwidths that were broader than those found by Helmholtz. Bekesy typically found values of $Q_{10dB} = 0.9$ for the rat and the guinea pig cochleas. The experimental data clearly showed that excitation propagated along the length of the cochlea and appeared to suggest that the cochlea behaves like an assembly of tuned oscillators, much as had been originally suggested. The problem was that the tuning was not as sharp physiologically as the psychoacoustics predicted (for a comprehensive historical review, see Ref. 339).

Bekesy himself, aware of the problem, thought there might be some sort of lateral inhibition operating in the

auditory system similar to that described in the retina to restrict receptive fields (23). Recordings from single auditory nerve fibers by Kiang et al. (188) and by Evans (87) only emphasized that although the "sharpening" mechanism was located in the cochlea, the principles were unclear. With the exception of some notable, but unreproduced, experiments by Rhode and Robles (266–268) in the early 1970s which clearly showed that sharp tuning of the basilar membrane occurred, the origin of the precise and sharp frequency selectivity of the cochlea remained experimentally unresolved.

Early attempts to capture the essence of a Bekesy traveling wave in mathematical models (257, 356) as well as experiments on scaled up mechanical models of the cochlea (described in Ref. 23) caused doubts as to whether the idea of an array resonator was a reasonable underpinning of the psychoacoustics and physiology at all. The literature contains a number of ingenious proposals as to how sharp auditory nerve tuning could arise (5, 6), in some cases including suggestions which have subsequently been taken up to explain the role of the tectorial membrane (357). At the lowest point in the popularity of resonant models of the cochlea, Huxley (151) summarized the situation with a paper entitled "Is resonance possible in the cochlea after all?"

The solution had in effect been proposed in 1948 by Gold and Pumphrey (120, 121). Aware that the viscosity of the fluids in the cochlea would damp down any resonance, Gold proposed that a passive oscillatory mechanism should be abandoned and the explanation was that the cochlea used active amplification to enhance the resonance. The suggestion was rediscovered by the auditory community around 1980 and has been influential ever since (119). The idea was familiar to radio engineers for the idea of feeding back the output of a sensor back into the input, (the "regeneration principle"), had been developed by E. H. Armstrong in the early 1920s to enhance selectivity in radio receivers. The degree of feedback is critical, and such systems can easily become unstable. A common example of such feedback occurs in public address systems that "howl" when the microphone picks up the loudspeaker. The possibility of instability suggested that a small fraction of the input sound energy might be re-emitted from the inner ear. Gold failed to find this emission for technical reasons and another 30 years passed before lower noise floor microphones enabled "otoacoustic emissions" to be unequivocally detected as a re-emitted sound measured in the ear canal (181).

With the benefit of hindsight, other arguments also pointed to active amplification within the cochlea. Until reliable measurements of basilar membrane mechanics were introduced (reviewed in Ref. 276), the precise location of Q enhancement was unclear. It is now appreciated that the mechanical properties of the basilar membrane (BM) sets the frequency selectivity of the cochlea. The earlier measurements of Rhode have been clearly vindicated (266, 267). The idea crystallized after two additional sets of results were reported in the early 1980s when less biologically intrusive measurements of the basilar membrane motion were made, using laser interferometry in cats (184, 185) and using Mössbauer techniques in guinea pigs (307). These measurements showed that the basilar membrane (BM) was sharply tuned. In the best cases, the tuning curves of the BM approximated the sharp tuning curves obtained from auditory nerve fibers, indicating that frequency selectivity of the auditory periphery is determined by the mechanics of the cochlea (233). There are still relatively few measurements of the basilar membrane motion at the apex of the cochlea (see, however, Ref. 53), and it remains a possibility that the mechanisms there differ from those at the base.

Frequency selectivity in the cochlea is particularly evident at low sound pressure levels, that is, in the range between 0 and 50 dB SPL. This can be seen if the BM gain function is plotted (i.e., the ratio of BM velocity to input sound level). Under these conditions, the overall gain at the best frequency is significantly enhanced at low sound levels by ~40–60 dB (i.e., 100–1,000 times). At higher sound levels (i.e., above 60 dB SPL), the gain begins to fall off and the selectivity declines as well. Between the low and high levels of sound level, there is a transitional region (276, 307). Gain enhancement disappears at all sound levels after manipulations that damage the cochlea. The BM tuning also collapses post mortem to a pattern of low Q curves resembling those found in the earlier measurements of Bekesy.

Measurements of the vibration pattern, particularly after the introduction by Nuttall of commercially available laser vibrometers (244) have extended these results to multiple apical and basal sites along the cochlear duct (53, 53, 277, 278). These techniques provide a near-complete characterization of the mechanics of the BM. The sensitivity of the measurement techniques is now sufficiently great that all the nonlinearities inherent in cochlear mechanics, the distortion products of the BM motion, and the transitional regimes between low and high SPLs can also be reliably and accurately recorded.

The origins of many of the nonlinearities in the mechanics of the cochlea remain a contentious issue. The main source of nonlinearity in the system is likely to be the mechanoelectrical transduction step in the hair cell where a linear BM displacement is transformed into current that is itself a nonlinear function of displacement (149, 196, 241). A number of cochlear models have been developed that take as their starting point the inherent nonlinearity of cochlear mechanics (39, 52, 76, 81, 170). These models have developed some generic approaches to understanding the nonlinear interaction between tones

in the auditory system, but will not be considered extensively here.

C. Physics of Cochlear Amplification

An amplifier is a device that takes an input signal and converts it to an output that is in some sense "larger." A physically implemented device requires an energy source to perform this operation, as physical systems in general dissipate energy. A device that attenuates a signal can do so without any energy sources. In addition, signals need to be amplified in the presence of noise, both intrinsic and extrinsic. In the cochlea, sensory transduction is limited by classical, not quantum, considerations. This is a different situation from that found in visual system where the quantum of light, the photon, ensures that the threshold of seeing is determined by the limits imposed by statistical nature of light, or equivalently, because of the high energy associated with an individual photon. In the auditory system, the quantum of sound is the phonon. It has energy $h\nu$ (where h is Planck's constant and ν is the frequency). In the cochlea, the ratio between the phonon of acoustic energy and $k_B T$ (where k_B is Boltzmann's constant and T is absolute temperature) determines the amount of energy per degree of freedom of each mechanical component of the system. The ratio $h\nu/k_B T$ is $\sim 10^{-10}$ at acoustic frequencies; the ratio for a photon of blue light is 100, which is 12 orders of magnitude larger. Auditory detection is a classical problem limited by thermal noise: a single phonon is unlikely to be detected by an auditory mechanism (29). Thermal noise can, however, be detected. Experimental evidence shows that a frog hair cell can transduce Brownian noise (the thermal fluctuations of the bundle) at its input (68, 69). It is surprising that displacements this small can be detected without further noise from the transduction channels.

Gold (120) recognized that there would have to be a source of energy to provide the feedback to cancel the dissipative forces of viscosity. He proposed, in a remarkably far-sighted manner, that the source of the energy would be ". . . supplied by some form of electrochemical action. . . . and that acoustic energy would be required to modulate the electric current." Gold proposed active amplification in the cochlea so that *1*) the resonant system becomes more highly tuned (i.e., Q increases) and *2*) the system amplifies (i.e., the peak amplitude of the resonance increases). In this scheme, both selectivity and amplification are inherently linked. It is worth noting, however, that there are some cochlear models where the two are decoupled. In these, the effective viscosity of the fluid in the cochlea is not cancelled but to the stiffness of the BM is dynamically adjusted (191, 192, 194). In such schemes, the resonant peak is sharpened by reducing the response to frequencies away from the best frequency by decreasing the BM velocity on the basal side of the traveling wave peak.

Halliwell Davis, one of the pioneers of modern cochlear physiology, brought together a number of the ideas about how tuning comes about by coining the phrase *the cochlear amplifier* (66). The cochlear amplifier is the set of processes which produces *1*) sharper frequency selectivity and *2*) higher sensitivity to sound at low sound levels. Davis's argument depended, initially, on the behavior of the cochlear microphonic (CM), the extracellular potential which can be recorded from within and around the cochlea. The CM reflects the transduction current flowing through the population of OHCs. The CM input/output function also shows an enhancement at low sound levels compared with high sound levels, and this finding parallels the enhancement found in the mechanical measurements of the BM.

The "cochlear amplifier" idea has been useful as it summarizes the experimental observations and to some extent it bridges the field of cochlear mechanics and the underlying physiology. Nevertheless, it has also confounded what exactly is meant by an amplifier; quite often "active" has been used, probably unjustifiably, as a synonym for "in vivo." Physiological integrity of the inner ear is a necessary, but not sufficient, condition for a correctly tuned BM.

D. Cellular Origin of Cochlear Amplification

OHCs form one of the two distinct classes of sensory hair cells found in the mammalian cochlea (see Fig. 1) They are cylindrical cells 15–70 μm long and are three to four times as numerous as the IHCs. They are positioned in the organ of Corti near the center of the basilar membrane. Based on the work of several groups, it had been known since the mid 1970s that the loss of OHCs, by noise damage or by chemical ablation, parallels the loss of tuning and rise of threshold in the auditory nerve (61, 88, 187, 282). These data provided clear physiological evidence for OHCs as the instrument of amplification within the cochlea. Nevertheless, the precise role of OHCs remained enigmatic for a surprisingly long time. It might even be argued that there is still not complete agreement as to how they contribute to normal cochlear function. The OHCs' relatively poor afferent supply but extensive efferent innervation, remarked above, had already suggested parallels between the OHC population and an effector cell system (96). The details were unclear when this proposal was made, although it was further fueled by the novel identification of actin in hair cell stereocilia by its decoration with S1 myosin. Although ultimately for the wrong reason, the evidence thus suggested parallels between OHCs and muscles.

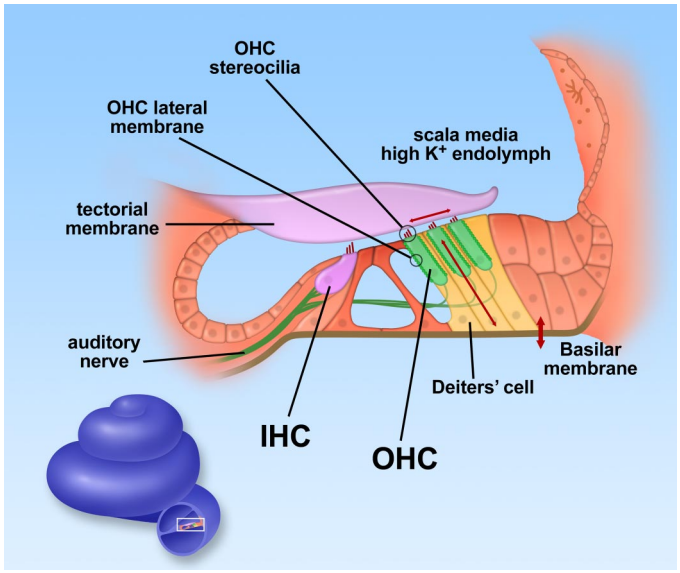

FIG. 1. Organization of the mammalian organ of Corti and the hair cells on the basilar membrane. The schematic shows a cross section of the organ of Corti with the inner hair cells (IHCs) and outer hair cells (OHCs) in place over the basilar membrane in series with the Deiters' cells. Both IHCs and OHCs are stimulated by a shear force applied to the stereocilia through the tectorial membrane. Changes in the OHC membrane potential produce a longitudinal force in the cell acting through the motor. The effect of OHC feedback (which may in principle either be positive or negative) is to produce a local alteration of the partition mechanics, i.e., the basilar membrane (BM) motion. The possible forces generated by the stereocilia are discussed at the end of the review. The traveling wave in the cochlea coordinates the response of many such cross-sectional units.

As well as such cellular evidence, it was found that when the stereocilia of the hair cells in the frog vestibular system were mechanically deflected, the recovery occurred in a manner that depended on extracellular calcium (97, 98, 255). The recovery rate was reduced in media that induced muscle relaxation. Bundle measurements of this type were performed on frog hair cells as well as in the vestibular system of the eel (279, 280). The results suggested that the hair bundle could perhaps be able to interact with the mechanics of the cochlea. Although circumstantial, this assembly of observations pointed to some hair cells also being capable of motor function as well as their more conventional sensory role. The available data at that time pointed towards the stereocilia as being the source of the force. The discovery of outer hair cell motility shifted the emphasis away from the apical surface of the cell to its basolateral surface.

E. OHCs Change Length

The original observation that isolated OHCs change length when stimulated electrically was reported by Brownell et al. (34). The movement was referred to as "motility." In these experiments, the cells were electrically polarized either by using intracellular electrodes or by passing extracellular current along the cell. The key observation was that hyperpolarization by current led to a lengthening of the cell, and depolarization by current led to the cell becoming shorter.

The technical advance that made the observation possible was an improved microelectrode recording technique. Developed for the purpose of recording from isolated retinal photoreceptors (18), the technique found application to the cochlea. The second advance was the redevelopment of techniques for working with isolated OHCs. These techniques were pioneered by Flock and his co-workers at the Karolinska Institute in Stockholm. The observation of isolated single OHCs precedes this by a considerable period and is due to Held in 1902 (134) who found that the cells could be dissected readily from intact tissue. Nevertheless, the idea that a population of OHCs which change length was rapidly recognized as a potential mechanism that could modify the mechanics of the cochlear partition (171).

These initial experiments reported results using OHCs isolated from the guinea pig cochlea. The guinea pig has remained a preferred system for subsequent studies as guinea pigs (as do gerbils) have an acoustic range which, at the low frequency end, is commensurate with human hearing. There is also an extensive database on the physiology of guinea pig hearing. Electrically evoked length changes are nevertheless not unique to guinea pig OHCs. Isolated human OHCs also respond to electrophysiological stimuli (247, 248); such studies show that the animal results translate to understanding human hearing. Studies have been carried out using other cochlear systems as well. Mouse, gerbil, and rat systems are all attractive for various reasons related to their availability, their genetics, and/or their hearing ranges. OHC motility has been reported in mouse (1, 217), rat (24), and gerbil (131). It is clear, however, that special precautions have to be taken when using hair cells from cochlear positions corresponding to high-frequency hearing, for the cells are often smaller and do not survive isolation procedures well for reasons that are not fully understood.

F. Speed of OHC Length Changes

To participate in acoustic tuning, OHC forces need to be fast enough to follow cyclical changes up to the mammalian hearing limits of nearly 100 kHz. This is not an absolute requirement as some models of cochlear mechanics require only that the "active element" tonically alter the properties of the cochlear partition. Nevertheless, low-frequency changes in OHC length (i.e., up to ~10 Hz) can be captured by video microscopy (171). This technique remains inherently limited by video capture

rates (maximally a few tens of frames per second) unless stroboscopic techniques are employed.

The original report on OHC motility left open the precise question of whether there was an upper limit to the frequency of the motile response. The question was partially answered by using alternatives to video imaging to measure fast, nanometer displacements of the cell. Originally developed to detect hair bundle movement in nonmammalian hair cells (54), fast response photodiodes aligned on optical boundaries of the hair cell image can be used to detect linear changes of cell dimension. With the use of this approach, it was shown that transcellular stimulation could produce measurable length changes of OHCs up to at least 8 kHz (14). With the use of whole cell patch recording techniques to record from OHCs, techniques first introduced to record from nonmammalian hair cells (150, 197), and detection methods used to follow rapid motility of the hair bundle (54), the OHC motion could be followed reliably. The recordings unequivocally showed that OHC lengthening and shortening was as fast as whole cell recording permitted (13). The limits were set by the patch-clamp bandwidth. Thus OHCs are certainly not excluded from being part of the mechanism for mechanical feedback to the basilar membrane at acoustic frequencies (348). Whole cell patch-clamp recording emphasized that the speed of OHC motility measurements is often limited by the recording technologies (293).

Although the whole cell tight-seal recording techniques provide major insights into the currents of hair cells, the access resistance of the recording pipette in the patch clamp limits the frequencies that can be reached. In whole cell recording, a practical upper bandwidth limit of ~10 kHz is seldom achieved. Higher bandwidths can be obtained when recording patches of membrane with much larger diameter pipettes and, in these cases, submicrosecond responses are possible (corresponding to frequencies higher than 200 kHz) (138). The problem of stimulating whole hair cells at high rates can also be partially circumvented by using suction pipettes. Originally developed to study the currents in photoreceptor outer segments (21, 22, 342), such pipettes can be used to suck the whole cell, rather than portions of membrane, into a pipette. Introduced to measure OHC motility, the pipette was rebranded as a "microchamber" (86). Long cylindrical cells, such as OHCs from the apical end of the guinea pig cochlea, can be drawn into a suction pipette and stimulated with a current passed down the pipette. The method is noninvasive in the sense that the plasma membrane is not punctured and intracellular contents remain undisturbed even though the suction pipette internal diameter and the cell diameter have to be very closely matched. The technique offers good stability for the recording of cell length changes even though it does not permit the intracellular potentials or currents to be measured directly. The microchamber also permits different solutions to be presented to the apical and the basolateral surfaces of the cell, thus more closely mimicking the situation in vivo. The configuration allows an elegant demonstration that deflection of the stereocilia does indeed lead to the electromotile changes in an OHC, for the projecting stereocilia can be manipulated while motion of the cell body is measured (85).

Only extracellular current stimulation is used in microchamber experiments. As current is passed down the pipette it will hyperpolarize (or depolarize) the membrane within the microchamber and depolarize (or hyperpolarize, respectively) the externally exposed membrane. The effectiveness of the stimulus depends critically on the quality of the seal between the cell and the rim of the pipette. By sucking cells into the pipette to varying extents, one can measure the effects of transmembrane current at different sites. Inter alia, this technique provides evidence that motility arises in from the lateral membrane (58).

It was remarked that, if the cell was sucked halfway into the microchamber, the electrical circuit of the stimulated cell is that of a capacitance divider. Thus, if the time constants of the cell inside and outside the microchamber are equal, the transcellular current is not attenuated and the cells can be stimulated at much higher frequencies (56, 57). Such experiments reported that the upper limit of electromotility was above 22 kHz. That higher rates could not be measured more precisely was probably a consequence of the limited bandwidth of the instrumentation, and in that case the photodiode system employed. Such limitations have subsequently been removed and, by enhancing the signal-to-noise ratio of the optical measurement by using a laser vibrometer to measure light reflected from an atomic force microscope cantilever placed on the cell axis (100), a much higher frequency limit of the electromotility has been determined. The 3-dB point of the frequency response was found to be 79 kHz for cells from the basal, high-frequency end of the cochlea, and at a slightly lower frequency for cells from the apical, low-frequency end of the cochlea. Over a range of frequencies, the electromotile response is described by an overdamped second-order resonant system with an apparent Q_{3dB} of 0.42. Such measurements suggest that internal damping and inertia of the hair cell itself may be limiting any higher response frequencies.

G. Strains and Stresses of OHC Motility

The dependence of an OHC's length as a function of voltage is described quantitatively by a curve that saturates at positive and negative potentials. The functional dependence can be parameterized by a "Boltzmann" function familiar from statistical mechanics

$$\Phi_B(V) = 1/\{1 + \exp[-\beta(V - V_o)]\} \quad (1)$$

where $\Phi_B(V)$ is a sigmoidal function that varies between 0 and 1. At $V = V_o$, $\Phi_B(V) = 0.5$; β is a free parameter to be determined experimentally. By differentiation, the maximum slope of Φ_B occurs at $V = V_o$ and has the value $\beta/4$. The nomenclature for V_o is not fixed in the literature (e.g., V_{PkCm} and V_{pkCm} is used in Refs. 172, 296 and $V_{1/2}$ in Refs. 250, 251).

The length L of a electrically stimulated cell is found to vary between a maximum (L_{max}) and a minimum length (L_{min}) and is a sigmoidal function of membrane potential given by (13, 55, 58, 293)

$$L(V) = L_{max} + (L_{min} - L_{max})\,\Phi_B(V) \quad (2)$$

In experiments where the intracellular membrane potential could be determined (i.e., in patch-clamp experiments), the value of the slope ($=\beta/4$) was found to be $\sim$1/120 mV^{-1} (13, 289, 293). Thus the critical parameter β has a value of $\sim$1/30 mV^{-1}. The range of values found for β and V_o will be discussed below. In experiments where the cell is stimulated by an extracellular current (i.e., in experiments with microchamber stimulation, Ref. 86), the value of β depends on the precision with which the membrane potential can be determined. Often the potential is not measured directly, but *Equation 2* provides a semiquantitative description.

The maximum length change that can be induced by electrical stimulation of an OHC is $\sim$4% [i.e., a strain 2 $(L_{max} - L_{min})/(L_{max} + L_{min}) = 0.04$] (141). For a cell 50 μm long, this value corresponds to a maximal length change of $\sim$2 μm and is easily observable by light microscopy. The length of a cell is maintained while the potential is held constant. The maximum voltage sensitivity of extension is consequently 2 μm/120 mV = 18 nm/mV. Stated in an alternative way, the voltage dependence of the strain in an OHC is $0.04/120 = 0.0003$ mV^{-1}.

The function that describes the potential dependence of OHC length, *Equation 2*, is surprisingly simple. It is the clue to the mechanism. To distinguish motility driven by potential from length changes produced by movement of water in and out of the cell, to be described below, OHC length changes produced by electrical stimulation has been termed *electromotility* (55). No other cell type in the mammalian cochlea exhibits electromotility. An effect of this magnitude has not been found in hair cells of nonmammalian hair cells. Thus electromotility seems to be a property exhibited exclusively by mammalian OHCs.

The forces generated by OHCs are important as they offer insights into the possible mechanisms. An early estimate was that the force produced by an OHC was $\sim$0.1 nN/mV based on the maximal rate of extension of an isolated cell against the viscous damping of the surrounding fluid (13). Subsequent experiments used flexible probes held against the cell near the cuticular plate whilst the cell was driven with voltage pulses delivered from a patch pipette under whole cell voltage clamp. This method was used to deduce the isometric force generated by an OHC. The experiments also gave a value of $\sim$0.1 nN/mV (158). With the use of an atomic force microscope cantilever held against the cell, allowing a much higher measurement bandwidth, the isometric force produced by an OHC has been found to be constant up to at least up to 50 kHz (100). The isometric force was measured to be 53 pN/mV. This value is therefore consistent with earlier estimates. These data permit a simple point mechanical model of OHC stiffness and a displacement generator to be combined with internal viscous elements when higher frequencies (above 10 kHz) need to be considered (100). Models that incorporate the interaction between lateral wall properties and the surrounding fluids have further explored the limiting mechanics of OHC (321–323).

Combining compliance and strain data, OHCs have a stiffness of 510 nN/unit strain (158). Because the maximal strain of an OHC is $\sim$4%, the force that can be produced by an OHC is about the same magnitude as the force required to stretch the cell. In a more detailed report of hair cell stiffness using axial compression of cells with a calibrated glass fiber probe, it was found that OHCs behave like linear springs for strains up to $\sim$0.5% with stiffnesses in the range 1–25 nN/μm (126). Longer cells were more compliant, and shorter cells were less compliant. This observation would be expected if each axial element of the cell behaved as though it were mechanically uniform and responded independently of its nearest neighbors.

The similarity between the effective numerical magnitude of the OHC forces and the OHC stiffness has made disentangling the biophysics of motor mechanics less straightforward. The axial stiffness of an OHC is itself voltage dependent (129, 130). It is also clear that the stiffness is also modulated by osmotic stresses on the cell (127). The stiffness of the lateral wall of the OHC is itself determined by agents such as salicylate (208) and chlorpromazine (209). The changes in stiffness of the whole cell produced by these agents are severalfold, whereas the changes in length are only a few percent. The experimental observations are consistent with the cell being represented by a model in which an ideal displacement-generating element is in series with an internal stiffness element at least for low frequencies. In principle, either the displacement generating element, the stiffness element, or a combination of both could be potential dependent (62). If it is the stiffness that is potential dependent, then changes in length only occur if the cell is preloaded (for example, if there is a further "spring," such as the actin cytoskeleton, which maintains the length of an isolated cell). If it is the displacement element that is poten-

tial dependent, a variety of different conformational changes in the underlying structures might be responsible. These might be changes in a uniform symmetrical area motor (157) or a changes in model in an L-shaped structure (described by the authors as a "boomerang" model) where the basic element exhibits two different angles between the two "legs" or conformational states (62, 128). There are, therefore, alternative modeling approaches to the description stiffness and motility (70), but the resolution of this problem will depend ultimately on the detailed molecular dynamics of the motor molecule underlying the mechanical forces of OHCs.

III. CELLULAR MECHANISMS OF OUTER HAIR CELL MOTILITY

The OHC is a cylindrical cell whose length varies from ~1.5 to 7 times its diameter (see Fig. 2). The precise ratio depends on cochlear position within the organ of Corti. OHCs from the high-frequency end of the cochlear are generally shorter. The cellular structures that keep the cell in this shape are mainly cytoskeletal (139, 142, 143). However, the lateral membrane of the cell is visible under the microscope. It is not a single plasma membrane but includes a system of endoplasmic structures, the lateral cisternae (124). It has even been suggested that this distinguishing organelle of OHCs could be a contributing factor to OHC motility (171). The proposal has only limited support. Nevertheless, the lateral cisternae have remained an enigmatic feature of the cell. They are implicated in the movement of membrane within the cells (176), and the presence of a Ca^{2+}-ATPase in the organelle suggests that they may be calcium stores (306). The detailed structure and function are yet to be fully clarified.

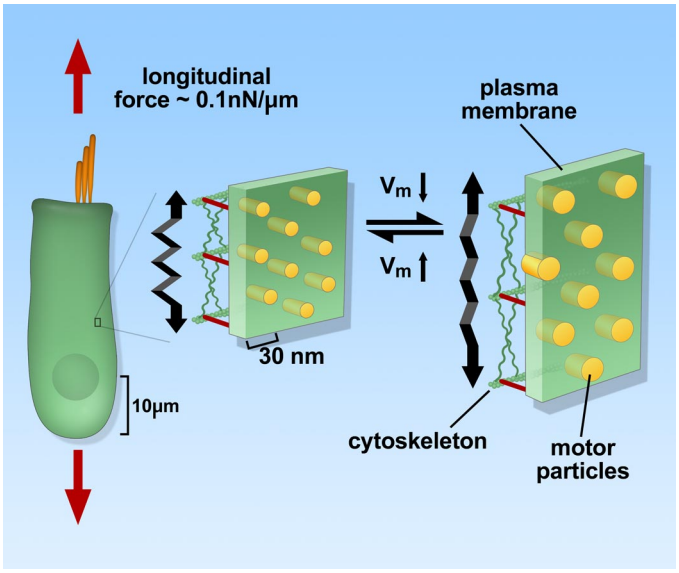

FIG. 2. Local membrane response of the OHC generates longitudinal forces. Molecular crowding of an area motor generates change in length of the cell when the motor works against the planar constraints of the cytoskeleton. The area motor is driven by membrane potential.

OHCs exhibit a number of novel features for a motile cell. OHC motility is not blocked by metabolic uncouplers. For example, the metabolic poison iodoacetate permeates the cell membrane and decouples energy-generating steps yet does not block electromotility (171). The energy required for shape change does not come directly from internal (e.g., mitochondrial) stores. ATP is definitely not required for motility as inhibitors of ATP synthesis in mitochondria, FCCP and CCCP, do not block the movements (141), nor does dialyzing the nonhydrolyzable ATP analog AMP-PNP into the OHC through a patch pipette inhibit length changes. Agents targeted against actin-based motility mechanisms (phalloidin) and agents shown to inhibit microtubule assembly and disassembly (cytochalasin B and cytochalasin D) also prove ineffective. It might also be supposed that electromotility depended on microtubule-based mechanisms, yet agents targeted against tubulin assembly and stabilization (including colchicine, nocodazole, and colcemid) also fail to inhibit electromotility. Electromotility can therefore not be reconciled with other types of more conventional mechanisms of cell motility (141).

The temperature dependence of OHC motility is lower than would be expected for a mechanism where multiple biochemical steps are involved. A Q_{10} between 1.3 and 1.5 describes kinetic parameters of electromotility (16, 109, 294). Such values suggest that the rate-limiting step for the change in length may even be limited by the diffusion of some mobile molecule. Thus OHC motility is not a modification of more conventional motility mechanism, but can instead be identified, tentatively, as a novel form of cellular motility (55, 59).

OHCs are osmotically active cells. They are sensitive to the osmotic strength of the external solution, swelling or shrinking as the solution becomes hypo- or hyperosmotic (77, 79, 139, 265). Because of the simple physics of a cylindrical cell, swelling leads to the cell shortening, and volume shrinkage leads to the cell elongating. Although some degree of volume regulation occurs in OHCs, the high osmosensitivity produces changes in turgor pressure of the cell. Collapse of the cell occurs at an average of 8 mosM above the standard medium, suggesting that normal cells have an effective intracellular pressure of ~130 mmHg (50). When exposed to slow rates of osmolarity change, cells tend to maintain their volume, whereas fast changes in osmolarity produce rapid alterations of cell shape. Cells do not recover their initial volumes readily, and this usually limits the experimental time available for in vitro studies. During electrical stimulation with extracellular current, responses can be enhanced by reducing the ionic strength of the solution by adding sucrose (171). Although partly a consequence of the change in current

flow, the main explanation for the observation must be that electromotility depends on the cells having a slightly positive internal (turgor) pressure: cells which are collapsed and shrunken do not exhibit electromotility.

A. OHC Motility Is Determined by Membrane Potential

In vitro stimulation of OHCs can be carried out by using extracellular current, by using sharp microelectrodes, or by using patch recording pipettes. The responses are tonic: the length change is maintained for as long as the stimulus continues. The question is thus: does membrane potential or membrane current determine OHC length change? In principle, it could be either. Whole cell patch-clamp recording, by changing the intracellular contents of the cell with a defined medium, allows a ready answer to the question. If OHCs are recorded with Na^+ replacing K^+ in the pipette, the current-voltage (*I-V*) curve of the cell changes but the dependence of length on membrane voltage does not (13). The complementary experiment, where the external solution is replaced with one containing Ba^{2+}, shows that there is a range of membrane potentials where depolarization from rest produces an inward current yet the cell mechanically continues to shorten, i.e., the direction of the length change is unchanged but the current direction is changed (293). Taken together, these lines of evidence strongly point to membrane potential as the determinant of electromotility. A back-of-the-envelope calculation suggests that when an OHC does work against viscous forces in an experimental chamber, the energy required is ~1 aJ (10^{-18} J) per cycle (12, 58). The energy in this case comes from the electrical recording system. The energy required to charge the membrane capacitance is about an order of magnitude larger. Thus there seems to be sufficient energy in the electrical field across the plasma membrane to drive OHC motility.

B. OHC Motility Depends on the Lateral Plasma Membrane

By stimulating the cell with a patch pipette at various positions along its lateral membrane, it can be shown that the cell moves relative to the fixed point of the pipette. This experiment shows that the force-generating mechanism is distributed throughout the length of the cell (141). In a different design of experiment, where the cell is drawn into a microchamber, the inside and outside portions of the cell move in opposite directions, an observation only readily compatible with membrane-bound motor (58).

The clearest evidence for a plasma membrane-based mechanism is, however, derived from experiments where the cellular contents of the cell are completely removed by internal digestion with the enzyme trypsin (148, 174). In these experiments, the cells often round up. Even in such near-spherical cells, movement can still be detected in small regions of membrane. The authors also reported that patches of membrane withdrawn into the patch pipette in cell-attached configuration continued to move even when the cells rounded up, indicating that motility may be a consequence of local properties of the basolateral membrane rather than a global property of the entire and intact cell (see also Ref. 109). When the membrane was hyperpolarized, the patch moved into the pipette and the curvature of the patch decreased. The observation is compatible with the idea that hyperpolarization leads to an increase in membrane area and that each elemental area of the membrane operates independently (Fig. 2).

The evidence thus supports the hypothesis that OHC motility is due to a "motor" in the lateral plasma membrane. Based on observations of lateral markers on the cell (141, 344) and by observation of the movement of membrane patches (174), an attractive hypothesis is that the area of any local patch of membrane varies in a way that depends solely on membrane potential (reviewed in Ref. 8). The idea was formally developed in two papers (60, 157), where it was proposed that the OHC motor should be described as an "area" motor. An area motor is a structure in the plane of the lateral membrane that can be switched between two states, extended and compact, by a change of membrane polarization.

What is the identity of the OHC area motor? In principle, the properties of a lipid bilayer alone might be able to trigger cell length changes (this will be described below), although the evidence is now in favor of a specific membrane protein. The lateral membrane of OHCs contains a dense array of particles, first indicated in freeze-fracture images in the inner surface of the cytoplasmic leaflet (124) and associated with a complex pattern of cytoskeletal elements and submembranous endoplasmic reticula (285). These particles are 8–10 nm in diameter and present at high density. The precise diameter cannot be determined as the observed scanning electron microscope images depend on the preparation and the shadowing methods used. The densities found in mature OHCs are ~3,000 μm^{-2} (174), although some reports give densities twice as high at 6,000 μm^{-2} (99). Electrophysiological measurements, using methods to be described below, have suggested the figure may be as high as 8,000 μm^{-2} (295). Although this particle population may represent several different membrane proteins, the specialized lateral membrane and the exceptionally high packing density of particles makes the particle a prime candidate for the OHC area motor. Tight packing of any molecular motor will ensure that any small change in molecular structure will be reflected in the behavior of the whole cell. The proposal that an area motor is responsible for

OHC motility is thus an effective way of combining functional and structural data.

It is possible that the particles are not the unit "motors" (i.e., individual force-producing elements) but part of a system on which membrane potential acts. As an example of such thinking (171), it could be that the electric fields within the cell, close to the membrane, could act as the origin of OHC motive forces (165). For example, it might be imagined that voltage gradients within the cell act electrophoretically on some special feature of the particles embedded in the plasma membrane and generate longitudinal forces. Such hypotheses are hard to maintain in the face of evidence that transmembrane potential is the essential stimulus (13, 293) unless there were to be a significant nonhomogeneity of the membrane potential. At high frequencies, a short cylindrical OHC could depart progressively from isopotentiality, with one end of the cell depolarized more than another. In this case, complex modes of excitation might occur. Some of these modes have been explored by placing OHCs in a custom microchamber that allows the top and bottom of the lateral membrane to be stimulated extracellular current at 1–100 kHz (259). The findings show complex piezoelectric resonant modes of the cell where transverse electrical resonances become modulated by axial forces.

C. OHC Motility as a Piezoelectric Phenomenon

Rigorously speaking, the OHC is not powered by a motor as the cell does not cycle through a series of mechanical states when it is "triggered" to start. There is no internal source of energy. OHC electromotility arises from what is more precisely an "actuator": the cell switches between states when externally supplied by an energy source. This is also the case for piezoelectric devices that change dimensions under the influence of potential. OHC electromotility is observed in isolated cells when the membrane potential changes, and this leads to a (sustained) change in length. If an OHC is stretched or compressed axially, then potentials are generated. Although initially observed as an effect on the voltage-dependent capacitance when forces were applied to the membrane (156), the underlying redistribution of charge can be observed as a transient whole cell current when the cell is rapidly stretched along its axis (107, 172). The same effect can be observed in groups of (mechanically coupled) cells in strips of organ of Corti: a transient current is recorded in an OHC when its neighbor is depolarized and shortens (286, 351). The consequences of this coupling seem unlikely to have more than a second-order effect for cochlear mechanics. Nevertheless, the reciprocity (or interchangeability) of membrane voltage and axial force in an OHC is highly reminiscent of piezoelectricity. The similarity has been remarked upon and developed in several studies (32, 75, 107, 155). There is an important difference however: the OHC is much more compliant than a piezoelectric crystal. On the other hand, the piezoelectric coefficient that describes the conversion of voltage to displacement in OHCs is four orders of magnitude greater than found in man-made crystals used in electronic devices or manipulators (75).

The notion of biological piezoelectricity has been useful in modeling hair cells (reviewed in Ref. 32). It brings the data from isolated cells into the domain of cochlear mechanics. In the organ of Corti, the cells are held in a matrix of other cells, and any changes in length are small (although observable with sufficiently sensitive techniques, Refs. 100, 137, 210, 211, 224, 304). It has been pointed out from simple electrical arguments that if the OHC were represented as a piezoelectric element in a cochlear mechanical model, any load on the cell could extend the range of frequencies to which the cell responds (226). Loading the cell causes the electrical impedance of the cell to increase because of piezoelectric reciprocity. In turn, this mechanism would increase the frequency bandwidth of the cell's response.

The observation of apparent piezoelectricity in a biological structure permits explanations for electromotility which depend on continuum models of the membrane. The ideas have been developed by several authors (35, 166, 167, 261). The hypothesis is that an electric field across the membrane is converted into an in-plane force and therefore leads to length changes in the cell. Electrophoretic mechanisms have been mentioned above; local ion fluxes produced by the electric field (electro-osmosis) have also been proposed. Both of these mechanisms are needed to account quantitatively for the high frequencies at which electromotility can be driven.

The idea that electrical forces could also produce direct distortion of the lipid bilayer has also received attention (35, 261). In these schemes, dielectric forces on the plasma membrane are converted to local curvature changes ("flexoelectricity"). The model generates longitudinal cell forces by linking membrane bending forces to attachment sites along the actin-spectrin cytoskeleton. The model has the virtue of using classical membrane biophysical theory and provides an explanation for the observation that the disruption of spectrin, (normally part of the cytoskeleton conferring rigidity on the plasma membrane, Ref. 143), by diamide reduces force generation in the cell (2). In an interesting use of the atomic force microscope, it has also been proposed that the particles observed in the lateral membrane determine the dielectric constant of the membrane (349) and so can lead to a change in the transmembrane forces. If this were to produce a change in the bending of the membrane, then the cell length would also change. Such models, although plausible, do not explain why a very specific molecule,

prestin, to be described below, is found at such high density in the lateral membrane of OHCs.

D. Charge Movement and Membrane Capacitance in OHCs

During normal whole cell recording conditions, it is possible to compensate for the cell membrane capacitance as part of the conventional electrophysiological recording procedures. In OHCs, the cell membrane capacitance cannot be compensated over the whole experimental voltage range (9, 290). The underlying cause for the apparent difficulty can be traced to a pronounced charge movement when the membrane potential is stepped to any new value. This charge movement appears as a transient current and resembles a gating current of the type known in ion channels in excitable membranes (310) and in excitation-coupling in skeletal and cardiac muscle cells (95). In such systems, whether charge or membrane capacitance is measured is a matter of taste, since the capacitance-voltage (*C-V*) curve is the derivative of the charge-voltage (*Q-V*) curve.

Charge movements are best measured by integrating the transient currents produced when the membrane potential is rapidly stepped. The widest recording bandwidth is required for accurate estimates. The analysis produces a *Q-V* curve. Alternatively, and equivalently, a *C-V* curve for the system can be measured by measuring the membrane capacitance at each membrane voltage *V*. Since the capacitance is not a constant function of voltage, this curve is often referred to as a nonlinear capacitance (NLC) on the hair cell literature. *C-V* curves can be measured easily, and a variety of techniques exist to measure it. For example, membrane capacitance can be measured using sinusoidal stimuli (169, 239, 332) or multiple sinusoidal commands (288). It is also implemented in the controlling software of many patch-clamp recording amplifiers (49, 115).

The OHC charge movements are exceptionally large. They are distinguished from the charge displacements in other systems by their magnitude. In cardiac muscle cells, the maximum charge displacement from excitation-contraction coupling is ~5 nC/μF (95). The maximal charge in OHCs, calculated from the transient current, is 2–3 pC, and hence, the comparable normalized figure for OHCs would be 2.5 pC/25 pF or 100 nC/μF, over an order of magnitude greater than found in cardiac cells. The consequence is that, for 70-μm-long OHC from the low frequency end of the cochlea, the membrane capacitance is a strongly nonlinear function of holding potential, and the apparent capacitance can nearly be doubled, from 25 pF expected from the geometric area of the cell to nearly 50 pF at −30 mV.

The measured dependence of *Q* on membrane potential is also described by a simple sigmoidal function whose symmetry suggests that it should be a Boltzmann function

$$Q(V) = Q_{max}\,\Phi_B(V) = Q_{max}\,1/\{1 + \exp[\beta(V - V_o)]\} \quad (3)$$

Here Q_{max} is the maximal charge displaced, and V_o is the voltage at which $Q = 0.5Q_{max}$. This is the same Boltzmann function that is used to describe the length change (*Eq. 1*). In this case, the parameter β has an interpretation based on the statistical mechanics of a charge distributed across the electric field of the plasma membrane and is given by $\beta = ze/k_BT$, where $e = 1.6 \times 10^{-19}$ Coulombs is the elementary charge on electron, z is the valence of the charge moved, $k_B = 1.35 \times 10^{-16}$ J/^{0}K is Boltzmann's constant, and T (in degrees K) is the absolute temperature. In OHCs, the parameter β is found to be ~1/30 mV^{-1} (10, 13, 292), implying that either a fraction of ~0.8 of an elementary charge is moved across the cell membrane. Equivalently, this value represents a single elementary charge moved across the 0.8 of the membrane electric field. The value of β is thus comparable to the value found in length change experiments; by combining *Equations 1* and *2*, the electrically induced shortening of an OHC, $\delta L = (L - L_{max})$ is proportional to the charge displacement $Q(V)$. This observation can be experimentally verified by showing that change in cell length follows the area under the current transient (10). The charge moved at the onset of a depolarizing pulse is equal and opposite to the charge moved at the offset (291) (see Fig. 3).

The corresponding *C-V* curve associated with the total charge $Q(V)$ moved during a voltage step from a hyperpolarized potential is given by the derivative

$$C_{NL} = dQ/dV = Q_{max}\,\beta[1 - \Phi_B(V)] \times \Phi_B(V) \quad (4)$$

where C_{NL} is the nonlinear capacitance of the cell (i.e., to the NLC). The linear capacitance of the cell (C_{linear}) can be established from the geometric cell area and a specific membrane capacitance of 1 μF/cm^2. At a membrane potential $V = V_o$, the cell capacitance is

$$C_m = C_{linear} + C_{NL,max} = C_{linear} + Q_{max}\,\beta/4 \quad (5)$$

Thus the maximum nonlinear capacitance $C_{NL,max}$ depends on the maximum slope of the *Q-V* curve and the number of elementary charges moved.

The value of V_o is variable. It can vary between −70 and −10 mV even under normal experimental conditions. Even within a single study, the coefficient of variation (c.v.) may exceed 0.25 (e.g., Refs. 47, 332). In isolated cells, V_0 is generally negative and close to reported values of OHC resting potentials measured with microelectrodes (64). It is clear, however, that it depends on many factors, which include the developmental stage of the hair cell

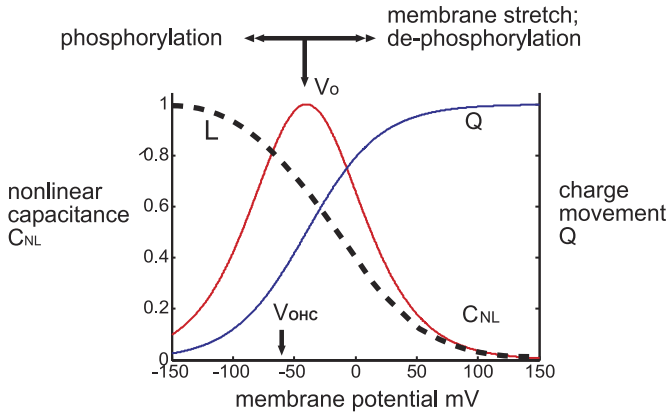

FIG. 3. Dependence of nonlinear capacitance (C), charge movement (Q), and length change (δL) on membrane potentials. The curves are all normalized and plotted according to *Eqs. 3* and *4* with $\beta = 1/30$ mV^{-1} and $V_0 = -40$ mV. V_{OHC} represents a typical OHC resting potential. The curves' position on the potential axis depends on experimental conditions described in the text.

(250), the phosphorylation state of the intracellular proteins (63, 104) and on levels of intracellular calcium (104), the tension in the cell membrane (172), the prior holding potential of the cell (296), and the presence of certain drugs in the medium. As an example of the latter, 20 mM extracellular furosemide shifts V_o to depolarizing values by 80 mV (302). The value of β is less variable (c.v. = 0.1, typically), but this depends on the fitting procedures used, on the experimental data and on the precise conditions: for example, β changes from ~1/30 mV^{-1} to 1/45 mV^{-1} when the OHC is stretched (172). Thus the values of both V_o and $C_{NL,max}$ depend on the experimental conditions. This issue will be further discussed below.

E. Tension Sensitivity of the Membrane Charge Movement

The details of charge movement $Q(V)$ depend on membrane tension. OHC membrane tension can be changed either by swelling or shrinking the cell with external solutions or by applying hydraulic pressures via the patch pipette. By using external hyposmotic solution and stretching the cell membrane, Iwasa (156) found that the membrane capacitance of an OHC, clamped at a fixed negative potential, reduced when the cell swelled; this result is consistent with a shift of the *C-V* curve to positive potentials. He deduced that for a two-state (expanded/contracted) model of the membrane motor, the change in area of the motor was ~2.2 nm^2. The converse experiment, where a hyposmotic solution (−14 mosM) is introduced into the pipette, made an OHC lengthen as the volume decreased and shifted the *C-V* curve by 30 mV to more hyperpolarized potentials (172). This result can also be obtained by applying a negative pressure to the pipette. Similar conclusions on the tension sensitivity of the lateral membrane can also be reached using isolated patches of OHC lateral membrane (108).

The same types of experiment have also been carried out in heterologous expression systems. Following the identification of a candidate OHC motor molecule, prestin (SLC26A5, see below), expression systems show nonlinear capacitance and tension sensitivity. The sensitivity of the *C-V* curves to pressure in such systems are lower than in OHCs (299). This may reflect, compared with the OHC, low expression levels for the molecule or a missing subunit of the presumed motor in the cell line. A similar conclusion has also been reached by quantitative analysis of the change in the motor protein area when the candidate motor molecule is expressed in a heterologous system. In that case, a smaller area change was found than in OHCs (74).

Equation 3 fits the *C-V* data, to within experimental error, over the range of physiologically reasonable potentials. Over a larger range of potentials, deviations can be detected. If the potentials extend below −150 mV or above +100 mV, the fit is less satisfactory, and the asymptotic capacitances do not reach the same steady asymptotic levels predicted by *Equation 3*. At hyperpolarized potentials, the nonlinear capacitance is greater by ~10% than would be predicted by a simple Boltzmann fit (296). It should be noted that special precautions are required to measure capacitance at large potentials close to the breakdown of the membrane (235). The observed deviations from the simple Boltzmann predictions may occur because the motor itself may be placed under strain through the membrane at the extreme potentials. In this case, and argued in Reference 296, additional membrane tension caused by the cell lengthening at hyperpolarized potentials will contribute to a free energy term in the energy of the motor and could produce a deviation from *Equation 3*. Alternatively, there may be additional tethered charges in the membrane which contribute to the charge displacement. In this case, it can be shown that membrane charge, associated with other membrane proteins say, will produce a small linear contribution from the "linear" capacitance (i.e., equal to $C_{linear}V$) and a force in the membrane which depends quadratically on V (92). This second term, known from classical membrane biophysics, has been invoked to explain small membrane deformations induced in excitable membranes during the propagation of an action potential (329) and may contribute to the curve's asymmetry. Consistent with this suggestion, prestin-transfected cells show a similar asymmetry in the *C-V* curves (92), even though the protein density is more than an order of magnitude smaller than in OHCs (297). It has been suggested that the effective capacitance of the membrane protein complex may be altered at extreme potentials as well.

F. Mathematical Models of OHC Motility

There have been many studies that attempt to bridge the gap between unconstrained and constrained force generation by hair cells. Understanding the "active" (i.e., the effect of external energy sources) and passive properties of the full, two-dimensional, lateral cell wall is critical before good models of the cell can be constructed. The passive properties of the cell wall (i.e., the structure which includes plasma membrane, cytoskeleton, and underlying membrane structures) can be described by a linear two-dimensional viscoelastic model. The equations that describe the mechanical properties of a cylindrical OHC were first formulated by Tolomeo and Steele (330, 331), who were also the first to include the effects of electromotility. These equations, generalized by subsequent authors (75, 155, 198, 319, 320, 323), include the effects of nonisotropic stiffness and viscosity of the cell wall as well as the contributions from the hair cell motor.

The motor can be included in these models by adding a piezoelectric element in which membrane stress terms depend on transmembrane potential and, conversely, electric current can be generated across the cell membrane in response to cell deformation. Two independent stress vectors are required for a cylindrical cell, one a vector oriented axially along the cell and the other a vector directed along the circumference. Finally, both ends of the cell are closed, and the effects of the viscosity of the cytoplasm need to be included. The internal viscosity of OHCs has not been determined directly, and only informed guesses can be made (198). It is usually assumed that OHC cytoplasmic viscosity is about the same as that of the cytoplasm of many other cells (typically 5–6 times greater than that of water), but it could be imagined that this quantity depends critically on the internal calcium concentration. The viscous component of this hair cell model is determined mainly by the viscosity of the lateral membrane complex (263).

The result of such modeling suggests that mechanical behavior of an isolated cell will be limited by its effective viscosity. Beyond ~2 kHz, the length changes of an OHC 60 μm long will be attenuated. The fall-off is rapid so that above 20 kHz hardly any motion will be detected (198, 331). A shorter cell, 20 μm long, will have a higher corner frequency at ~20 kHz. The predictions of these models are in good agreement with measurements of cells in a microchamber (60) and consistent with the later measurements of high-frequency motility (100) if the boundary conditions are suitably adjusted. The effect of reducing the viscous damping completely is to produce a resonant behavior in the OHC length. For an OHC 60 μm long, the predicted (highly damped) resonance would occur at ~3 kHz. A consequence of this approach is the conclusion that this resonant behavior is unlikely in experimental conditions, and certainly cannot account for a tuned mechanical resonance reported in experiments on isolated OHCs (36–38, 40).

IV. MOLECULAR BASIS OF MOTILITY

A. The Motor Molecule as an Area Motor

The evidence that the OHC motor mechanism depends on local membrane events can be shown by experiments involving electrical stimulation (58, 128, 141, 174). The simplest explanation is that the lateral membrane contains an array of voltage-sensitive elements that respond to membrane potential by changing area. As described above, this is not the only explanation as the change in the cylindrical cell shape involves different proportional changes in diameter and length. It is conceivable, therefore, that the motor could be an asymmetric element that functionally changes more along the length than along the diameter (58). Alternatively, local bending of a tethered plasma membrane under the influence of the electric field could, perhaps, produce forces propagated by the cytoskeleton of the cell (261).

For reasons of simplicity however, the idea of an area motor remains the most attractive model. An area motor, in its most schematic form, is a voltage-sensitive element in the plane of the membrane, which responds to transmembrane voltage and responds by changing its area in that plane (8, 159). In this model of OHC electromotility, the cell volume remains constant and the observed changes in cell length are a consequence of changes in the membrane tension induced by changes of the area of the surface of a cylindrical cell. The evidence for OHC electromotility occurring at constant volume is not as strong as it could be as the area changes in cell dimensions can be below the resolving power of the light microscope for all but the largest potential changes. The data imaged from isolated cells are, however, consistent with a constant volume change (13, 221, 222).

The plasma membrane in this scheme is maintained locally planar by a submembranous cytoskeleton containing both actin and spectrin filaments (142, 143). The formal description of this area motor was presented both by Dallos et al. (60) and by Iwasa (157). The model proposes that, on a molecular level, the motor can occupy one of only two states, a compact state or an extended state. In the model, the transition between the two is stochastic, with the probability depending on membrane potential. This is the origin of the Boltzmann function found in the experimental data. It is a consequence of the statistical mechanics of such a two-state system. Thus the probability P_c (P_e) of being in the compact (extended) state is

$$P_c = \Phi_B(V) \quad \text{and} \quad P_e = 1 - P_c = 1 - \Phi_B(V) \qquad (6)$$

where Φ_B is given by *Equation 1*. A small additional correction is required to fit experimental data. Membrane

tension and area change of the motor itself contribute to the free energy of the motor state (155). Including this correction produces alteration in the effective value of V_o and β. However, under load-free conditions, the 4% area change of the motor produces a small shift to the left of the length-voltage curve and a nonsignificant reduction in the slope β (157). Membrane tension does, however, produce a shift in the voltage dependence of the *Q-V* (or equivalently the *C-V*) curve (172) in a manner which can be incorporated in the model. If there are intermediate states of an area motor, the computed probability distributions are experimentally indistinguishable from a two-state motor (305).

B. Biophysical Considerations

The underlying rate of lengthening and of the charge movement of OHC motility is weakly temperature dependent (16). The kinetics of the charge movement has a temperature Q_{10} of ~1.5 both in membrane patches (109) and in whole cell recording (294), pointing to a relatively simple underlying physical mechanism. The low value (less by a factor of 2–3 of any process involving a second messenger system) is helpful experimentally as it implies that experiments performed at room temperature are a reasonable indicator of kinetics at 37°C. The voltage dependence of the *Q-V* curve shifts negatively by 19.2 mV/10°C, however (294, 298), and this suggests that the magnitude of V_o is underestimated by measurements made on isolated OHCs at room temperature. There are also slow changes of length that are temperature sensitive. The static length of a cell increases with temperature (116) by 0.22 $\mu m/^0C$ and suggests that the shape itself may also be controlled by cytoplasmic reactions, such as the phosphorylation state of the motor proteins (67).

The speed of the motor constrains the underlying biophysics of coupling membrane voltage and the charge movement. Although ion channels also exhibit a gating charge, the kinetics of such charge movements are often characterized by several components, which barely approach the microsecond range (310). The charge displacements seen in ion channels are thus still insufficiently fast to explain motions of the molecule that can be shown to undergo cyclic behavior at frequencies of 80 kHz (100). At these frequencies, the comparable relaxation time constant would be $\tau = 1/(2\pi \times 80\ \text{kHz}) = 2\ \mu s$, or nearly an order of magnitude faster than found for ion channels.

Another class of membrane protein capable, in principle, of operating at high rates are membrane transporters. A number of transporters exhibit gating charge movements; charge translocation has often been used as an electrophysiological fingerprint of their activity. Such transporters include ion translocating proteins (110, 231). For example, the classical sodium pump, an Na^+-K^+-ATPase, exhibits a transient current on a rapid change of membrane potential. It has been argued that this is a consequence of sodium ion transfer across a fraction of the membrane potential field (106, 231, 284). The movement of a small ion through 3–4 nm of the protein within an electric field takes nanoseconds if the ion is freely diffusing. The transit can be observed electrophysiologically using the wide bandwidth afforded by recording in macropatches (138). The resulting time constant for this process is on a submicrosecond time scale.

We have seen above that the OHC motor can be stimulated to move at frequencies in excess of 50 kHz (56, 57, 100), and charge movement in the membrane can be measured at frequencies in excess of 30 kHz (73, 109). On the basis of such observations, the motor charge in OHCs shares properties with charge translocation in transport proteins.

C. The Candidate Motor Molecule: Prestin (SLC26A5)

The search for the molecular basis of electromotility occupied several laboratories for the best part of a decade until the problem was neatly solved in 2000. With hindsight, a very obvious strategy for identifying the protein was used by Dallos and co-workers (355), but however a strategy which depended on the refinement of molecular biological techniques developed only during the 1990s. Separate cDNA libraries were constructed for IHCs and for OHCs separated from microdissected gerbil cochleas. The cells are readily distinguishable on a microscope stage. From these, a subtracted library was constructed for genes expressed preferentially in OHCs. Fifteen distinct gene clones were identified. Of these, one corresponded to an ORF of a protein containing 744 amino acids with molecular mass of 81.4 kDa. It was highly expressed in cochlear tissue.

The protein was named "prestin" because it was able to confer on cells the ability to move *presto* (fast in Italian). The prestin protein can be expressed in heterologous systems. Expressed in TSA201 cells (a T antigen expressing human embryonic kidney cell line), prestin produced cells that exhibited both a nonlinear capacitance and electromotility (355). The raw data show that the nonlinear capacitance is not as large as in native hair cells, although it is otherwise similar in voltage dependence. The transfected, but not untransfected, cells behaved like electromotile OHCs when the cells were elongated by sucking them up into a microchamber. Although the motility was only measured with a photodiode at 200 Hz, the data left little doubt that the identified protein prestin could underlie the high-frequency OHC electromotility. The motility in the expression system could be blocked by application of 10 mM salicylate, one of the few

known blockers of OHC motility (71, 309, 332). Although not shown in the original paper, subsequent antibody generation showed that prestin is expressed along the basolateral membrane of OHCs but not on the apical membrane (3, 343) as well as, surprisingly, in the cells of the vestibular system.

D. Prestin Knockout Mice and the Cochlear Amplifier

A mouse in which the prestin gene has been partially deleted has been created (199). The deletion was not complete but removed exons 3–7, which encode 245 amino acids of the NH_2-terminal (one-third of the protein). Homozygous mutant mice show a loss of OHC electromotility in vitro and a 40- to 60-dB loss of cochlear sensitivity in vivo measured by using the auditory brain stem responses (ABR) and distortion product emissions (DPOAE). The cochlear microphonic is relatively unimpaired in these mice, indicating that mechanoelectrical transduction in OHCs is not significantly affected. In heterozygote mice, there was a slight reduction in OHC motility and only a modest 6-dB increase in cochlear thresholds. In comparison, the homozygotes had a uniform 40- to 60-dB hearing loss across all frequencies, compatible with loss of cochlear amplification. The OHCs in prestin knockout mice were also ~15% shorter than their wild-type littermates. The conclusion of Liberman et al. (199) is that there is no need to invoke additional active processes, other than somatic motility (electromotility), to explain cochlear sensitivity in the mammalian cochlea.

Cheatham et al. (47) have pointed out that the reduction in OHC motility in heterozygotes should have produced a much larger reduction of cochlear sensitivity as the process of amplification is highly nonlinear. Indeed, most cochlear models would suggest that there should be large (>20 dB) threshold shifts. Nevertheless, a careful comparison of both cellular and in vivo measures of OHC performance between wild-type mice and those with careful selection for one copy of the prestin gene found no significant differences. With the use of real-time RT-PCR to measure transcript level, it was found that although there was less prestin mRNA in the heterozygotes, there was thus evidence for autoregulation of prestin protein levels in the OHCs of such mice so that deleterious effects on auditory peripheral function were minimized. In humans, there is late-onset deafness arising from mutations at the prestin gene locus (201); in heterozygote mice, there is no apparent haplo-insufficiency. This transgenic line of mice shows the importance of working at sound pressure levels low enough to involve OHC operation. Surprisingly, the prestin knockout animals exhibited DPOAEs at high SPLs indistinguishable from those of the wild type (200), indicating that although the cochlear amplifier is critical for an explanation of responses at low sound levels, there are residual nonlinearities in the mechanics of the system. These findings indicate that even physical models of the cochlea must be constructed with care to incorporate structural nonlinearities.

Noise exposure that produces deafness has been shown to affect the levels of prestin expression in rats (48). Intense levels of sound (110 dB SPL for 4 h) produced a hair cell loss at the base of the cochlea. The cochlear microphonic recovered after 7 days, indicating that the more apical regions of the cochlea were not so profoundly affected. However, the study reports that prestin gene expression levels, measured by real-time PCR, increased and peaked 3 days after exposure and provides some evidence for continuous turnover of prestin protein in the cochlea, although it is not known whether this is occurring in OHCs.

E. Genetics of Prestin

Prestin is member number A5 of a superfamily SLC26 of integral membrane proteins (203) (see Fig. 4). Identified from a genome-wide search, the SLC26 family is characterized by a sulfate transport motif in the amino acid sequence. The motif is a characteristic of the defining member SLC26A1 of the family. The SLC26 family is broadly described as a family of anion-bicarbonate transporters, each of which has specific tissue expression (225). The family now contains 10 vertebrate members, but homologs are found across many phyla including organisms as distant as yeast, plants, and most invertebrates.

Four mutations of prestin, SLC26A5, have been identified in human populations. Four splicing isoforms of the human SLC26A5 gene are known and designated SLC26A5A through -D (202). The human SLC26A5 gene contains 21 exons. Genes for SLC26A5B through -D all share the same terminal 3′-exon, but differ in their intervening cDNA sequences. SLC26A5A and -B share the majority of the sequence and differ only at the terminal 3′-exon. The gene is localized on chromosome 7 at position 7q22.1. At least two complete families are currently known with a hereditary hearing loss due to mutations in prestin. The mutation is recessive and has been identified to occur at the intron 2/exon 3 boundary.

Significant disease pathologies arise from mutations in the gene mutations of other members of the SLC26 family. The majority of disease mutations are mutations in the hydrophobic regions, but about one-third arise from mutations in the COOH-terminal end, producing faulty targeting or retention in intracellular sites. Even though prestin is the only member of the family associated with fast charge movements, other members of the SLC26

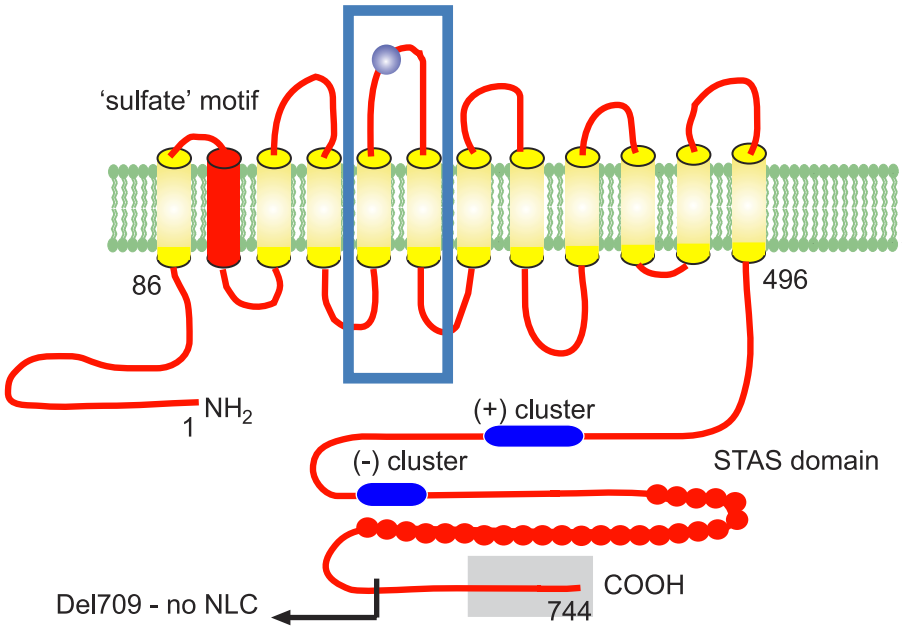

FIG. 4. A schematic representation of prestin (SLC26A5) shown with 12 transmembrane (TM) α-helical regions. TM2 contains the sulfate motif defining the family. The long COOH-terminal region from amino acids 496 to 744 contains runs of both positive and negative charges as well as a sequence defined as a STAS domain. The box surrounding TM5–6 and including a phosphorylation site shown as a distinct element highlights the region where Refs. 67 and 234 suggest there may be alternative structures, reducing prestin from a 12 α-helix to a 10 α-helix structure.

family, especially SLC26A6 and SLC26A9 (225), have yet to be fully investigated with the biophysical attention devoted to prestin.

Prestin is highly conserved between many species. It has been described in detail in several other organisms and appears to be associated with hearing organs (335). Sequence comparison shows SLC26 proteins in zebrafish, eel, mosquitoes, and flies. The fly and zebrafish homologs were clearly expressed in auditory organs by in situ hybridization and, in the case of the mosquito, by using riboprobes directed against rat prestin. There, the homolog of prestin is found in the chordotonal organ, a structure responsible for hearing found in some insects. Hence, prestin-related SLC26 proteins are seen to be widespread. It is clear that the prestin homologs are not necessarily associated with motility. It seems that although expressed with sound detection mechanisms, its presence is likely to be associated with other functions.

F. Prestin as an Incomplete Transporter

The simplest explanation for the charge movement is that it arises from chloride anions moving part way through the membrane in a cytoplasmic pore formed by prestin (see Fig. 5). The critical experiments were carried out by Oliver and co-workers (251, 253). There are no obvious regions of the prestin sequence corresponding to a voltage sensor of the type found in voltage-gated ion channels. Instead, specific charged amino acids are critical. On mutating a number of residues on the external and cytoplasmic surfaces of the prestin molecule, Oliver et al. (251) found alterations in the parameters of the *Q-V* curve (strictly the *C-V* curve) of rat prestin in CHO cells (251). Large negative shifts of up to 80 mV could be achieved by mutating several charged locations associated with the hydrophobic portion of the molecule to neutral residues (for example, the mutation D154N, changing an aspartate to a neutral asparagine, causes the largest shift; a positive shift of V_0 from −72 mV to +14 mV could be obtained by the mutation D342Q). However, mutating clusters of charged residues on the COOH-terminal end did not produce a shift of the *Q-V* curve, suggesting that the protein COOH-terminal region does not contribute to the potential field in or around the protein.

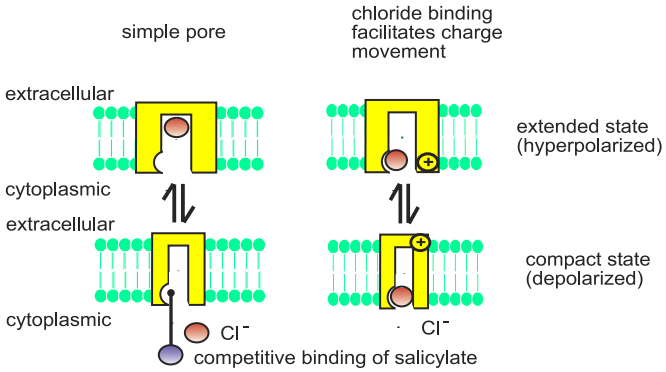

FIG. 5. Two simple models for prestin as an area motor (59, 251). *Left*: intracellular chloride (red) can be driven by the membrane potential field into a cytoplasm-facing pore, and its binding to a site within the molecule leads to lateral change in shape. There may be a cytoplasmic binding site for salicylate, serving as a competitive inhibitor of chloride binding. The data are also consistent with a model (*right*) where there is an intrinsic charge movement allosterically linked to chloride binding. The kinetics of charge movement would be limited in these models by the diffusion time for the ion transit and/or the conformational kinetics of the protein.

In experiments where cells were dialyzed with different intracellular anions, and in patches pulled from rat OHCs, the NLC was abolished by removal of cytoplasmic chloride (251). The results provide strong support for the proposal that charge movement arises from rapid movement of chloride ions into a pore region of the molecule under the influence of potential. Because there is no sustained current, the process has been described as transport where the cycle is "incomplete." This means that the transporter does not complete the full cycle, returning to its initial state, but remains at an equilibrium state determined by the membrane potential.

Reducing the chloride concentration on the intracellular surface shifts the peak of the NLC to more positive values. A number of anions, including bicarbonate and alkali halides, substitute for Cl^- (251). The shape of the *C-V* curve is consistent with an anion penetrating about 0.8 of the way through the membrane field. A smaller value for the valence z is found for larger monovalents: $\beta = ze/k_BT$ varies from 1/35 mV^{-1} (or $ze = 0.74$) to 1/65 mV^{-1} ($z = 0.4$) for butyrate.

There are some inconsistencies in a simple pore model of prestin. Reducing the internal chloride reduces the peak charge moved (89), an effect which requires more elaborate models, to be described below (227). In addition, replacing intracellular chloride with sulfate is reported to have little effect on β (283), although a divalent anion would be expected to produce a different z. These latter experiments also reported a large shift in V_0. The experiments in Reference 251 describe a voltage dependence of the NLC that was insensitive to external chloride. In the special case where the intracellular Cl^- is kept below 1 mM, using intracellular Tris sulfate, the NLC can depend on external Cl^-, and lowering the external chloride increases V_0 of the *C-V* curve to move to still further positive values (283).

G. Structure of Prestin

The structure of the prestin protein was not fully defined in the original report (355). There is currently still not an agreed structure, and it has not been ascertained whether there really is a pore. In part, this situation reflects the current lack of information about many integral membrane proteins, and so far, no member of the SLC26 family has been crystallized for structure determination. The hydropathy plot for prestin indicates a protein with a hydrophobic region extending over ~450 amino acids, similar to many transporters of the major facilitator superfamily. It has a relatively short NH_2-terminal region and an extended COOH-terminal end. Prestin has a hydropathy plot similar to that of pendrin, another member of the SLC26 family also expressed in cochlear tissue (203). It is certainly agreed that an even number of helices span the membrane as both NH_2-terminal and COOH-terminal ends lie within the cytoplasm, established experimentally by tagging the ends and expressing the protein in heterologous systems (207, 354). In the original report, Zheng et al. (355) did not commit themselves to a definite structure and, depending on the algorithm used, computer modeling gives ambiguous numbers of transmembrane α-helices. Subsequent reports have been more definite and identified 12 transmembrane α-helices (251), 10 alpha-helices inserting across the membrane with 2 nonspanning helices present in the set of helices (67) or 10 helices transmembrane helices alone (234). The quaternary structure awaits much firmer and decisive experimental evidence.

H. Function of the Hydrophobic Core of Prestin

Some clues about other properties of prestin have yielded to bioinformatic approaches. Prestin is member number A5 of the family of SLC26 anion-bicarbonate transporter proteins and highly conserved between species (203). Nevertheless, unlike prestin (SLC26A5), the most closely related homolog, SLC26A6, does not exhibit a charge displacement phenotype (251). In what follows, we shall be citing amino acid positions from mouse prestin, but the amino acid homology with other species is high and in some cases approaches 100%.

The hydrophobic core of prestin shares considerable homology with other member of the SLC26 family and also contains a sulfate transport domain motif, a common motif shared by all members of the family between amino acids (aa) 109–130. The whole hydrophobic region, and the one therefore likely to be within the membrane, lies between aa 100 and 550. Two proposed *N*-glycosylation sites of prestin are proposed to be on the extracellular surface: N163 and N166 do not affect membrane targeting, but it is reported that deglycosylation shifts the measured *C-V* curve to more depolarized values (220). These glycosylation sites may be the same as those identified by the binding of fluorescently conjugated wheat germ agglutinin (WGA) to the external coat of hair cells, indicative of sialic acid or *N*-acetyl-D-glucosamine on the extracellular surface of cochlear hair cell plasma membranes, but the labeling is consistent with the normal distribution of these glycoconjugates in the cell coat (114). The same report also showed that with *Helix pomatia* agglutinin (HPA) binds inside the plasma membrane of OHCs and implies the presence of glycoconjugates with terminal *N*-acetyl-D-galactosamines inconsistent with distribution of glycoproteins on the internal membrane systems of OHCs. This early result and the later observation (234) are therefore consistent.

Lack of structural information leaves it unclear which subsequences of prestin are critical for the

charge movement and for any structural changes it undergoes when the charge moves. Among the numbers of recent attempts to identify critical regions of the prestin protein, a combination of bioinformatic methods, to identify candidate regions, and mutagenesis studies seem to be promising (260). Mutations of amino acids near the "sulfate transporter motif" of gerbil prestin, particularly in transmembrane helices 1 and 2, produced significant alteration of its expression in the membrane or behavior in a potential field. Mutations in this part of the protein suggest that this region or its packing may be critical for prestin function. The comparative approach, identifying functional differences between prestins from widely different species, also point to critical evolutionary changes in sulfate transport, although these cannot at the moment be identified with changes in molecular motifs. Thus both zebrafish prestin and chick prestin when expressed in CHO cells act as electrogenic sulfate transporters (1:1 exchange of SO_4^{2-} for Cl^-) (303). On the other hand, zebrafish prestin does not generate motile responses in expression systems, but it does have a charge movement. This prestin homolog shows a weaker voltage dependence ($\beta = 1/54$ mV^{-1}) in the NLC, suggesting that the structure differs. The NLC of zebrafish prestin is also displaced to very positive potentials ($V_0 = +95$ mV) and, when transient currents are measured for the *Q-V* curve, the relaxation kinetics are slower (4).

I. Function of the Terminal Ends of Prestin

The COOH-terminal region contains two prominent charge clusters, a positive cluster between aa 557–580 and a negative cluster between aa 596–613. Mutagenesis of these blocks of residues does not interfere with the measurement of a charge movement, although it may change the voltage and magnitude of the charge (19), and therefore, it might be concluded that these regions of the prestin protein lie outside the membrane electric field. A STAS (sulfate transport anti-sigma factor antagonist) domain is also identifiable in the COOH-terminal segment of the protein between aa 635–705. These domains, widely described in plant systems, may contribute to the catalytic, biosynthetic, or regulatory aspects of anion transporters in both animal and plant systems (7). The STAS domain of many SLC26 transporters (but not so far including prestin) activates the cystic fibrosis transmembrane receptor (CFTR) by a protein kinase A (PKA)-dependent binding to the CFTR R domain (189).

As with other membrane proteins, nearly the full length of the COOH-terminal end of prestin is necessary for correct targeting of prestin to the membrane (353) but is not sufficient (260). Deleting the terminal end below aa 719 leads to a partial or complete failure of the protein to insert into the membrane; instead, the protein is retained in the Golgi apparatus or in the cytoplasm. Deleting the terminal end at or below aa 709 fails to produce any measurable nonlinear capacitance. A similar result is reported by another group (234). In both of these studies the absence of a charge transfer is reported; work on the zebrafish prestin should alert researchers that a slowed kinetics of charge transfer as a result of the mutation could be missed because of the way that the *C-V* curves are conventionally measured (4). Zheng et al. (353) also reported that the chimeric COOH-terminal construct, made by replacing part or all of the COOH terminus with the analogous COOH-terminal ends from pendrin (SLC26A4) or PAT1 (SLC26A6), also fails to produce expression of prestin for there is no NLC. With different COOH-terminal lengths, these chimeric proteins also showed altered cellular distribution.

The NH_2-terminal region of prestin contains the first 95 amino acids before the α-helix; the precise number depends on the overall predicted topology. For example, by constraining the structure prediction to 10 transmembrane regions, a shorter NH_2-terminal complex is obtained (234). Deletion of more than the first 20 amino acids from the NH_2-terminal end of prestin abolishes NLC, although it is reported that the reason is that construct does not reach the plasma membrane.

J. A Model for Prestin

Although the properties of prestin as an area motor can be captured by stochastic models (60, 155, 157), some information can be obtained by considering prestin as an anion antiporter (227) (see Fig. 6). A simple pore facing the cytoplasm into which Cl^- anions can be driven does not lead, as found (89), to an NLC which becomes smaller as the cytoplasmic Cl^- is reduced. A simple pore reproduces the observed displacements of the *C-V* curve (a situation which applies to the charge movement in sodium pump, Ref. 106) but not the concentration dependence. To reproduce the experimental data, prestin has to be modeled as a transporter in which there is a voltage-dependent access (and associated conformational change) to the anion binding site within the membrane electric field; the rates need to be chosen to match its "incomplete" transporter status. Consistent with its membership of the SLC26 family, the transporter can be represented as a SO_4^{2-}/Cl^- electrogenic exchanger. The model suggests that there needs to be further internal charge movements that contribute to the NLC. Experimental investigation suggests that mammalian prestin does not readily transport SO_4^{2-}, even though nonmammalian prestins act as 1:1 SO_4^{2-}/Cl^- electrogenic transporters (303). Refinement of this class of model is still required.

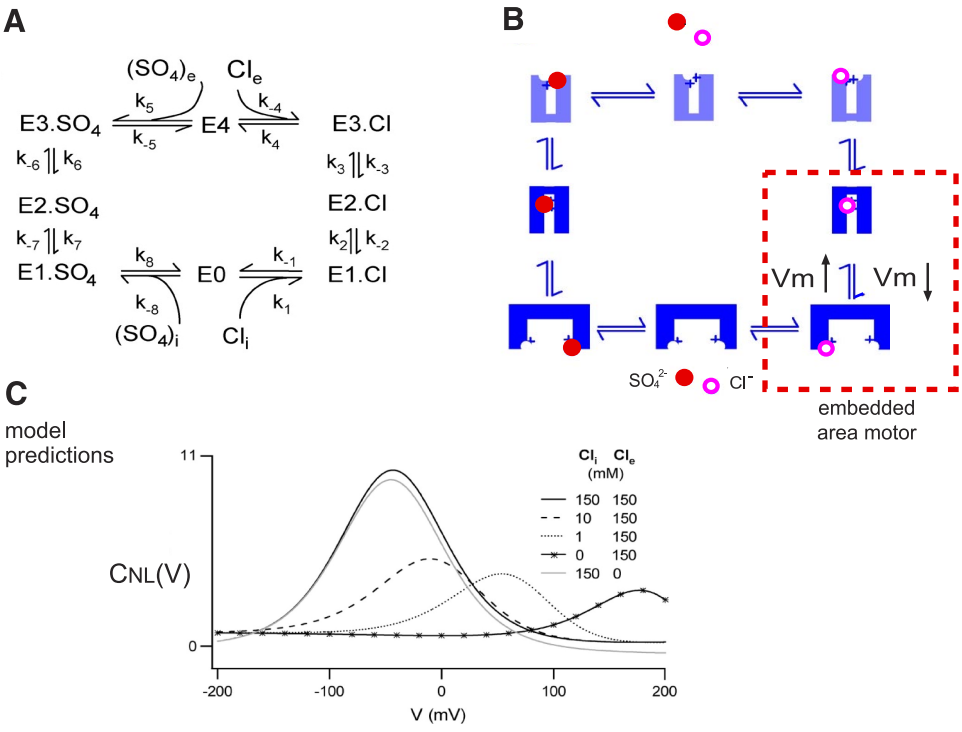

FIG. 6. Prestin as an anion transporter. *A*: the state diagram for a transporter acting as a chloride-sulfate antiporter. The kinetic parameters, k_i, are chosen subject to experimental and physical constraints (227). *B*: diagram of the physical representation of the states showing an assignment of the extended and compact forms of the states. This model also contains fixed charge movements of the protein so that depolarization of the membrane is not associated with a movement of Cl^- into the pore. *C*: the predicted capacitance (*C*)-voltage (*V*) curve of the model shows a reasonable agreement with the experimental data. It shows the experimental finding that the peak capacitance is reduced as the intracellular Cl^- is reduced. [Redrawn from Muallem and Ashmore (227).]

V. SPECIALIZED PROPERTIES OF THE OUTER HAIR CELL BASOLATERAL MEMBRANE

The lateral membranes of cochlear hair cells determine the membrane potential of the cells. Current entering the cell through the mechanotransducer channels in the apical membrane will always tend to depolarize the cell as the channel acts as a pathway for current entry from scala media, a compartment with a potential of +80 mV. The dominant ion channels of the basolateral membrane are K^+ channels. The properties of these and other channels maintain a predominantly negative potential inside the cell. The question of whether the specialized region of the OHC membrane containing prestin contains other integral membrane proteins is not completely resolved.

A. Density of the Motor Protein

The lateral membrane of OHCs has a complex structure where the motor molecule is inserted at high density in a membrane which is supported by attachment structures to the underlying cytoskeletal meshwork. The high packing of the motor structure in this membrane makes this membrane a useful test site in which to study a high-density transport array.

Considerable attention has been devoted to the relation between the particle density and the density of mobile charge measured electrophysiologically in OHCs. Early estimates of particle density vary between 3,000 μm^{-2} (174) and 6,000 μm^{-2} (99). There is a reported difference between the particle density in OHCs from either end of the cochlea so that the density in apical (low-frequency) cochlear OHCs is 4,000 μm^{-2}, whereas it is 4,800 μm^{-2} in basal (high-frequency) cochlear OHCs. For a face-centered close packed array, the theoretical maximum density would be ~10,000 μm^{-2} and exclude all the membrane lipid. This theoretical limit is clearly not appropriate in OHCs.

The size of the particles, 8–10 nm in diameter (174), is compatible with ~40–50 transmembrane α-helix structures. Too large to be a single prestin molecule, each individual particle is thus probably a multimer of prestin. Even though there must be an additional contribution of the platinum coating as well as from glycocalyx on the surface of the plasma membrane, it seems most probable that the particle would represent a tetrameric assembly formed from the hydrophobic portions of prestin. Chemical cross-linking experiments suggest that prestin forms at least a dimer with pairs of monomers cross-linked by disulfide bonds embedded in the hydrophobic core of the molecule (352). This leaves open the possibility that the molecule assembles, for example, as a dimer of dimers into the larger particles seen by electron microscopy.

The present ultrastructural data cannot exclude the particle being a heteromer of prestin in conjunction with some other subunit. Resolution of this question is on the boundary of what can be determined by electron micros-

copy. A different technique, atomic force microscopy, which has an, in principle, resolution in biological samples on the 1-nm scale, has also been used to investigate prestin expressed in CHO cells, but the structure can only be resolved in a model-dependent way and remains unclear (228).

Electrical measurements of charge movement suggest that the apparent charge per square micron of OHC membrane can vary more significantly. The number of elementary charges per cell can be calculated from the *Q-V* or *C-V* curves as Q_{max}/ze (*Eq. 4*). The number of elementary charges calculated for an apical OHC is on the order of 10^7. If the lateral membrane of an OHC extends ~50 μm down the length of the cell, the density of charges moved would be ~6,500 μm^{-2}, within the range of particle densities. The match is not quite exact but does support the hypothesis that the charge-generating mechanism is associated with the OHC lateral particles, with 1–2 charges moved per particle. The precise relation remains to be clarified.

Nonlinear capacitance can certainly be measured in both apical and basal cells (12). The parameters of the *C-V* curves are approximately the same for both apical and basal OHCs, although the peak charge moved is greater in the longer apical cochlear OHCs. By carefully studying the nonlinear capacitance in a large sample of OHCs, the slope β (*Eq. 3*) remains approximately constant and corresponds to $z = 0.8$, although there is a slight decrease of the value in cells from the more basal cochlea (295). The ratio of nonlinear capacitance to the geometrically determined linear capacitance increased by a factor of ~3 (increasing from a ratio of 0.6 to 2) as the cell length decreased. By omitting the (estimated) membrane areas at the synaptic pole and the apical transducer site, the charge moved per square micron of motor area was estimated to be ~5,000 $e^-/\mu m^{-2}$ for apical cells (i.e., close to the particle density) but ~30,000 $e^-/\mu m^{-2}$ for basal OHCs, considerably higher than found for the particle density. This type of calculation is prone to error as the geometric corrections for cell shape are critical. Nevertheless, the result suggests that the motor at the base of the cochlea may differ from that at the apex. As pointed out in the paper, the OHC motor charge density must track the location of the cell along the length of the cochlea.

There is no reason to expect that the distribution of prestin might be functionally uniform within a single cell. In expression systems, such as in HEK cells, the lateral diffusion of GFP-labeled prestin appears, on the basis of FRAP experiments, to be considerably lower than expected for freely diffusing proteins (254). This study suggests that there may be intermolecular interactions between prestin and a lipid membrane and/or the underlying cytoskeleton, even in these cells. Indeed, prestin may be associated specifically with cholesterol-rich membrane domains (324). In OHCs, there is evidence for functional microdomains along the lateral membrane (287). One electrophysiological technique used to address this question has been "electrical amputation" in which an OHC is simultaneously sucked into a suction pipette while the membrane is recorded with a whole cell patch pipette. This technique allows partial electrical isolation of different cell regions and suggests that motor charge properties can be heterogeneous and locally differ from that of the whole cell. In principle, this result should also be measurable with cell-attached patches (108) provided that the different regions of the basal cell surface can be recorded.

B. Cochlear Development and the Motor Protein

The appearance of electromotility in the cochlea is not synchronized with the first emergence of hair cells in the organ of Corti during early embryogenesis, but occurs later during a well-defined developmental window. Hair cell mechanotransduction currents can be detected in the mouse vestibular system from embryonic day 16 (E16) onward (112, 113). Although not measured with the same developmental precision in the cochlea, a similar timing seems likely. It is worth recalling that rodents do not "hear" or exhibit complete behavioral responses to sound until 2 wk later.

By postnatal day 3 (P3) in the rat, ~300 copies of prestin mRNA can be found per OHC (123). The expression of electromotility is functionally detectable in gerbils only from P7 and reaches mature levels (i.e., with maximal length changes of 4–5%) only at P14, slightly preceding the establishment of adult hearing thresholds (131). A similar time course for the emergence of electromotility has also been reported in mouse (217) and rat (24), where the half-maximal expression levels of nonlinear capacitance occurs around P9. The full molecular description of the emergence of electromotility remains to be described. A recent quantitative RT-PCR study on the mouse suggests that the development of electromotility occurs in stages, with the insertion of protein near-complete around P10 before the final development of adult properties of nonlinear capacitance by P14 (1). The factors contributing to this second stage of maturation are not known.

The detection of electromotility in OHCs is not an all-or-none event and depends on how thresholds are set experimentally. It seems probable that the process of development of electromotility in OHCs may start quite early. There is clear evidence that lateral membrane of gerbil contains intramembrane particles (IMP, equivalent to "motor" particles) that occur at low density by P2 (317). The density increases from 2,200 IMP/μm^2 at P2 to 4,100 IMP/μm^2 at P8 but continue to increase in density until mature values are attained at P16. This observation is consistent within error with the RT-PCR observations

(1). The emergence of electromotility starts before the appearance of subsurface cisternae (which begin to appear at P8) and submembranous pillar structures, linked to the cytoskeletal lattice, first appear at P10. In the gerbil, the process of constructing a system of OHCs extends over more than 10 days, with remodeling of the organ of Corti to include the tunnel of Corti and the spaces of Nuel around the OHCs only beginning to reach their mature form from P10 (273, 318).

One puzzling feature of motor particle insertion is the parallel change of the NLC voltage dependence. The voltage dependence of the *C-V* curves changes during hair cell maturation. Using rat as the developmental model, the NLC of OHCs can be followed in both apical and basal turns of the cochlea (250). Consistent with the electron microscopy, NLC cannot be detected at P0 in the basal turn of rat, although a small value, ~1% of the mature value, can be detected in the apical OHCs, possibly indicative of a cochlear gradient in the development of the hair cell membrane. A steep increase in the NLC is reported between P6 and P11, consistent with electromotility and IMP measurements, with a final steady state being reached at around P12. However, at early developmental stages, the V_0, the peak of the *C-V* curve, is initially found near −90 mV and progressively moves to the reported adult values (about −40 mV) at maturity. Since this shift in the NLC peak was abolished during wash out of excised patches, it must be concluded that there is as yet an unidentified modulating factor of the lateral membrane motor during OHC development.

C. Water Transport

OHCs change length slowly when the external solution is changed to one containing elevated external K (345). The time scale (seconds to minutes) has caused this phenomenon to be called "slow motility." It is observed independently of external calcium, calcium entry, and any additional K^+ permeability induced by the K^+ ionophore valinomycin. The phenomenon appears to be a consequence of water entry as a result of sustained depolarization by potassium (77, 79).

Water entry has been studied directly by exposing the cells to changes of external osmotic pressures. The first direct measurements of water permeability showed that the permeability was compatible with water transport through a lipid bilayer (264). The value obtained for the hydraulic conductivity (P_f) was $\sim 10^{-4}$ cm/s. This value is low compared with values reported for different lipid bilayers and two orders of magnitude lower than the hydraulic conductivity of red blood cells. A more mathematical and detailed analysis of water flow through specific ultrastructural elements of the OHC may account for the low values (262).

Similar experiments have been carried out in both guinea pig OHCs and neonatal rat OHCs where values for P_f are reported to be slightly higher (25, 43). The water volume flow through an adult OHC can be estimated to be $\sim 10^{-2}$ cm^2/s, a value within the range estimated for flow due to aquaporin channels. An anti-peptide antibody specific for aquaporins labels the lateral plasma membrane of the OHC. The flow is blocked by Hg^{2+}, which is compatible with the presence of some aquaporin channel types. In neonatal rat OHCs, a lower value of 10^{-3} cm^2/s was found, although this increases between postnatal days 8 and 12 to values closer to those found in adult OHCs. Thus early in OHC maturity, values for P_f are at least five times smaller. However, the water flux into the OHC is dependent on membrane potential (25, 111) so that if permeability is measured in depolarized cells, low values for P_f are found. There thus seems to be an intimate relationship between electromotility mechanisms and water transport.

D. Sugar Transport

An immunohistochemical study indicates that antibodies raised against the sugar transporter GLUT5 also label components of the basolateral membrane of gerbil OHCs (232). GLUT5 contains 551 aa and a hydrophobic region that is predicted to contain 12 transmembrane α-helices (122). It is specifically a fructose rather than a glucose transporter. To test for the presence of this protein in isolated cells OHCs, glucose in the external solution was isosmotically replaced with fructose. OHCs reversibly shortened, compatible with the proposal that water was moving into the cells along with transported fructose (15, 111). The uptake was compatible with transport with a Michaelis constant K_m of 16 mM and comparable to that found for the fructose transporter GLUT5 in other systems. The uptake of fructose also shifted the voltage dependence of the nonlinear capacitance. Although these studies pointed to the involvement of a GLUT5 epitope in the immunohistochemistry, the evidence is not conclusive.

The discovery of prestin relegates the strict requirement of a sugar transporter in OHCs to a position of somewhat academic interest. Nevertheless, heterologously expressed prestin also transports fructose (43). The effect can be demonstrated by showing that cells presented with solutions where the glucose has been replaced isosmotically with fructose, like OHCs, swell with a K_m of 24 mM, close to that found in OHCs. The transport rates for the whole cell that can be inferred are smaller than in OHCs, which is likely to reflect the lower copy numbers in the cell line. The calculated uptake of water is 175 molecules water per fructose transported. Similar water transport values for "water pumps" have been described for the Na-glucose

cotransporter SGLT1 (205). In that case, 200 water molecules are transported per glucose. The transport of fructose (and water) is a property also shared by pendrin (SLC26A4) and possibly other members of the SLC26 family. Surprisingly, GLUT5 protein associates with prestin protein in expression systems when assayed with an imaging techniques (341). This suggests that that these two proteins can heteromerize, as the similarity of their common hydropathy plots hint. Nevertheless, the fructose transport pathway in expressed prestin remains unknown. It might be mediated either by the monomeric form, as suggested for the sugar transporters, or by a pore formed by a multimeric configuration of prestin, or by the presence of an additional cofactor, as yet unidentified.

E. Chloride Transport and Permeability

The lateral membrane of OHCs exhibits some permeability to chloride. Although members of the ClC chloride channel family have been identified by RT-PCR in OHCs (179, 180), the direct functional observation of chloride permeation in the lateral membrane has proven to be more complex. The intracellular dependence of the motor on the anion Cl^- and the membership of the prestin to the anion-bicarbonate transporter family SLC26 makes chloride permeation through the lateral membrane a distinct possibility. Several laboratories have described methods to reduce swelling of cochlear tissue, and particularly of the sensory cells, by replacing chloride in the medium with an impermeant anion, such as lactobionate (30, 82), suggesting that chloride is a permeant anion in OHCs.

On the basis of single channel-like recording from the lateral membrane, it had been suggested that the OHC membrane contains a chloride conductance (118). An early (42) identified chloride movement across OHC membranes by exposing OHCs to low external chloride with HEPES as the buffer. This produced an initial shortening, which was rapidly followed by an increase in length. Continued exposure to Cl^--free saline produced a reversible extension to a maximal length where the cell volume was effectively zero. The phenomenon was interpreted as due to co-movement of K^+ and Cl^-. The biphasic length change is difficult to explain, although chloride (and water) leaving a cylindrical cell would account for the length increase.

Imaging methods can also be used to show that OHCs are chloride permeable. A Cl^--sensitive dye MQAE has been used to show that exposure of OHCs to low external chloride reduces intracellular Cl^- (316). In its role as a chloride ionophore, the organometallic and ototoxic compound tributyltin (TBT) has been used to control intracellular chloride levels. Use of nanomolar quantities of TBT allows intra- and extracellular levels of chloride to be equilibrated in isolated cells and therefore is a powerful method of probing the intracellular dependence of the motor on anions. The effect of TBT in the intact cochlea has now been investigated while measuring the motion of the BM in vivo (300). Cochlear infusion of 50 μM TBT reversibly reduced the peak BM velocity at the 16-kHz point by ~40%. It is reported that in preparations where the response had already been reduced by 1 mM salicylate or by operative surgery, TBT, instead, increased the response. The response of the cochlea to alterations of the anion homeostasis is thus complex.

In experiments where intracellular chloride is reduced below 1 mM in isolated cells using Tris sulfate as the internal media, iontophoretic reapplication of high chloride concentrations along the lateral surface of the cells allows an (outward) chloride current to be mapped along the length of the basolateral membrane coextensive with the distribution of prestin (283). The study also showed that that conventional channels were not responsible for the observed results and suggested that an anion-permeable stretch-activated channel, with a conductance termed G_{metL}, may modulate the behavior of prestin (298). Paradoxically, niflumic acid, a chloride channel blocker, increased rather than decreased the whole cell anion current. Although there are consequences for models of OHC action in the cochlea of stretch-activated channels (see below), there remain unresolved questions in the detail in this proposal.

F. Bicarbonate Transport

Early measurements of intracellular pH (pH_i) with fluorescent dyes such as BCECF showed that pH_i is regulated in OHCs (154). These measurements suggested that the pH_i in cells is regulated by a chloride/bicarbonate exchanger. The proposal that a bicarbonate/chloride exchanger was present was at the time difficult to maintain but receives some support if prestin is indeed an exchanger like other members of the SLC26 family and is operating as a regulator of pH_i. Bicarbonate acts as a substitute for the chloride anion at the intracellular surface of the prestin where it has a binding site with an equilibrium constant K_m of 44 mM (251). In addition, OHCs contain substantial quantities of carbonic anhydrase, suggesting that bicarbonate buffering is probably critical for cell function (146, 152, 249).

G. Potassium Channels

There is clear evidence that the basolateral membrane of OHCs contains several different types of K channel. These channels serve as the exit pathway for K^+ entering through the apical transducer channel. As in many hearing organs, the distribution of K channels in OHCs changes with the position of the cell in the organ. A

full discussion is outside the scope of this review, but K channels deserve mention as they localize differentially with prestin. The evidence for distinct channels is derived both from whole cell recording and from single-channel recordings (e.g., Ref. 333) derived from cell-attached patches from the lateral membrane. The channels described in OHCs include the large-conductance BK channel (17, 117, 240), an SK channel, the final target of the action of the cholinergic efferent system (252), and an inward rectifier channel expressed transiently in some species (216).

One type of K^+ channel active at resting membrane potentials (between −70 and −60 mV) is likely to be the main determinant of the OHC resting potential. It provides the pathway for the K^+ efflux from the cell. It is named I_{Kn} (144). I_{Kn} arises from the voltage-gated potassium channel KCNQ4 (Kv7.4), although its subunit structure has yet to be clarified. The KCNQ4 channel is mutated in the nonsyndromic deafness gene locus DFNA2 (195) but differs from I_{Kn} in having a different and more positive activation range. This observation suggests that there may be extra subunits coassembling with the K channel in the hair cells (44). The analysis in isolated OHCs is complicated by the differential hair cell K channels distributions along the cochlea (212, 213).

Within a single OHC, the K channels reside mainly at the synaptic pole (186, 336). By puffing on barium as a K^+ channel blocker, it can be shown functionally that a potassium permeability is localized predominantly at the basal pole (230). The method is not refined enough to provide a high degree of localization or to rule out currents along the lateral membrane. Another method, "electrical amputation" gives an electrical rather than a pharmacological demonstration of the same phenomenon. In this method, an OHC is sucked up to varying extents into a "microchamber" while being recorded under whole cell clamp (147). This method also suggests that the K^+ conductance is predominantly at the basal pole of the cell in mature OHCs. Gigaseals can be formed between the lateral membrane and a recording pipette (108, 109) and, while showing that single patches of lateral membrane move under the influence of membrane potential and exhibit a gating charge, there has been no report of a significant potassium current colocalizing with prestin in the lateral membrane in adult cells.

In neonatal mouse cells between P0 and P7, the entire basolateral membrane is immunopositive for the potassium channel KCNQ4 (186, 336). As the cell matures, the localization of the epitope moves progressively to the basal pole of the cell, while the lateral plasma membrane densely fills with the motor molecule. The adult distribution at the synaptic pole is only achieved at P14. In the period P7–P14, prestin and KCNQ4 segregate to different regions of the lateral membrane (336). Both the prestin and the Kcnq4 genes are part of a concerted program orchestrated by the thyroid hormone triiodothyronine (T_3) acting through the receptors TRβ and TRα1, respectively (340). The resolution of immunohistochemistry is not sufficiently sensitive to show whether there is a residual K channel distribution in the adult lateral OHC membrane, but two types of experiment show that if there is K^+ channel distribution there it is small. Localization of the ion channels using electrophysiological means has not as yet been described in developing hair cells.

H. Nonspecific Cation and Stretch-Activated Channels

As well as the localization of potassium currents at the basal pole of the OHC and a possible anion permeability of the lateral membrane, the presence of nonspecific cation channels in the lateral membrane has been suggested in several reports. The current-voltage curve of OHCs (but not IHCs) is dominated by a large leak conductance that may contribute by the difficulty of recording from the small hair cells in the basal turn of the cochlea (144). Whether such leak conductances arise from calcium loading of the cell is unresolved. Cationic calcium-activated channels have been reported by single-channel recording (333). These channels exhibited a low permeability to Ca^{2+}, to Ba^{2+}, and to *N*-methyl-D-glucamine. The measured permeability ratio of $P_{Na}/P_{Cl} = 18$ suggests that these channels were not chloride channels, although they were partially blocked by flufenamic acid (100 μM) and by 3′,5′-dichlorodiphenylamine-2-carboxylic acid (DCDPC, 10 μM). A similar conclusion was reached in whole cell recording (162). There have been reports of stretch-activated channels in patches of the lateral membrane of OHCs (72) with a unit conductance of 150 pS. Such channels are proposed to underlie stretch-induced whole cell currents that lead to cell hyperpolarization (160). These channels have been hard to record. In particular, the selectivity of the stretch-activated channel has not been fully described, although the initial report (72) suggested that it was K selective.

As we have seen above, it reported that OHCs contain a stretch-activated anion channel intimately related to OHC motility (283, 298) but in this case from whole cell recording experiments only. The conducting channel, termed G_{metL}, has been described as being anion permeant and possibly providing part of the motor unit, regulating the chloride anion environment of prestin. The channel is reported to have a nonlinear temperature dependence, with Q_{10} increasing to 4 above 34°C from a value of 1.5 when measured experimentally at room temperature. It is not clear whether this conductance is an unidentified molecular entity, a channel already described elsewhere but with unidentified mechanical sensitivity, or a functional feature of prestin.

A single report identified a 16-pS cyclic nucleotide-activated channel in patches pulled from the lateral OHC membrane. The channel was reversibly blocked by millimolar Ca^{2+} or Mg^{2+} and L-*cis*-diltiazem. (190). Although similar to the olfactory cell cyclic nucleotide-gated channel, it was not activated by intracellular cGMP as found in photoreceptors but by cAMP. Whether this cAMP-activated channel is a cation-selective channel needs to be reviewed in the light of later evidence which showed that some OHC currents, mainly K currents, were activated by PKA (163, 164). The identity of the role and identity of ion channels in the basolateral membrane is still not well understood and deserves further attention.

VI. OTHER FORMS OF OUTER HAIR CELL MOTILITY

A. Slow Length Changes in OHCs

A distinction is often made in the literature between fast and slow motility of OHCs. Fast motility described above is associated with membrane polarization. Slow motility, on the other hand, is also characterized by shape changes of the cells (sometimes in excess of 20% of the resting length) which take seconds to occur. It can be induced by mechanical stimuli (such as changes of the osmotic strength of the solution) or by chemical stimuli, such as potassium concentration changes. The distinction between slow and fast motility, the latter tacitly assumed to be electromotility, is not completely satisfactory as the dividing time scale is not explicit. Since extracellular K^+ also depolarizes the membrane, there has at times been confusion between electromotility and slow motility: the mechanisms are however different.

A more recent helpful distinction between these forms of cell shape change is that OHC motility should be categorized as either *prestin-dependent* or *prestin-independent* (222) (see Fig. 7). In prestin-dependent motility, a defining characteristic is that the length change occurs at constant volume. In this case, the change in length will necessarily be accompanied by a cross-sectional area reduction. Electromotility in OHCs can thus be defined by a shape change that occurs as a result only in membrane area change with no change in volume (Fig. 7). In prestin-independent motility, the volume is not so constrained.

This idea has been extended by making specific measurements of volume V, length L, and longitudinal cross-sectional area A (i.e., the area section along the axis of the cell) (222). The volume of a cylindrical cell of diameter D is given by $V = \pi D^2 L/4$. Hence, taking derivatives one easily finds (since $A = DL$) that

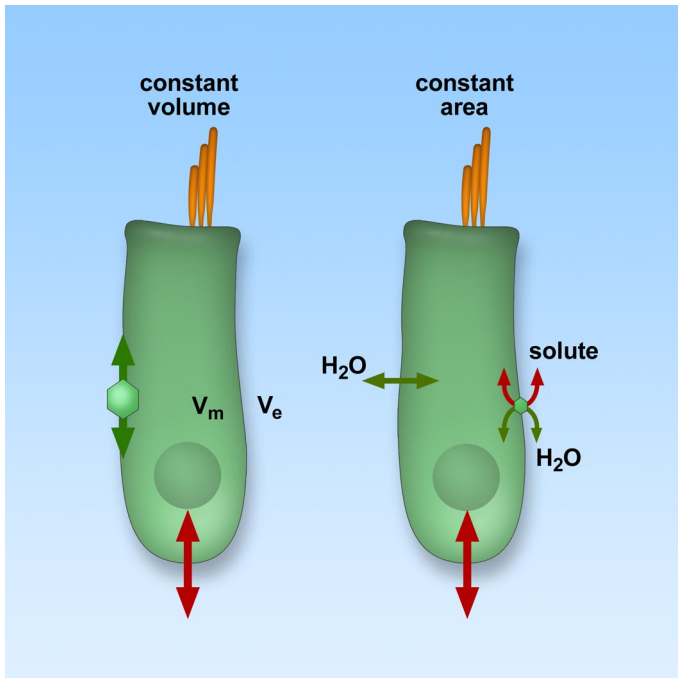

FIG. 7. Distinct mechanisms of OHC motility. Two mechanisms by which a cell can change length: a constant volume (prestin-dependent) mechanism (*scheme a*) and a constant area (prestin-independent) mechanism where the volume changes (*scheme b*). *Scheme b*, on a slower time scale than *scheme a*, can occur through entry of water (e.g., as a result of an osmotic gradient or solute entry). Water entry could arise through a "water pump" mechanism with the entry of solute (e.g., Ref. 43). Changes of internal Ca^{2+}, for example, might affect the stiffness and OHC static length.

$$\delta V/V = 2\delta D/D + \delta L/L = 2\delta A/A - \delta L/L \qquad (7)$$

where δ signifies incremental change. These proportional changes in geometric parameters of the cell can be measured by imaging techniques. The changes usually amount to a few percent. This empirical finding is useful to determine any small volume changes since the length of the cell is an accessible parameter for measurement. In electromotile OHCs, the maximal normalized length change (=strain) produced by electrical depolarization is ~4% (141). In the case of electrically driven motility, the volume is constant ($\delta V/V = 0$), and good agreement with the prediction $2\delta A/A = \delta L/L$ is obtained (25, 221).

In contradistinction, prestin-independent length changes appear to be better characterized by the condition $\delta A/A = 0$, up to cell length changes of up to 30% (221). Such changes can be induced by exposing the cells to high potassium (77–80, 345, 346). The partially reversible shortening in this case seems almost certainly to be a consequence of water movement (25).

Other ions, and in particular calcium, have been implicated in the slow shortening of OHCs. The reports are sometimes contradictory. External Ca^{2+} is reported to modulate the potassium-induced shortening so that low-

ering external Ca^{2+} reduces the maximum K^+-induced shortening (41, 91). Ionomycin, a calcium ionophore, can alter internal Ca^{2+} levels and also produce changes in cell length (79, 80, 313). When ionomycin is applied to an isolated OHC, intracellular Ca^{2+} rises and the cell lengthens (41). The same paper reports that OHCs, permeabilized with DMSO and exposed to Ca^{2+}-, shorten only if ATP is present. Such studies suggest that a mechanical interaction between the cytoskeleton and the external membrane of the OHC is playing a role. Indeed, it is known that the OHC Ca^{2+} sensitivity and electromotility appear over the same developmental window (27).

Fixatives such as glutaraldehyde change the shape of OHCs (312), an observation of importance for studies of the cellular organization of the cochlea. On the other hand, acetylcholine applied around the cell leads to a shortening of the cell (325–327) with a slow time constant which may be indicative either of direct calcium entry or of a trigger of a signal transduction cascade whose final target is the cell cytoskeleton. It has been suggested that mobilization of calcium stores may affect hair cell electromotility, by controlling a calmodulin-dependent phosphorylation step which in turns affects the cytoskeleton (328). Such complex pathways need further examination.

Slow length changes induced by osmotic stimulation are particularly apparent in long cylindrical cells. The effects can be attributed to movement of water into the cell to neutralize the osmotic gradient across the membrane. Measured by exposing the cells to hyposmotic stimuli, the water permeability increases during maturation of the cochlear hair cells and can be inhibited by mercurous chloride $HgCl_2$ which block aquaporin-mediated water transport (25). Thus, although compatible with a selective water pathway, the water could also enter through any of the membrane proteins, including prestin.

B. Bending Motions of OHCs

OHCs, especially from the apical, low-frequency end of the guinea pig cochlea, exhibit a pronounced curvature. This is a consequence of the structure of the low-frequency portion of the organ of Corti where the wider basilar membrane produces an articulation of the tissue different from that at the basal (high frequency) end. In addition, apical OHCs tend to be longer especially in guinea pig, so that, during electrical stimulation, some cells appear to have a pronounced lateral as well as longitudinal motion. Using low-frequency external electrical stimulation (2–3 Hz) oriented across the long axis of the cell, it has been reported that cells could show a pronounced bending movement of as large as 0.7 μm (103). Agents that blocked longitudinal movements [e.g., specific sulfhydryl cross-linking reagents *p*-chloromercuriphenylsulfonic acid (pCMS) and *p*-hydroxymercuriphenylsulfonic acid (pHMS)] also blocked the bending motion. This result suggests that a bending motion is due to the lateral membrane OHC motor, with the stimulus depolarizing one side and hyperpolarizing the other side. Whether there is sufficient current flow in the intact cochlea to induce a similar bending motion is not known.

C. Constrained Motions of OHCs In Situ

The experiments described above are carried out, generally, on isolated cells. In the living organ of Corti, the OHCs are constrained by the surrounding tissue so that they generate force under near isometric conditions, rather than being allowed to freely change length. Direct measurements do show that OHCs generate sufficient force to distort the organ of Corti when stimulated electrically (125, 136, 211, 224, 304). These data show that nanometer movements can be recorded using interferometric techniques. Estimates of the motion of the basilar membrane (on a scale of 1–10 nm) and the accessible surfaces of the organ of Corti indicate that the stiffness of the surrounding cells may match that of the OHCs, allowing a good transfer of force from the OHC to the other tissues (211). The stiffness of the Deiters cells intervening between the OHCs and the BM then becomes critical when transferring forces to the BM: too stiff and the OHCs have no effect, too compliant and the forces generated by the OHCs are not transmitted at all (191, 193).

The resolution of OHC-induced movement over the frequency range of 0–50 kHz is sufficient to address the nature of fluid flow in the subtectorial space (243). This allows at last a detailed study of the radial motions of the organ of Corti, essential data for future realistic three-dimensional models of the cochlear partition. Imaging the intact structures with light microscopy in the temporal bone (101, 161) or in the hemisected cochlea (274) can be used to show that the OHC forces do measurably influence the mechanics. In the smaller cochlea of the gerbil, electrically evoked OHC activity likewise produces complex collective motions of the cells (177, 178). Improved imaging techniques are likely to provide critical data for understanding realistic three-dimensional cochlear models.

VII. PHARMACOLOGY OF OUTER HAIR CELL MOTILITY

A. Modifiers of Electromotility

There are several agents that modify the quantitative properties of OHC motility, although none of them can be described as high-affinity antagonists. A number of these agents alter the voltage dependence of the *Q-V* (or equiv-

alently the *C-V*) curves; some alter the peak charge moved, some alter the voltage dependence of the curve, and some alter both. Since *Q-V* curves and strain-voltage curves track each other, at least for those conditions where the mechanical properties of the cell are not significantly altered, these compounds are able to alter the forces produced by OHCs and hence directly to affect cochlear micromechanics in vivo; that is, of course, if they can pass the blood-cochlea barrier. The precise molecular site of action has not been established for many of these agents.

B. Lanthanides and Charged Cationic Species

A number of metal ions of the lanthanide series, triply charged cations, affect electromotility. The action is relatively nonspecific. These cations also have pharmacological actions on ion channels at the same dose or lower. Gadolinium (Gd^{3+}), known to block mechanosensitive channels at micromolar concentrations, reduces electromotility when applied at concentrations between 0.5 and 1 mM (290). The effect is reversible. These high concentrations of Gd^{3+} shift the *C-V* curve in the depolarizing direction but also reduce the maximum capacitance, suggesting both nonspecific binding and charge screening effects of the ion. At lower concentrations (typically 100 μM), lutetium (Lu^{3+}) and lanthanum (La^{3+}) also displace the *C-V* curve but in the negative direction (173). Gd^{3+} is reported to increase the stiffness of OHCs when applied around cells in the microchamber (129). The required dose is higher than required to change the electrical properties (20), and concentrations of 5 mM are necessary to obtain measurable stiffness changes. The high concentrations required indicate that (conventional) stretch-activated channels are not involved in such OHC electromotility responses.

A cationic peptide toxin isolated from a tarantula venom has been found to be effective against stretch-activated channels. This toxin, GsMTx4, also affects the membrane motor of OHCs (90). The effect is similar to the more highly charged cationic agents and produces a shift of 26 mV of the *C-V* curve in the depolarizing direction. The dissociation constant for this peptide is reported to be 3.1 μM. Although the affinity is high, it may still prove to be insufficiently high to act as a tool to isolate the motor protein from cells.

C. Salicylate

The link between the clinical observation that aspirin leads to a temporary hearing loss and OHC was made in a previous review (33). It had been known for a long time that aspirin elevated auditory thresholds and, with the advent of precise otoacoustic emission measurements, it was also found that acute doses of aspirin also reversibly abolished human OAEs (204, 338). Aspirin abolishes OHC electomotility (71). Although the study also reported structural alterations in the endoplasmic reticulum in guinea pig hair cells, these observations may have been a consequence of the slow deterioration of OHCs in short-term tissue culture. It is clear that with suitable doses, where a full washout and recovery is possible, OHC motility is inhibited. Aspirin or its unmethylated congener, salicylate, may alter submembranous structures to the extent that fluorescent dyes interact differently with the lateral membrane (258). The detailed mechanisms in these cases have not been established. More recent measurements using optical tweezers to measure tethering forces of membrane blebs pulled from the lateral membrane of OHCs suggest that salicylate may be having an effect on hearing function more through its interaction with anion binding sites in OHCs than on membrane mechanics (84). Aspirin at millimolar doses, such as used in these reports, also produces pH changes in cells (332). It may be that structural changes are consequent on the acidification of the cytoplasm in these experimental conditions.

Salicylate is amphipathic. It can, however, permeate the membrane as salicylic acid, and then dissociate to acidify the cell. As an amphipath, it is able to interact with the inner surface of the plasma membrane. External concentrations of 0.05–10 mM salicylate produce measurable reduction of electromotility (309) and also alter the magnitude (but not the voltage dependence) of the charge movement itself (332). The inhibition by extracellular salicylate is characterized by an IC_{50} of between 1.6 and 4 mM. The Hill coefficient of the dose-response curve is one, indicating a relatively simple mode of inhibition (173). With the use of inside-out patches of rat lateral membrane and studies of the competition with chloride, the intracellular binding site for salicylate has been estimated to have a much lower K_D of 200 μM (251). In these experiments too, salicylate does not significantly shift in the voltage dependence but reduces the peak of the *C-V* curve. Pretreatment of the cytoplasmic surface of the OHC membrane with trypsin is not reported to affect the action of salicylate (173). This observation suggests that the salicylate interaction occurs at a relatively well-protected site of the motor molecule.

D. Protein Reactive Agents

In pursuit of agents binding tightly to the motor protein, it was noticed that agents which bind to exposed sulfhydryl (-SH) groups also effect electromotility (175). Incubation of OHCs with *p*-chloromercuriphenylsulfonate (pCMPS) reduce electromotility but not completely. As well as pCMPS, *p*-hydroxymercuriphenylsulfonic acid

(pHMPS) also suppresses longitudinal OHC movements produced in an external field (103). *N*-ethylmaleimide (NEM), dithiothreitol (DTT), and diamide, all reagents which react with exposed SH-groups, produce no significant effects on the electrical properties of the cell (175). The early measurements were relatively qualitative. Subsequent reevaluation of the effects broadly agree (301), and when the observations were repeated with high-resolution capacitance measurements, only a small shift in the peak of the *C-V* curves could be detected in the presence of these protein reactive agents.

E. Agents Affecting the Cytoskeleton

Although diamide has no significant effect on the electrical properties of OHCs, it does cause changes in the mechanical properties of the cell. At concentrations up to 5 mM, it produces OHCs whose stiffness is reduced by a factor of up to 3 (2). The effect on forces produced by cells can be measured by a calibrated probe pressing against one end of the cell while the cell is held by the patch pipette. It is found that the force is also reduced by the same factor. Functionally, therefore, diamide reduces the motor output of an OHC.

F. Agents Affecting the Lipid Environment of the Motor

Several agents that interact with lipids and modify the lipid bilayer have been investigated systematically for their effect on the OHC capacitance (301). It is difficult to estimate the precise concentration of these agents as they would have partitioned into the lipid out of the aqueous phase and the partition coefficients are not known. For example, chloroform (as an aqueous saturated solution) shifts the *C-V* curve negatively by 30 mV and slightly reduces the maximum charge Q_{max}. A positive shift of +37 mV was obtained with the lysophospholipid hexadecylphosphocholine (HePC), which is known to intercalate into cell plasma membranes. Other agents, such as phospholipase A_2 (PLA_2), and filipin , which can bind to cholesterol in membranes, had no significant effect (301). In the event that the lipid access is restricted because of the tight packing of the motor or that the OHC lipid type is in some way exceptional, it might be profitable to investigate the effects of these agents in expression systems rather than in native cells. Some results along these lines are known. When prestin is expressed in HEK293 cells, depletion of the cell's cholesterol with methyl-β-cyclodextrin (MβCD) shifts the peak of the NLC positively by 80 mV (324). Lipid-prestin interactions thus deserve closer scrutiny.

Chlorpromazine (CPZ) is a member of a class of compounds described as cationic amphipaths. Although CPZ has antipsychotic effects in humans at submicromolar levels, it has been reported to shift the *Q-V* curve by 30 mV in the depolarizing direction when applied to OHCS at concentrations of 100 μM (209). In vivo systemic introduction of CPZ inhibits cochlear function by raising auditory threshold and by reducing otoacoustic emissions (246). The interest in this compound arises as its mechanical effects are well documented in red blood cells: CPZ causes an inward bending of red blood cell membranes (308). CPZ intercalates into lipid membranes and, depending on the charge on the lipid moiety, will increase or decrease the radius of curvature of the membrane. Such considerations can be built in to a model of the OHC lateral wall (35, 223, 261). Anionic compounds such as CPZ should increase the radius of curvature and therefore interfere with action of a motor system. These results raise the possibility that the effect on prestin arises from local mechanical effects on the phospholipid bilayer, or from the interaction between the phospholipid and the tethering cytoskeleton (229). A recent report also suggests that mutations in the sulfate transporter motif region of prestin (near aa 100 in the sequence) affect the forces that prestin can exert in the membrane. These mutations only minimally affect the static mechanical properties of the membrane per se (350).

G. Phosphorylating Agents

A systematic study of the effect of phosphorylation state of the motor molecule has been reported by Frolenkov et al. (104). Hyperpolarizing shifts of the voltage dependence of the *Q-V* curve are induced by membrane-permeable agents that promoted phosphorylation. Thus okadaic acid produced a hyperpolarizing shift in the NLC. In contrast, agents that are implicated in protein dephosphorylation such as trifluoperazine and W-7, both antagonists of calmodulin, caused a depolarizing shift. A comparable finding has been reported by Deak et al. (67), where it was proposed that prestin can be phosphorylated by a PKG; this induced only a small (a few mV) hyperpolarizing shift in the *Q-V* curve. On the other hand, the nonhydrolyzable cyclic nucleotide agonist dibutyryl cGMP enhanced the charge magnitude by a factor of 2. From mutation studies on prestin, PKG acts at serine residue S238. Since neither PKG nor ATP was present externally in these experiments, this result suggests that the phosphorylated site is intracellular. As a result, this study proposed that helices S5 and S6 of the prestin molecule loop back into the cytoplasm (see Fig. 4).

A related observation has been made on the effect of 2,3-butanedione monoxime (BDM) on nonlinear capacitance. BDM is often described as an inorganic phosphatase and used widely in the studies of ATPases. The action on OHCs is in the same direction as those agents that

operate by phosphorylation of the protein. When applied extracellularly at 5 mM, the compound induced a large hyperpolarization (of about −50 mV) of the peak of the *C-V* curve (105). It therefore appears as though BDM may be a compound that specifically targets a site on the motor protein for kinases.

VIII. CONCLUSIONS

In this review we have seen how the OHC motility emerged as an experimental observation that provides a cellular explanation for the system biology of auditory frequency selectivity. The phenomenon itself, ultrafast force generation by a subpopulation of the sensory hair cells of the cochlea, has given rise to experimental results that inform other areas of physiology. To makes sense of many of the complexities of the experimental data, mathematical models have usefully been employed in cochlear physiology at all scales of the system. There are, however, two issues that continue to preoccupy cochlear physiology (as seen in recent reviews. e.g., Ref. 65): *1*) Is OHC motility really the explanation for "cochlear amplification"? *2*) What is the molecular basis for the rapid force generation step? These will be dealt with in turn.

A. Cochlear Amplification and OHC Motility

The major criticism of schemes to incorporate OHC motility into a theory of cochlear amplification arises from the apparent electrical filtering of the cell receptor potential. The motor can be driven at high frequencies in experimental conditions when isolated cells are being studied. In situ, any membrane potential change in an OHC results from deflection of the stereocilia and the consequent gating of current into the cell. At frequencies above a corner frequency determined by the membrane time constant, the membrane potential response is attenuated (by 6 dB/octave). For apical and basal cells in the guinea pig, these corner frequencies have been estimated to be ~150 and 600 Hz, respectively (144). Although this is not an issue for low-frequency hearing, and this includes many nonmammalian hearing organs, there are difficulties in explaining how OHC motility can be useful at frequencies significantly above 1 kHz. The high-frequency range of hearing is where the cochlear amplifier takes on particular significance and importance for that is where the quality factors (Q_{10dB}) of the tuning curves are greatest. Indeed, it might even be argued that the role of OHCs is being overemphasized, since mutations in the tectorial membrane, a structure thought to couple the OHCs into the mechanics, leads to an enhanced BM and neural tuning curve in the high-frequency region (281).

Various ways out of this dilemma have been proposed. First, it could be that the transducer current in OHCs is not constant but is larger in hair cells from the more basal end of the cochlea. As a result, the OHC receptor potential attenuation would be offset by the larger input currents passing through the transducer. Such assumptions are built into some linear and nonlinear models of cochlear mechanics (214, 241, 242). There is experimental evidence that this situation does occur in some hearing organs. In the turtle auditory papilla, where recordings can be made directly at different best frequency sites, hair cell transducer currents increase significantly in high-frequency cells (94, 269–271). The available evidence in mammalian hair cells indicates that there is an increase in the magnitude of the transduction current (132) as well as an increase in the rate of channel adaptation in higher frequency cells (272). Underlying these changes may be an alteration in the unitary conductance of the transducer channel of the OHC (28). The experimental data are thus consistent with the model requirements. Nevertheless, these data have yet to show the full quantitative increases in the transduction current in the small basal cells predicted by theoretical models of cochlear mechanics.

Second, it could be that there are mechanisms that cancel the effects of membrane time constant. One of these has been described associated with the chloride permeability of the membrane where a stretch-activated anion conductance, G_{metL}, has been proposed as a direct allosteric modulator of prestin, allowing activation of the motor at high frequencies (283, 298). Another ingenious proposal, so far unsubstantiated experimentally, has been that the K^+ currents in OHCs have kinetic properties that maximize the impedance of the cell at its best frequency (256). The analysis of the underlying cochlear mechanics concludes that it is not the RC time constant of the cell which determines the filtering but that it is the product of the electrical membrane capacitance C_m and a drag coefficient. As a result, the inferred cutoff for OHC motility is estimated to be between 10 and 13 kHz, rather than the order of magnitude less observed in isolated cells. This is similar to the theme that only meaningful conclusions can be obtained by modeling the cells in situ (226). Nevertheless, a cutoff at 10 kHz is still not sufficient for known cochlear function. Further extension of the cutoff to even higher frequencies can be achieved if there is a fast-activating K^+ current in the cell whose kinetics cancel the effect of the membrane capacitance C_m. So far experimental support for this idea has not been forthcoming.

Third, it could be that greater attention needs to be paid to the extracellular current flow around hair cells. Since the OHC motor is driven by transmembrane voltage, the extracellular field takes on a particular significance (56, 57). Although it is clear that there are significant extracellular potential fields produced by the activity of neighboring hair cells (245), it is difficult to measure these at the sites near the OHC lateral membrane with certainty

about the correct phasing. The problem has been addressed by in vivo recordings (102). Both electric potentials inside the organ of Corti and basilar membrane vibration were measured during tone bursts. The available data suggest that the extracellular potentials could indeed drive the OHC motors, although, subject to uncertainty as to whether the mechanical and electrical measurements were made at the same point, it presently looks as though the magnitude of the effect is not quite sufficient.

Fourth, there has been reevaluation of the role of the precise architecture of the cochlea in determining cochlear amplification and how this contributes to the traveling wave. Recent work suggests that the bandwidth problem for single OHCs may not be a complete determinant of gain for the whole cochlea if the manner in which the assembly hair cell feedback is taken into account in the context of the whole cochlear system (206). The proposal is that under certain circumstances the OHCs can provide negative feedback at the basal high-frequency side of the traveling wave peak. Under closed loop conditions, which occur in the intact cochlea and where the OHCs are embedded in the organ of Corti, a relatively low-gain OHC system can still work to propagate the input sound energy to the resonant place even though the receptor potential is severely attenuated. A similar suggestion is also apparent in other earlier, systems engineering approaches to the cochlea (226) where it has been tentatively proposed that negative feedback may work in favor of enabling a wider frequency response. This is in stark contrast to mechanisms where positive feedback is invoked (120) to cancel fluid viscosity. Positive feedback leads to models of the cochlea with an undamping element to enhance the resonance (214, 236–238). Negative-feedback mechanisms, being inherently more stable, have advantages over positive-feedback systems as they are less prone to parasitic oscillations. Such explanations of cochlear function, built on modeled system properties of the cochlea, invoke more subtle complex behavior than we have hitherto been accustomed, and it may take a while yet before such approaches can be fully tested.

Finally, there has been considerable and renewed interest in the possibility that the hair cell stereocilia are responsible for cochlear amplification. It has to be remembered that OHCs are part of a mechanical feedback loop in which the forces act on the sensor (the transducer channels in the stereocilia) and on the cell body as the basilar membrane moves up and down during each cycle induced by sound. In vivo, it is hard to ascertain at which phase of the cycle the forces within the cochlear partition act on the stereocilia and at which phase the forces might be generating forces in their own right. However, were the OHC stereocilia to generate forces which augmented, with the appropriate phase, the forces acting on them, the feedback could effectively become regenerative. Hair cell stereocilia are not just passive levers but even in their neutral position move mechanically with displacements above the thermal noise floor (54). In the bullfrog, deflection of the hair bundle produces a small fast, voltage-dependent "twitch" that augments the forces pulling in the same direction (51). The data are consistent with a mechanism that depends on a transmembrane event in the stereocilia which is not necessarily identical with the gating step of the transducer channel. Described first in gating compliance measurements and distinct from adaptational movements of the bundle (145), the twitch phenomenon can now be explored robustly in amphibian systems (26, 218, 219). This mechanism has been proposed as a source of feedback forces in mammalian hair bundles, where the frequency response needs to be at least two orders of magnitude higher. In this case, the forward transduction step is undoubtedly very fast. The feedback step, however, is determined by the speed of so-called "fast adaptation." Whether the forces are generated fast enough remains to be determined.

Experimental data from the excised rat organ of Corti, not from isolated cells, shows that there is a rapidly developing force component of the response and that this force can be measured when the OHC hair bundle is pushed by a small calibrated fiber designed to engage with the stereocilia (182). The force is linked to adaptation and is calcium dependent. As it is linked to the transduction step, it could therefore operate at high frequencies, and only technical limitations prevent microsecond time scales from being observed. In a different experimental design using an isolated preparation of the gerbil cochlea, stimulation of the basilar membrane produced larger deflections of the IHC stereocilia and deviations of the vibration pattern from a linear response to sound predicted from a simple passive hair bundle (45, 46). The data provide some evidence for stereociliary involvement in cochlea mechanics.

These recent data reignite the idea that hair cell stereocilia generate rapid forces and that these forces may be responsible for cochlear amplification. Such proposals thereby side-step the function of somatic motility. The debate is currently unresolved. There are persuasive arguments being advanced for the bundle being the origin of the forces powering the cochlear amplifier (196). A cautionary note comes from measurements of hair bundle motion in intact mammalian OHC systems (168). Stimulation of the OHCs in either mouse or gerbil in situ organs of Corti with a sinusoidal voltage command produced a deflection of the hair bundle even when the cells are locked into the epithelium of the organ of Corti. The reported movements are large (peak deflections of the stereocilial tips by 830 nm). Thus there appears to be coupling between somatic motility and movement of the hair bundle. This suggestion was made, in fact, when electromotility was first observed (347). In rat cochlear cultures the OHC somatic electromotility also contributes

to the active motion of stereocilia (93, 183). The case for sufficient hair bundle force to power the amplifier thus remains weak until somatic motility and bundle motility can be convincingly decoupled in experimental measurements.

B. Mechanistic Basis of OHC Motility

There is no clear molecular structure for prestin. It has so far resisted analysis by crystallographic techniques. The structure is necessary before the motor can really be graced by being called a small nano-machine. Although the area motor model seems to account for many of the features of the cell motility (157, 174), it is not clear which part or parts of the molecule undergo rearrangement. Nor is it clear whether the "deep pore" on the cytoplasmic surface of prestin and implied by an anion sensor model is indeed a structural feature of the protein (251) or part of an allosterically induced change in the protein topology. Evidence, notably from the Santos-Sacchi group (283), suggests that other charge components in the protein may have to move in the membrane field to explain all of the residual charge movement in the absence of a chloride anion within the cell. Indeed, quantitative modeling of the protein as an anion transporter indicates that the simple anion sensor model of Oliver et al. (251) may require some modification, and further moving charges are required (227).

The expression levels of prestin have been a problem for studies that require sufficient quantities for structure-function studies. Methods have been published that have endeavored to maximize the number of hair cells for protein yield (133, 140), but so far it has not been possible to express prestin in a bacterial system to obtain protein in sufficient quantity for structural and biochemical studies. Insect cells and mammalian cells lines, such as Chinese hamster ovary cells, kidney cell lines, and some epithelial cell lines, seem to offer the best expression systems (153). It is possible that improved viral transfection methods may improve the yield. Taking a page from the potassium channel literature, where successful crystallization is commonplace, the bacterial homolog of SLC26 transporters may be required first before true structural data become available.

Many of the features of the cochlea depend on mechanisms that operate at microsecond time scales or less. Although there remain many attractive theoretical models that help us understand cochlear mechanics and tuning, the experimental data are still in short supply. The high bandwidth of acoustic signals, which can go up to frequencies of several tens of kilohertz, put severe strains on many physiological recording techniques designed to uncover neural mechanisms. Whole cell or single-channel recordings are not designed to investigate the high kilohertz region, and for this reason, a number of quite special techniques have been developed. We know much about the electrophysiology of hair cells associated with the lower frequencies of the mammalian hearing range. Many of the recording technologies become deficient precisely where mammalian cochlear function is at its most remarkable, at frequencies at 10 kHz or above. Even the limiting speed of mechanotransduction channel in the hair cell stereocilia, or its precise molecular identity, is currently unknown.

As Hallowell Davis presciently remarked in 1983 (66): "The mechanism of the CA (cochlear amplifier) is unknown, and the problem remains of how its action can be triggered by submolecular movements near threshold." It seems as though Davis was wise enough to know the answer to that problem would still not be solved over two decades later.

ACKNOWLEDGMENTS

I am indebted to Drs. Pascal Martin, Pavel Mistrik, and Daniella Muallem as well as members of the Unite de Genetique des Deficits Sensoriels, Institut Pasteur, for discussion and to two anonymous referees for remarks that significantly improved the accuracy of this review.

Address for reprint requests and other correspondence: J. Ashmore, Dept. of Physiology and UCL Ear Institute, University College London, Gower St., London WC1E 6BT, UK (e-mail: j.ashmore@ucl.ac.uk).

GRANTS

This work was supported by the Wellcome Trust and EU Integrated Project EuroHear LSHG-CT-2004-512063.

REFERENCES

1. **Abe T, Kakehata S, Kitani R, Maruya SI, Navaratnam D, Santos-Sacchi J, Shinkawa H.** Developmental expression of the outer hair cell motor prestin in the mouse. *J Membr Biol* 215: 49–56, 2007.
2. **Adachi M, Iwasa KH.** Effect of diamide on force generation and axial stiffness of the cochlear outer hair cell. *Biophys J* 73: 2809–2818, 1997.
3. **Adler HJ, Belyantseva IA, Merritt RC Jr, Frolenkov GI, Dougherty GW, Kachar B.** Expression of prestin, a membrane motor protein, in the mammalian auditory and vestibular periphery. *Hear Res* 184: 27–40, 2003.
4. **Albert JT, Winter H, Schaechinger TJ, Weber T, Wang X, He DZ, Hendrich O, Geisler HS, Zimmermann U, Oelmann K, Knipper M, Gopfert MC, Oliver D.** Voltage-sensitive prestin orthologue expressed in zebrafish hair cells. *J Physiol* 580: 451–461, 2007.
5. **Allen JB.** Cochlear micromechanics—a mechanism for transforming mechanical to neural tuning within the cochlea. *J Acoust Soc Am* 62: 930–939, 1977.
6. **Allen JB.** Cochlear micromechanics—a physical model of transduction. *J Acoust Soc Am* 68: 1660–1670, 1980.
7. **Aravind L, Koonin EV.** The STAS domain: a link between anion transporters and antisigma-factor antagonists. *Curr Biol* 10: R53–R55, 2000.
8. **Ashmore J.** The ear's fast cellular motor. *Curr Biol* 3: 38–40, 1993.
9. **Ashmore JF.** Motor coupling in mammalian outer hair cells. In: *Cochlear Mechanisms*, edited by Wilson JP and Kemp DT. New York: Plenum, 1989, p. 107–114.

10. **Ashmore JF.** Forward and reverse transduction in the mammalian cochlea. *Neurosci Res Suppl* 12: S39–S50, 1990.
11. **Ashmore JF.** The electrophysiology of hair cells. *Annu Rev Physiol* 53: 465–476, 1991.
12. **Ashmore JF.** Mammalian hearing and the cellular mechanisms of the cochlear amplifier. In: *Sensory Transduction*, edited by Corey D and Roper S. New York: Rockefeller Univ, Press, 1992, p. 395–412.
13. **Ashmore JF.** A fast motile response in guinea-pig outer hair cells: the cellular basis of the cochlear amplifier. *J Physiol* 388: 323–347, 1987.
14. **Ashmore JF, Brownell WE.** Kilohertz movements induced by electrical stimulation in outer hair cells isolated from the guinea pig cochlea. *J*. Physiol 377: 41P, 1986.
15. **Ashmore JF, Geleoc GS, Harbott L.** Molecular mechanisms of sound amplification in the mammalian cochlea. *Proc Natl Acad Sci USA* 97: 11759–11764, 2000.
16. **Ashmore JF, Holley MC.** Temperature-dependence of a fast motile response in isolated outer hair cells of the guinea-pig cochlea. *Q J Exp Physiol* 73: 143–145, 1988.
17. **Ashmore JF, Meech RW.** Ionic basis of membrane potential in outer hair cells of guinea pig cochlea. *Nature* 322: 368–371, 1986.
18. **Bader CR, Macleish PR, Schwartz EA.** Responses to light of solitary rod photoreceptors isolated from tiger salamander retina. *Proc Natl Acad Sci USA* 75: 3507–3511, 1978.
19. **Bai JP, Navaratnam D, Samaranayake H, Santos-Sacchi J.** En block C-terminal charge cluster reversals in prestin (SLC26A5): effects on voltage-dependent electromechanical activity. *Neurosci Lett* 404: 270–275, 2006.
20. **Batta TJ, Panyi G, Gaspar R, Sziklai I.** Active and passive behaviour in the regulation of stiffness of the lateral wall in outer hair cells of the guinea-pig. *Pflügers Arch* 447: 328–336, 2003.
21. **Baylor DA, Lamb TD, Yau KW.** Responses of retinal rods to single photons. *J Physiol* 288: 613–634, 1979.
22. **Baylor DA, Lamb TD, Yau KW.** The membrane current of single rod outer segments. *J Physiol* 288: 589–611, 1979.
23. **Bekesy G.** *Experiments in Hearing*. New York: McGraw-Hill, 1960.
24. **Belyantseva IA, Adler HJ, Curi R, Frolenkov GI, Kachar B.** Expression and localization of prestin and the sugar transporter GLUT-5 during development of electromotility in cochlear outer hair cells. *J Neurosci* 20: RC116, 2000.
25. **Belyantseva IA, Frolenkov GI, Wade JB, Mammano F, Kachar B.** Water permeability of cochlear outer hair cells: characterization and relationship to electromotility. *J Neurosci* 20: 8996–9003, 2000.
26. **Benser ME, Marquis RE, Hudspeth AJ.** Rapid, active hair bundle movements in hair cells from the bullfrog's sacculus. *J Neurosci* 16: 5629–5643, 1996.
27. **Beurg M, Bouleau Y, Dulon D.** The voltage-sensitive motor protein and the Ca^{2+}-sensitive cytoskeleton in developing rat cochlear outer hair cells. *Eur J Neurosci* 14: 1947–1952, 2001.
28. **Beurg M, Evans MG, Hackney CM, Fettiplace R.** A large-conductance calcium-selective mechanotransducer channel in mammalian cochlear hair cells. *J Neurosci* 26: 10992–11000, 2006.
29. **Block SM.** Biophysical principles of sensory transduction. *Soc Gen Physiol Ser* 47: 1–17, 1992.
30. **Brandt N, Kuhn S, Munkner S, Braig C, Winter H, Blin N, Vonthein R, Knipper M, Engel J.** Thyroid hormone deficiency affects postnatal spiking activity and expression of Ca^{2+} and K^{+} channels in rodent inner hair cells. *J Neurosci* 27: 3174–3186, 2007.
31. **Brown MC, Liberman MC, Benson TE, Ryugo DK.** Brainstem branches from olivocochlear axons in cats and rodents. *J Comp Neurol* 278: 591–603, 1988.
32. **Brownell WE.** The piezoelectric outer hair cell. In: *Vertebrate Hair Cells*, edited by Eatock RA, Fay RR, and Popper AN. New York: Springer, 2006, p. 313–347.
33. **Brownell WE.** Outer hair cell electromotility and otoacoustic emissions. *Ear Hear* 11: 82–92, 1990.
34. **Brownell WE, Bader CR, Bertrand D, De RY.** Evoked mechanical responses of isolated cochlear outer hair cells. *Science* 227: 194–196, 1985.
35. **Brownell WE, Spector AA, Raphael RM, Popel AS.** Micro- and nanomechanics of the cochlear outer hair cell. *Annu Rev Biomed Eng* 3: 169–194, 2001.
36. **Brundin L, Flock A, Canlon B.** Sound-induced motility of isolated cochlear outer hair cells is frequency-specific. *Nature* 342: 814–816, 1989.
37. **Brundin L, Flock A, Canlon B.** Tuned motile responses of isolated cochlear outer hair cells. *Acta Otolaryngol Suppl* 467: 229–234, 1989.
38. **Brundin L, Russell I.** Tuned phasic and tonic motile responses of isolated outer hair cells to direct mechanical stimulation of the cell body. *Hear Res* 73: 35–45, 1994.
39. **Camalet S, Duke T, Julicher F, Prost J.** Auditory sensitivity provided by self-tuned critical oscillations of hair cells. *Proc Natl Acad Sci USA* 97: 3183–3188, 2000.
40. **Canlon B, Brundin L, Flock A.** Acoustic stimulation causes tonotopic alterations in the length of isolated outer hair cells from guinea pig hearing organ. *Proc Natl Acad Sci USA* 85: 7033–7035, 1988.
41. **Canlon B, Dulon D.** Dissociation between the calcium-induced and voltage-driven motility in cochlear outer hair cells from the waltzing guinea pig. *J Cell Sci* 104: 1137–1143, 1993.
42. **Cecola RP, Bobbin RP.** Lowering extracellular chloride concentration alters outer hair cell shape. *Hear Res* 61: 65–72, 1992.
43. **Chambard JM, Ashmore JF.** Sugar transport by mammalian members of the SLC26 superfamily of anion-bicarbonate exchangers. *J Physiol* 550: 667–677, 2003.
44. **Chambard JM, Ashmore JF.** Regulation of the voltage-gated potassium channel KCNQ4 in the auditory pathway. *Pflügers Arch* 450: 34–44, 2005.
45. **Chan DK, Hudspeth AJ.** Ca^{2+} current-driven nonlinear amplification by the mammalian cochlea in vitro. *Nat Neurosci* 8: 149–155, 2005.
46. **Chan DK, Hudspeth AJ.** Mechanical responses of the organ of corti to acoustic and electrical stimulation in vitro. *Biophys J* 89: 4382–4395, 2005.
47. **Cheatham MA, Zheng J, Huynh K, Du GG, Gao J, Zuo J, Navarrete E, Dallos P.** Cochlear function in mice with only one copy of the prestin gene. *J Physiol* 569: 229–241, 2005.
48. **Chen GD.** Prestin gene expression in the rat cochlea following intense noise exposure. *Hear Res* 222: 54–61, 2006.
49. **Chen P, Gillis KD.** The noise of membrane capacitance measurements in the whole-cell recording configuration. *Biophys J* 79: 2162–2170, 2000.
50. **Chertoff ME, Brownell WE.** Characterization of cochlear outer hair cell turgor. *Am J Physiol Cell Physiol* 266: C467–C479, 1994.
51. **Cheung EL, Corey DP.** Ca^{2+} changes the force sensitivity of the hair-cell transduction channel. *Biophys J* 90: 124–139, 2006.
52. **Choe Y, Magnasco MO, Hudspeth AJ.** A model for amplification of hair-bundle motion by cyclical binding of Ca^{2+} to mechanoelectrical-transduction channels. *Proc Natl Acad Sci USA* 95: 15321–15326, 1998.
53. **Cooper NP, Rhode WS.** Mechanical responses to two-tone distortion products in the apical and basal turns of the mammalian cochlea. *J Neurophysiol* 78: 261–270, 1997.
54. **Crawford AC, Fettiplace R.** The mechanical properties of ciliary bundles of turtle cochlear hair cells. *J Physiol* 364: 359–379, 1985.
55. **Dallos P, Corey ME.** The role of outer hair cell motility in cochlear tuning. *Curr Opin Neurobiol* 1: 215–220, 1991.
56. **Dallos P, Evans BN.** High-frequency motility of outer hair cells and the cochlear amplifier. *Science* 267: 2006–2009, 1995.
57. **Dallos P, Evans BN.** High-frequency outer hair cell motility: corrections and addendum. *Science* 268: 1420–1421, 1995.
58. **Dallos P, Evans BN, Hallworth R.** Nature of the motor element in electrokinetic shape changes of cochlear outer hair cells. *Nature* 350: 155–157, 1991.
59. **Dallos P, Fakler B.** Prestin, a new type of motor protein. *Nat Rev Mol Cell Biol* 3: 104–111, 2002.
60. **Dallos P, Hallworth R, Evans BN.** Theory of electrically driven shape changes of cochlear outer hair cells. *J Neurophysiol* 70: 299–323, 1993.
61. **Dallos P, Harris D.** Properties of auditory nerve responses in absence of outer hair cells. *J Neurophysiol* 41: 365–383, 1978.

62. **Dallos P, He DZ.** Two models of outer hair cell stiffness and motility. *J Assoc Res Otolaryngol* 1: 283–291, 2000.
63. **Dallos P, He DZ, Lin X, Sziklai I, Mehta S, Evans BN.** Acetylcholine, outer hair cell electromotility, the cochlear amplifier. *J Neurosci* 17: 2212–2226, 1997.
64. **Dallos P, Santos-Sacchi J, Flock A.** Intracellular recordings from cochlear outer hair cells. *Science* 218: 582–584, 1982.
65. **Dallos P, Zheng J, Cheatham MA.** Prestin and the cochlear amplifier. *J Physiol* 576: 37–42, 2006.
66. **Davis H.** An active process in cochlear mechanics. *Hear Res* 9: 79–90, 1983.
67. **Deak L, Zheng J, Orem A, Du GG, Aguinaga S, Matsuda K, Dallos P.** Effects of cyclic nucleotides on the function of prestin. *J Physiol* 563: 483–496, 2005.
68. **Denk W, Webb WW.** Forward and reverse transduction at the limit of sensitivity studied by correlating electrical and mechanical fluctuations in frog saccular hair cells. *Hear Res* 60: 89–102, 1992.
69. **Denk W, Webb WW, Hudspeth AJ.** Mechanical properties of sensory hair bundles are reflected in their Brownian motion measured with a laser differential interferometer. *Proc Natl Acad Sci USA* 86: 5371–5375, 1989.
70. **Deo N, Grosh K.** Two-state model for outer hair cell stiffness and motility. *Biophys J* 86: 3519–3528, 2004.
71. **Dieler R, Shehata-Dieler WE, Brownell WE.** Concomitant salicylate-induced alterations of outer hair cell subsurface cisternae and electromotility. *J Neurocytol* 20: 637–653, 1991.
72. **Ding JP, Salvi RJ, Sachs F.** Stretch-activated ion channels in guinea pig outer hair cells. *Hear Res* 56: 19–28, 1991.
73. **Dong X, Ehrenstein D, Iwasa KH.** Fluctuation of motor charge in the lateral membrane of the cochlear outer hair cell. *Biophys J* 79: 1876–1882, 2000.
74. **Dong XX, Iwasa KH.** Tension sensitivity of prestin: comparison with the membrane motor in outer hair cells. *Biophys J* 86: 1201–1208, 2004.
75. **Dong XX, Ospeck M, Iwasa KH.** Piezoelectric reciprocal relationship of the membrane motor in the cochlear outer hair cell. *Biophys J* 82: 1254–1259, 2002.
76. **Duke T, Julicher F.** Active traveling wave in the cochlea. *Phys Rev Lett* 90: 158101, 2003.
77. **Dulon D, Aran JM, Schacht J.** Potassium-depolarization induces motility in isolated outer hair cells by an osmotic mechanism. *Hear Res* 32: 123–129, 1988.
78. **Dulon D, Schacht J.** Motility of cochlear outer hair cells. *Am J Otol* 13: 108–112, 1992.
79. **Dulon D, Zajic G, Schacht J.** Increasing intracellular free calcium induces circumferential contractions in isolated cochlear outer hair cells. *J Neurosci* 10: 1388–1397, 1990.
80. **Dulon D, Zajic G, Schacht J.** Differential motile response of isolated inner and outer hair cells to stimulation by potassium and calcium ions. *Hear Res* 52: 225–231, 1991.
81. **Eguiluz VM, Ospeck M, Choe Y, Hudspeth AJ, Magnasco MO.** Essential nonlinearities in hearing. *Phys Rev Lett* 84: 5232–5235, 2000.
82. **Emadi G, Richter CP, Dallos P.** Stiffness of the gerbil basilar membrane: radial and longitudinal variations. *J Neurophysiol* 91: 474–488, 2004.
83. **Engstrom H, Wersall J.** The ultrastructural organization of the organ of Corti and of the vestibular sensory epithelia. *Exp Cell Res* 14: 460–492, 1958.
84. **Ermilov SA, Murdock DR, El-Daye D, Brownell WE, Anvari B.** Effects of salicylate on plasma membrane mechanics. *J Neurophysiol* 94: 2105–2110, 2005.
85. **Evans BN, Dallos P.** Stereocilia displacement induced somatic motility of cochlear outer hair cells. *Proc Natl Acad Sci USA* 90: 8347–8351, 1993.
86. **Evans BN, Hallworth R, Dallos P.** Outer hair cell electromotility: the sensitivity and vulnerability of the DC component. *Hear Res* 52: 288–304, 1991.
87. **Evans EF.** The frequency response and other properties of single fibers in the guinea-pig cochlear nerve. *J Physiol* 226: 263–287, 1972.
88. **Evans EF, Harrison RV.** Proceedings: correlation between cochlear outer hair cell damage and deterioration of cochlear nerve tuning properties in the guinea-pig. *J Physiol* 256: 43P–44P, 1976.
89. **Fakler B, Oliver D.** Functional properties of prestin: how the motor molecule works. In: *Biophysics of the Cochlea: From Molecules to Models*, edited by Gummer AW. Singapore: World Scientific, 2002, p. 110–115.
90. **Fang J, Iwasa KH.** Effects of tarantula toxin GsMTx4 on the membrane motor of outer hair cells. *Neurosci Lett* 404: 213–216, 2006.
91. **Farkas Z, Sziklai I.** Potassium-induced slow motility is partially calcium-dependent in isolated outer hair cells. *Acta Otolaryngol* 123: 160–163, 2003.
92. **Farrell B, Do SC, Brownell WE.** Voltage-dependent capacitance of human embryonic kidney cells. *Phys Rev E Stat Nonlin Soft Matter Phys* 73: 041930, 2006.
93. **Fettiplace R.** Active hair bundle movements in auditory hair cells. *J Physiol* 576: 29–36, 2006.
94. **Fettiplace R, Ricci AJ, Hackney CM.** Clues to the cochlear amplifier from the turtle ear. *Trends Neurosci* 24: 169–175, 2001.
95. **Field AC, Hill C, Lamb GD.** Asymmetric charge movement and calcium currents in ventricular myocytes of neonatal rat. *J Physiol* 406: 277–297, 1988.
96. **Flock A, Cheung HC, Flock B, Utter G.** Three sets of actin filaments in sensory cells of the inner ear. Identification and functional orientation determined by gel electrophoresis, immunofluorescence and electron microscopy. *J Neurocytol* 10: 133–147, 1981.
97. **Flock A, Orman S.** Micromechanical properties of sensory hairs on receptor cells of the inner ear. *Hear Res* 11: 249–260, 1983.
98. **Flock A, Orman S.** Sensory hairs as mechanical filters in crista ampullaris: passive through structure and active through contraction. *Acta Otolaryngol Suppl* 406: 59–60, 1984.
99. **Forge A.** Structural features of the lateral walls in mammalian cochlear outer hair cells. *Cell Tissue Res* 265: 473–483, 1991.
100. **Frank G, Hemmert W, Gummer AW.** Limiting dynamics of high-frequency electromechanical transduction of outer hair cells. *Proc Natl Acad Sci USA* 96: 4420–4425, 1999.
101. **Fridberger A, de Monvel JB.** Sound-induced differential motion within the hearing organ. *Nat Neurosci* 6: 446–448, 2003.
102. **Fridberger A, de Monvel JB, Zheng J, Hu N, Zou Y, Ren T, Nuttall A.** Organ of Corti potentials and the motion of the basilar membrane. *J Neurosci* 24: 10057–10063, 2004.
103. **Frolenkov GI, Kalinec F, Tavartkiladze GA, Kachar B.** Cochlear outer hair cell bending in an external electric field. *Biophys J* 73: 1665–1672, 1997.
104. **Frolenkov GI, Mammano F, Belyantseva IA, Coling D, Kachar B.** Two distinct Ca^{2+}-dependent signaling pathways regulate the motor output of cochlear outer hair cells. *J Neurosci* 20: 5940–5948, 2000.
105. **Frolenkov GI, Mammano F, Kachar B.** Action of 2,3-butanedione monoxime on capacitance and electromotility of guinea-pig cochlear outer hair cells. *J Physiol* 531: 667–676, 2001.
106. **Gadsby DC, Rakowski RF, De WP.** Extracellular access to the Na,K pump: pathway similar to ion channel. *Science* 260: 100–103, 1993.
107. **Gale JE, Ashmore JF.** Charge displacement induced by rapid stretch in the basolateral membrane of the guinea-pig outer hair cell. *Proc Biol Sci* 255: 243–249, 1994.
108. **Gale JE, Ashmore JF.** The outer hair cell motor in membrane patches. *Pflügers Arch* 434: 267–271, 1997.
109. **Gale JE, Ashmore JF.** An intrinsic frequency limit to the cochlear amplifier. *Nature* 389: 63–66, 1997.
110. **Galli A, Petersen CI, deBlaquiere M, Blakely RD, DeFelice LJ.** *Drosophila* serotonin transporters have voltage-dependent uptake coupled to a serotonin-gated ion channel. *J Neurosci* 17: 3401–3411, 1997.
111. **Geleoc GS, Casalotti SO, Forge A, Ashmore JF.** A sugar transporter as a candidate for the outer hair cell motor. *Nat Neurosci* 2: 713–719, 1999.
112. **Geleoc GS, Holt JR.** Developmental acquisition of sensory transduction in hair cells of the mouse inner ear. *Nat Neurosci* 6: 1019–1020, 2003.

113. **Geleoc GS, Risner JR, Holt JR.** Developmental acquisition of voltage-dependent conductances and sensory signaling in hair cells of the embryonic mouse inner ear. *J Neurosci* 24: 11148–11159, 2004.
114. **Gil-Loyzaga P, Brownell WE.** Wheat germ agglutinin and *Helix pomatia* agglutinin lectin binding on cochlear hair cells. *Hear Res* 34: 149–155, 1988.
115. **Gillis KD.** Admittance-based measurement of membrane capacitance using the EPC-9 patch-clamp amplifier. *Pflügers Arch* 439: 655–664, 2000.
116. **Gitter AH.** The length of isolated outer cells is temperature dependent. *ORL J Otorhinolaryngol Relat Spec* 54: 121–123, 1992.
117. **Gitter AH, Fromter E, Zenner HP.** C-type potassium channels in the latertal cell membrane of guinea-pig outer hair cells. *Hear Res* 60: 13–19, 1992.
118. **Gitter AH, Zenner HP, Fromter E.** Membrane potential and ion channels in isolated outer hair cells of guinea pig cochlea. *ORL J Otorhinolaryngol Relat Spec* 48: 68–75, 1986.
119. **Gold T.** Historical background to the proposal, 40 years ago, of an active model for cochlear frequency analysis. In: *Cochlear Mechanisms*, edited by Wilson JP and Kemp DT. New York: Plenum, 1989, p. 299–305.
120. **Gold T.** Hearing. II. The physical basis of the action of the cochlea. *Proc R Soc Lond B Biol Sci* 135: 492–498, 1948.
121. **Gold T, Pumphrey RJ.** Hearing. I. The cochlea as a frequency analyser. *Proc R Soc Lond B Biol Sci* 135: 462–491, 1948.
122. **Gould GW, Holman GD.** The glucose transporter family: structure, function and tissue-specific expression. *Biochem J* 295: 329–341, 1993.
123. **Gross J, Machulik A, Amarjargal N, Fuchs J, Mazurek B.** Expression of prestin mRNA in the organotypic culture of rat cochlea. *Hear Res* 204: 183–190, 2005.
124. **Gulley RL, Reese TS.** Regional specialization of the hair cell plasmalemma in the organ of corti. *Anat Rec* 189: 109–123, 1977.
125. **Gummer AW, Hemmert W, Zenner HP.** Resonant tectorial membrane motion in the inner ear: its crucial role in frequency tuning. *Proc Natl Acad Sci USA* 93: 8727–8732, 1996.
126. **Hallworth R.** Passive compliance and active force generation in the guinea pig outer hair cell. *J Neurophysiol* 74: 2319–2328, 1995.
127. **Hallworth R.** Modulation of outer hair cell compliance and force by agents that affect hearing. *Hear Res* 114: 204–212, 1997.
128. **Hallworth R, Evans BN, Dallos P.** The location and mechanism of electromotility in guinea pig outer hair cells. *J Neurophysiol* 70: 549–558, 1993.
129. **He DZ, Dallos P.** Properties of voltage-dependent somatic stiffness of cochlear outer hair cells. *J Assoc Res Otolaryngol* 1: 64–81, 2000.
130. **He DZ, Dallos P.** Somatic stiffness of cochlear outer hair cells is voltage-dependent. *Proc Natl Acad Sci USA* 96: 8223–8228, 1999.
131. **He DZ, Evans BN, Dallos P.** First appearance and development of electromotility in neonatal gerbil outer hair cells. *Hear Res* 78: 77–90, 1994.
132. **He DZ, Jia S, Dallos P.** Mechanoelectrical transduction of adult outer hair cells studied in a gerbil hemicochlea. *Nature* 429: 766–770, 2004.
133. **He DZ, Zheng J, Edge R, Dallos P.** Isolation of cochlear inner hair cells. *Hear Res* 145: 156–160, 2000.
134. **Held H.** Untersuchungen uber den feineren Bau des Ohrlabyrinths der Wirbeltiere. I. Zur Kenntnis des Cortischen Organs und der ubrigen Sinnesapparate des Labyrinthes bei Saugetieren. *Abh Math-Phys Kl Konigl SAchs Ges Wiss XXVIII* 1: 1–74, 1902.
135. **Helmholtz HLFv.** *On the Sensations of Tone as Physical Basis for the Theory of Music* (4th ed.), edited by Ellis WH. New York: Dover, 1954.
136. **Hemmert W, Zenner H, Gummer AW.** Characteristics of the travelling wave in the low-frequency region of a temporal-bone preparation of the guinea-pig cochlea. *Hear Res* 142: 184–202, 2000.
137. **Hemmert W, Zenner HP, Gummer AW.** Three-dimensional motion of the organ of Corti. *Biophys J* 78: 2285–2297, 2000.
138. **Hilgemann DW.** Channel-like function of the Na,K pump probed at microsecond resolution in giant membrane patches. *Science* 263: 1429–1432, 1994.
139. **Holley MC.** Outer Hair Cell Motility. In: *The Cochlea*, edited by Dallos P, Popper AN, Fay RR. New York: Springer, 1996, p. 386–434.
140. **Holley MC.** Purification of mammalian cochlear hair cells using small volume Percoll density gradients. *J Neurosci Methods* 27: 219–224, 1989.
141. **Holley MC, Ashmore JF.** On the mechanism of a high-frequency force generator in outer hair cells isolated from the guinea pig cochlea. *Proc R Soc Lond B Biol Sci* 232: 413–429, 1988.
142. **Holley MC, Ashmore JF.** A cytoskeletal spring in cochlear outer hair cells. *Nature* 335: 635–637, 1988.
143. **Holley MC, Ashmore JF.** Spectrin, actin and the structure of the cortical lattice in mammalian cochlear outer hair cells. *J Cell Sci* 96: 283–291, 1990.
144. **Housley GD, Ashmore JF.** Ionic currents of outer hair cells isolated from the guinea-pig cochlea. *J Physiol* 448: 73–98, 1992.
145. **Howard J, Hudspeth AJ.** Compliance of the hair bundle associated with gating of mechanoelectrical transduction channels in the bullfrog's saccular hair cell. *Neuron* 1: 189–199, 1988.
146. **Hsu CJ, Nomura Y.** Carbonic anhydrase activity in the inner ear. *Acta Otolaryngol Suppl* 418: 1–42, 1985.
147. **Huang G, Santos-Sacchi J.** Mapping the distribution of the outer hair cell motility voltage sensor by electrical amputation. *Biophys J* 65: 2228–2236, 1993.
148. **Huang G, Santos-Sacchi J.** Motility voltage sensor of the outer hair cell resides within the lateral plasma membrane. *Proc Natl Acad Sci USA* 91: 12268–12272, 1994.
149. **Hudspeth AJ.** How hearing happens. *Neuron* 19: 947–950, 1997.
150. **Hudspeth AJ, Lewis RS.** Kinetic analysis of voltage- and ion-dependent conductances in saccular hair cells of the bull-frog, *Rana catesbeiana*. *J Physiol* 400: 237–274, 1988.
151. **Huxley AF.** Is resonance possible in the cochlea after all? *Nature* 221: 935–940, 1969.
152. **Ichimiya I, Adams JC, Kimura RS.** Immunolocalization of Na^+,K^+-ATPase, Ca^{2+}-ATPase, calcium-binding proteins, carbonic anhydrase in the guinea pig inner ear. *Acta Otolaryngol* 114: 167–176, 1994.
153. **Iida K, Tsumoto K, Ikeda K, Kumagai I, Kobayashi T, Wada H.** Construction of an expression system for the motor protein prestin in Chinese hamster ovary cells. *Hear Res* 205: 262–270, 2005.
154. **Ikeda K, Saito Y, Nishiyama A, Takasaka T.** Intracellular pH regulation in isolated cochlear outer hair cells of the guinea-pig. *J Physiol* 447: 627–648, 1992.
155. **Iwasa KH.** A two-state piezoelectric model for outer hair cell motility. *Biophys J* 81: 2495–2506, 2001.
156. **Iwasa KH.** Effect of stress on the membrane capacitance of the auditory outer hair cell. *Biophys J* 65: 492–498, 1993.
157. **Iwasa KH.** A membrane motor model for the fast motility of the outer hair cell. *J Acoust Soc Am* 96: 2216–2224, 1994.
158. **Iwasa KH, Adachi M.** Force generation in the outer hair cell of the cochlea. *Biophys J* 73: 546–555, 1997.
159. **Iwasa KH, Chadwick RS.** Elasticity and active force generation of cochlear outer hair cells. *J Acoust Soc Am* 92: 3169–3173, 1992.
160. **Iwasa KH, Li MX, Jia M, Kachar B.** Stretch sensitivity of the lateral wall of the auditory outer hair cell from the guinea pig. *Neurosci Lett* 133: 171–174, 1991.
161. **Jacob S, Tomo I, Fridberger A, de Monvel JB, Ulfendahl M.** Rapid confocal imaging for measuring sound-induced motion of the hearing organ in the apical region. *J Biomed Opt* 12: 021005, 2007.
162. **Jagger DJ, Ashmore JF.** A potassium current in guinea-pig outer hair cells activated by ion channel blocker DCDPC. *Neuroreport* 9: 3887–3891, 1998.
163. **Jagger DJ, Ashmore JF.** Regulation of ionic currents by protein kinase A and intracellular calcium in outer hair cells isolated from the guinea-pig cochlea. *Pflügers Arch* 437: 409–416, 1999.
164. **Jagger DJ, Ashmore JF.** The fast activating potassium current, *I*(K,f), in guinea-pig inner hair cells is regulated by protein kinase A. *Neurosci Lett* 263: 145–148, 1999.
165. **Jen DH, Steele CR.** Electrokinetic model of cochlear hair cell motility. *J Acoust Soc Am* 82: 1667–1678, 1987.
166. **Jerry RA, Popel AS, Brownell WE.** Outer hair cell length changes in an external electric field. I. The role of intracellular

electro-osmotically generated pressure gradients. *J Acoust Soc Am* 98: 2000–2010, 1995.
167. **Jerry RA, Popel AS, Brownell WE.** Outer hair cell length changes in an external electric field. II. The role of electrokinetic forces on the cell surface. *J Acoust Soc Am* 98: 2011–2017, 1995.
168. **Jia S, He DZ.** Motility-associated hair-bundle motion in mammalian outer hair cells. *Nat Neurosci* 8: 1028–1034, 2005.
169. **Joshi C, Fernandez JM.** Capacitance measurements. An analysis of the phase detector technique used to study exocytosis and endocytosis. *Biophys J* 53: 885–892, 1988.
170. **Julicher F, Andor D, Duke T.** Physical basis of two-tone interference in hearing. *Proc Natl Acad Sci USA* 98: 9080–9085, 2001.
171. **Kachar B, Brownell WE, Altschuler R, Fex J.** Electrokinetic shape changes of cochlear outer hair cells. *Nature* 322: 365–368, 1986.
172. **Kakehata S, Santos-Sacchi J.** Membrane tension directly shifts voltage dependence of outer hair cell motility and associated gating charge. *Biophys J* 68: 2190–2197, 1995.
173. **Kakehata S, Santos-Sacchi J.** Effects of salicylate and lanthanides on outer hair cell motility and associated gating charge. *J Neurosci* 16: 4881–4889, 1996.
174. **Kalinec F, Holley MC, Iwasa KH, Lim DJ, Kachar B.** A membrane-based force generation mechanism in auditory sensory cells. *Proc Natl Acad Sci USA* 89: 8671–8675, 1992.
175. **Kalinec F, Kachar B.** Inhibition of outer hair cell electromotility by sulfhydryl specific reagents. *Neurosci Lett* 157: 231–234, 1993.
176. **Kaneko T, Harasztosi C, Mack AF, Gummer AW.** Membrane traffic in outer hair cells of the adult mammalian cochlea. *Eur J Neurosci* 23: 2712–2722, 2006.
177. **Karavitaki KD, Mountain DC.** Evidence for outer hair cell driven oscillatory fluid flow in the tunnel of corti. *Biophys J* 92: 3284–3293, 2007.
178. **Karavitaki KD, Mountain DC.** Imaging electrically evoked micromechanical motion within the organ of corti of the excised gerbil cochlea. *Biophys J* 92: 3294–3316, 2007.
179. **Kawasaki E, Hattori N, Miyamoto E, Yamashita T, Inagaki C.** Single-cell RT-PCR demonstrates expression of voltage-dependent chloride channels (ClC-1, ClC-2 and ClC-3) in outer hair cells of rat cochlea. *Brain Res* 838: 166–170, 1999.
180. **Kawasaki E, Hattori N, Miyamoto E, Yamashita T, Inagaki C.** mRNA expression of kidney-specific ClC-K1 chloride channel in single-cell reverse transcription-polymerase chain reaction analysis of outer hair cells of rat cochlea. *Neurosci Lett* 290: 76–78, 2000.
181. **Kemp DT.** Stimulated acoustic emissions from within the human auditory system. *J Acoust Soc Am* 64: 1386–1391, 1978.
182. **Kennedy HJ, Crawford AC, Fettiplace R.** Force generation by mammalian hair bundles supports a role in cochlear amplification. *Nature* 433: 880–883, 2005.
183. **Kennedy HJ, Evans MG, Crawford AC, Fettiplace R.** Depolarization of cochlear outer hair cells evokes active hair bundle motion by two mechanisms. *J Neurosci* 26: 2757–2766, 2006.
184. **Khanna SM, Leonard DG.** Basilar membrane tuning in the cat cochlea. *Science* 215: 305–306, 1982.
185. **Khanna SM, Leonard DG.** Measurement of basilar membrane vibrations and evaluation of the cochlear condition. *Hear Res* 23: 37–53, 1986.
186. **Kharkovets T, Hardelin JP, Safieddine S, Schweizer M, El-Amraoui A, Petit C, Jentsch TJ.** KCNQ4, a K^+ channel mutated in a form of dominant deafness, is expressed in the inner ear and the central auditory pathway. *Proc Natl Acad Sci USA* 97: 4333–4338, 2000.
187. **Kiang NY, Liberman MC, Levine RA.** Auditory-nerve activity in cats exposed to ototoxic drugs and high-intensity sounds. *Ann Otol Rhinol Laryngol* 85: 752–768, 1976.
188. **Kiang NY, Sachs MB, Peake WT.** Shapes of tuning curves for single auditory-nerve fibers. *J Acoust Soc Am* 42: 1341–1342, 1967.
189. **Ko SB, Zeng W, Dorwart MR, Luo X, Kim KH, Millen L, Goto H, Naruse S, Soyombo A, Thomas PJ, Muallem S.** Gating of CFTR by the STAS domain of SLC26 transporters. *Nat Cell Biol* 6: 343–350, 2004.
190. **Kolesnikov SS, Rebrik TI, Zhainazarov AB, Tavartkiladze GA, Kalamkarov GR.** A cyclic-AMP-gated conductance in cochlear hair cells. *FEBS Lett* 290: 167–170, 1991.
191. **Kolston PJ.** The importance of phase data and model dimensionality to cochlear mechanics. *Hear Res* 145: 25–36, 2000.
192. **Kolston PJ.** Sharp mechanical tuning in a cochlear model without negative damping. *J Acoust Soc Am* 83: 1481–1487, 1988.
193. **Kolston PJ, Ashmore JF.** Finite element micromechanical modeling of the cochlea in three dimensions. *J Acoust Soc Am* 99: 455–467, 1996.
194. **Kolston PJ, De BE, Viergever MA, Smoorenburg GF.** What type of force does the cochlear amplifier produce? *J Acoust Soc Am* 88: 1794–1801, 1990.
195. **Kubisch C, Schroeder BC, Friedrich T, Lutjohann B, El-Amraoui A, Marlin S, Petit C, Jentsch TJ.** KCNQ4, a novel potassium channel expressed in sensory outer hair cells, is mutated in dominant deafness. *Cell* 96: 437–446, 1999.
196. **LeMasurier M, Gillespie PG.** Hair-cell mechanotransduction and cochlear amplification. *Neuron* 48: 403–415, 2005.
197. **Lewis RS, Hudspeth AJ.** Voltage- and ion-dependent conductances in solitary vertebrate hair cells. *Nature* 304: 538–541, 1983.
198. **Liao Z, Popel AS, Brownell WE, Spector AA.** High-frequency force generation in the constrained cochlear outer hair cell: a model study. *J Assoc Res Otolaryngol* 1–12, 2005.
199. **Liberman MC, Gao J, He DZ, Wu X, Jia S, Zuo J.** Prestin is required for electromotility of the outer hair cell and for the cochlear amplifier. *Nature* 419: 300–304, 2002.
200. **Liberman MC, Zuo J, Guinan JJ Jr.** Otoacoustic emissions without somatic motility: can stereocilia mechanics drive the mammalian cochlea? *J Acoust Soc Am* 116: 1649–1655, 2004.
201. **Liu M, Pereira FA, Price SD, Chu MJ, Shope C, Himes D, Eatock RA, Brownell WE, Lysakowski A, Tsai MJ.** Essential role of BETA2/NeuroD1 in development of the vestibular and auditory systems. *Genes Dev* 14: 2839–2854, 2000.
202. **Liu XZ, Ouyang XM, Xia XJ, Zheng J, Pandya A, Li F, Du LL, Welch KO, Petit C, Smith RJ, Webb BT, Yan D, Arnos KS, Corey D, Dallos P, Nance WE, Chen ZY.** Prestin, a cochlear motor protein, is defective in nonsyndromic hearing loss. *Hum Mol Genet* 12: 1155–1162, 2003.
203. **Lohi H, Kujala M, Kerkela E, Saarialho-Kere U, Kestila M, Kere J.** Mapping of five new putative anion transporter genes in human and characterization of SLC26A6, a candidate gene for pancreatic anion exchanger. *Genomics* 70: 102–112, 2000.
204. **Long GR, Tubis A.** Modification of spontaneous and evoked otoacoustic emissions and associated psychoacoustic microstructure by aspirin consumption. *J Acoust Soc Am* 84: 1343–1353, 1988.
205. **Loo DD, Hirayama BA, Meinild AK, Chandy G, Zeuthen T, Wright EM.** Passive water and ion transport by cotransporters. *J Physiol* 518: 195–202, 1999.
206. **Lu TK, Zhak S, Dallos P, Sarpeshkar R.** Fast cochlear amplification with slow outer hair cells. *Hear Res* 214: 45–67, 2006.
207. **Ludwig J, Oliver D, Frank G, Klocker N, Gummer AW, Fakler B.** Reciprocal electromechanical properties of rat prestin: the motor molecule from rat outer hair cells. *Proc Natl Acad Sci USA* 98: 4178–4183, 2001.
208. **Lue AJ, Brownell WE.** Salicylate induced changes in outer hair cell lateral wall stiffness. *Hear Res* 135: 163–168, 1999.
209. **Lue AJ, Zhao HB, Brownell WE.** Chlorpromazine alters outer hair cell electromotility. *Otolaryngol Head Neck Surg* 125: 71–76, 2001.
210. **Maier H, Zinn C, Rothe A, Tiziani H, Gummer AW.** Development of a narrow water-immersion objective for laserinterferometric and electrophysiological applications in cell biology. *J Neurosci Methods* 77: 31–41, 1997.
211. **Mammano F, Ashmore JF.** Reverse transduction measured in the isolated cochlea by laser Michelson interferometry. *Nature* 365: 838–841, 1993.
212. **Mammano F, Ashmore JF.** Differential expression of outer hair cell potassium currents in the isolated cochlea of the guinea-pig. *J Physiol* 496: 639–646, 1996.
213. **Mammano F, Kros CJ, Ashmore JF.** Patch clamped responses from outer hair cells in the intact adult organ of Corti. *Pflügers Arch* 430: 745–750, 1995.
214. **Mammano F, Nobili R.** Biophysics of the cochlea: linear approximation. *J Acoust Soc Am* 93: 3320–3332, 1993.

215. **Manley GA.** Cochlear mechanisms from a phylogenetic viewpoint. *Proc Natl Acad Sci USA* 97: 11736–11743, 2000.
216. **Marcotti W, Geleoc GS, Lennan GW, Kros CJ.** Transient expression of an inwardly rectifying potassium conductance in developing inner and outer hair cells along the mouse cochlea. *Pflügers Arch* 439: 113–122, 1999.
217. **Marcotti W, Kros CJ.** Developmental expression of the potassium current *IK*,n contributes to maturation of mouse outer hair cells. *J Physiol* 520: 653–660, 1999.
218. **Martin P, Hudspeth AJ.** Active hair-bundle movements can amplify a hair cell's response to oscillatory mechanical stimuli. *Proc Natl Acad Sci USA* 96: 14306–14311, 1999.
219. **Martin P, Mehta AD, Hudspeth AJ.** Negative hair-bundle stiffness betrays a mechanism for mechanical amplification by the hair cell. *Proc Natl Acad Sci USA* 97: 12026–12031, 2000.
220. **Matsuda K, Zheng J, Du GG, Klocker N, Madison LD, Dallos P.** *N*-linked glycosylation sites of the motor protein prestin: effects on membrane targeting and electrophysiological function. *J Neurochem* 89: 928–938, 2004.
221. **Matsumoto N, Kalinec F.** Extraction of prestin-dependent and prestin-independent components from complex motile responses in guinea pig outer hair cells. *Biophys J* 89: 4343–4351, 2005.
222. **Matsumoto N, Kalinec F.** Prestin-dependent and prestin-independent motility of guinea pig outer hair cells. *Hear Res* 208: 1–13, 2005.
223. **Morimoto N, Raphael RM, Nygren A, Brownell WE.** Excess plasma membrane and effects of ionic amphipaths on mechanics of outer hair cell lateral wall. *Am J Physiol Cell Physiol* 282: C1076–C1086, 2002.
224. **Morioka I, Reuter G, Reiss P, Gummer AW, Hemmert W, Zenner HP.** Sound-induced displacement responses in the plane of the organ of Corti in the isolated guinea-pig cochlea. *Hear Res* 83: 142–150, 1995.
225. **Mount DB, Romero MF.** The SLC26 gene family of multifunctional anion exchangers. *Pflügers Arch* 447: 710–721, 2004.
226. **Mountain DC, Hubbard AE.** A piezoelectric model of outer hair cell function. *J Acoust Soc Am* 95: 350–354, 1994.
227. **Muallem D, Ashmore J.** An anion antiporter model of prestin, the outer hair cell motor protein. *Biophys J* 90: 4035–4045, 2006.
228. **Murakoshi M, Gomi T, Iida K, Kumano S, Tsumoto K, Kumagai I, Ikeda K, Kobayashi T, Wada H.** Imaging by atomic force microscopy of the plasma membrane of prestin-transfected Chinese hamster ovary cells. *J Assoc Res Otolaryngol* 7: 267–278, 2006.
229. **Murdock DR, Ermilov S, Spector AA, Popel AS, Brownell WE, Anvari B.** Effects of chlorpromazine on mechanical properties of the outer hair cell plasma membrane. *Biophys J* 2005.
230. **Nakagawa T, Kakehata S, Yamamoto T, Akaike N, Komune S, Uemura T.** Ionic properties of *IK*,n in outer hair cells of guinea pig cochlea. *Brain Res* 661: 293–297, 1994.
231. **Nakao M, Gadsby DC.** Voltage dependence of Na translocation by the Na/K pump. *Nature* 323: 628–630, 1986.
232. **Nakazawa K, Spicer SS, Schulte BA.** Postnatal expression of the facilitated glucose transporter, GLUT-5, in gerbil outer hair cells. *Hear Res* 82: 93–99, 1995.
233. **Narayan SS, Temchin AN, Recio A, Ruggero MA.** Frequency tuning of basilar membrane and auditory nerve fibers in the same cochleae. *Science* 282: 1882–1884, 1998.
234. **Navaratnam D, Bai JP, Samaranayake H, Santos-Sacchi J.** N-terminal-mediated homomultimerization of prestin, the outer hair cell motor protein. *Biophys J* 89: 3345–3352, 2005.
235. **Navarrete EG, Santos-Sacchi J.** On the affect of Prestin on the electrical breakdown of cell membranes. *Biophys J* 90: 967–974, 2005.
236. **Neely ST.** Mathematical modeling of cochlear mechanics. *J Acoust Soc Am* 78: 345–352, 1985.
237. **Neely ST, Kim DO.** An active cochlear model showing sharp tuning and high sensitivity. *Hear Res* 9: 123–130, 1983.
238. **Neely ST, Kim DO.** A model for active elements in cochlear biomechanics. *J Acoust Soc Am* 79: 1472–1480, 1986.
239. **Neher E, Marty A.** Discrete changes of cell membrane capacitance observed under conditions of enhanced secretion in bovine adrenal chromaffin cells. *Proc Natl Acad Sci USA* 79: 6712–6716, 1982.
240. **Nenov AP, Norris C, Bobbin RP.** Outwardly rectifying currents in guinea pig outer hair cells. *Hear Res* 105: 146–158, 1997.
241. **Nobili R, Mammano F.** Biophysics of the cochlea. II. Stationary nonlinear phenomenology. *J Acoust Soc Am* 99: 2244–2255, 1996.
242. **Nobili R, Mammano F, Ashmore J.** How well do we understand the cochlea? *Trends Neurosci* 21: 159–167, 1998.
243. **Nowotny M, Gummer AW.** Nanomechanics of the subtectorial space caused by electromechanics of cochlear outer hair cells. *Proc Natl Acad Sci USA* 103: 2120–2125, 2006.
244. **Nuttall AL, Dolan DF, Avinash G.** Laser Doppler velocimetry of basilar membrane vibration. *Hear Res* 51: 203–213, 1991.
245. **Oesterle E, Dallos P.** Intracellular recordings from supporting cells in the organ of Corti. *Hear Res* 22: 229–232, 1986.
246. **Oghalai JS.** Chlorpromazine inhibits cochlear function in guinea pigs. *Hear Res* 198: 59–68, 2004.
247. **Oghalai JS, Holt JR, Nakagawa T, Jung TM, Coker NJ, Jenkins HA, Eatock RA, Brownell WE.** Ionic currents and electromotility in inner ear hair cells from humans. *J Neurophysiol* 79: 2235–2239, 1998.
248. **Oghalai JS, Holt JR, Nakagawa T, Jung TM, Coker NJ, Jenkins HA, Eatock RA, Brownell WE.** Harvesting human hair cells. *Ann Otol Rhinol Laryngol* 109: 9–16, 2000.
249. **Okamura HO, Sugai N, Suzuki K, Ohtani I.** Enzyme-histochemical localization of carbonic anhydrase in the inner ear of the guinea pig and several improvements of the technique. *Histochem Cell Biol* 106: 425–430, 1996.
250. **Oliver D, Fakler B.** Expression density and functional characteristics of the outer hair cell motor protein are regulated during postnatal development in rat. *J Physiol* 519: 791–800, 1999.
251. **Oliver D, He DZ, Klocker N, Ludwig J, Schulte U, Waldegger S, Ruppersberg JP, Dallos P, Fakler B.** Intracellular anions as the voltage sensor of prestin, the outer hair cell motor protein. *Science* 292: 2340–2343, 2001.
252. **Oliver D, Ludwig J, Reisinger E, Zoellner W, Ruppersberg JP, Fakler B.** Memantine inhibits efferent cholinergic transmission in the cochlea by blocking nicotinic acetylcholine receptors of outer hair cells. *Mol Pharmacol* 60: 183–189, 2001.
253. **Oliver D, Schachinger T, Fakler B.** Interaction of prestin (SLC26A5) with monovalent intracellular anions. *Novartis Found Symp* 273: 244–253, 2006.
254. **Organ LE, Raphael RM.** Application of fluorescence recovery after photobleaching to study prestin lateral mobility in the human embryonic kidney cell. *J Biomed Opt* 12: 021003, 2007.
255. **Orman S, Flock A.** Active control of sensory hair mechanics implied by susceptibility to media that induce contraction in muscle. *Hear Res* 11: 261–266, 1983.
256. **Ospeck M, Dong XX, Iwasa KH.** Limiting frequency of the cochlear amplifier based on electromotility of outer hair cells. *Biophys J* 84: 739–749, 2003.
257. **Petersen LC, Bogert BP.** A dynamical theory of the cochlea. *J Acoust Soc Am* 22: 369–381, 1950.
258. **Pollice PA, Brownell WE.** Characterization of the outer hair cell's lateral wall membranes. *Hear Res* 70: 187–196, 1993.
259. **Rabbitt RD, Ayliffe HE, Christensen D, Pamarthy K, Durney C, Clifford S, Brownell WE.** Evidence of piezoelectric resonance in isolated outer hair cells. *Biophys J* 88: 2257–2265, 2005.
260. **Rajagopalan L, Patel N, Madabushi S, Goddard JA, Anjan V, Lin F, Shope C, Farrell B, Lichtarge O, Davidson AL, Brownell WE, Pereira FA.** Essential helix interactions in the anion transporter domain of prestin revealed by evolutionary trace analysis. *J Neurosci* 26: 12727–12734, 2006.
261. **Raphael RM, Popel AS, Brownell WE.** A membrane bending model of outer hair cell electromotility. *Biophys J* 78: 2844–2862, 2000.
262. **Ratnanather JT, Popel AS, Brownell WE.** An analysis of the hydraulic conductivity of the extracisternal space of the cochlear outer hair cell. *J Math Biol* 40: 372–382, 2000.
263. **Ratnanather JT, Spector AA, Popel AS, Brownell WE.** Is the outer hair cell wall viscoelastic. In: *Diversity in Auditory Mechanics*, edited by Lewis ER, Long GR, Lyon FR, Narins PM, Steele CR. Singapore: World Scientific, 1996, p. 601–607.

264. **Ratnanather JT, Zhi M, Brownell WE, Popel AS.** Measurements and a model of the outer hair cell hydraulic conductivity. *Hear Res* 96: 33–40, 1996.
265. **Ratnanather JT, Zhi M, Brownell WE, Popel AS.** The ratio of elastic moduli of cochlear outer hair cells derived from osmotic experiments. *J Acoust Soc Am* 99: 1025–1028, 1996.
266. **Rhode WS.** Observations of the vibration of the basilar membrane in squirrel monkeys using the Mossbauer technique. *J Acoust Soc Am* 49 *Suppl*: 1971.
267. **Rhode WS.** Measurement of vibration of the basilar membrane in the squirrel monkey. *Ann Otol Rhinol Laryngol* 83: 619–625, 1974.
268. **Rhode WS, Robles L.** Evidence from Mossbauer experiments for nonlinear vibration in the cochlea. *J Acoust Soc Am* 55: 588–596, 1974.
269. **Ricci AJ, Crawford AC, Fettiplace R.** Mechanisms of active hair bundle motion in auditory hair cells. *J Neurosci* 22: 44–52, 2002.
270. **Ricci AJ, Crawford AC, Fettiplace R.** Tonotopic variation in the conductance of the hair cell mechanotransducer channel. *Neuron* 40: 983–990, 2003.
271. **Ricci AJ, Gray-Keller M, Fettiplace R.** Tonotopic variations of calcium signalling in turtle auditory hair cells. *J Physiol* 524: 423–436, 2000.
272. **Ricci AJ, Kennedy HJ, Crawford AC, Fettiplace R.** The transduction channel filter in auditory hair cells. *J Neurosci* 25: 7831–7839, 2005.
273. **Richter CP, Edge R, He DZ, Dallos P.** Development of the gerbil inner ear observed in the hemicochlea. *J Assoc Res Otolaryngol* 1: 195–210, 2000.
274. **Richter CP, Evans BN, Edge R, Dallos P.** Basilar membrane vibration in the gerbil hemicochlea. *J Neurophysiol* 79: 2255–2264, 1998.
275. **Robertson D, Sellick PM, Patuzzi R.** The continuing search for outer hair cell afferents in the guinea pig spiral ganglion. *Hear Res* 136: 151–158, 1999.
276. **Robles L, Ruggero MA.** Mechanics of the mammalian cochlea. *Physiol Rev* 81: 1305–1352, 2001.
277. **Robles L, Ruggero MA, Rich NC.** Basilar membrane mechanics at the base of the chinchilla cochlea. I. Input-output functions, tuning curves, response phases. *J Acoust Soc Am* 80: 1364–1374, 1986.
278. **Robles L, Ruggero MA, Rich NC.** Two-tone distortion in the basilar membrane of the cochlea. *Nature* 349: 413–414, 1991.
279. **Rusch A, Thurm U.** Cupula displacement, hair bundle deflection, physiological responses in the transparent semicircular canal of young eel. *Pflügers Arch* 413: 533–545, 1989.
280. **Rusch A, Thurm U.** Spontaneous and electrically induced movements of ampullary kinocilia and stereovilli. *Hear Res* 48: 247–263, 1990.
281. **Russell IJ, Legan PK, Lukashkina VA, Lukashkin AN, Goodyear RJ, Richardson GP.** Sharpened cochlear tuning in a mouse with a genetically modified tectorial membrane. *Nat Neurosci* 10: 215–223, 2007.
282. **Ryan A, Dallos P.** Effect of absence of cochlear outer hair cells on behavioural auditory threshold. *Nature* 253: 44–46, 1975.
283. **Rybalchenko V, Santos-Sacchi J.** Cl^- flux through a non-selective, stretch-sensitive conductance influences the outer hair cell motor of the guinea-pig. *J Physiol* 547: 873–891, 2003.
284. **Sagar A, Rakowski RF.** Access channel model for the voltage dependence of the forward-running Na^+/K^+ pump. *J Gen Physiol* 103: 869–893, 1994.
285. **Saito K.** Fine structure of the sensory epithelium of guinea-pig organ of Corti: subsurface cisternae and lamellar bodies in the outer hair cells. *Cell Tissue Res* 229: 467–481, 1983.
286. **Santos-Sacchi J.** Cell coupling in Corti's organ. *Brain Res Rev* 32: 167–171, 2000.
287. **Santos-Sacchi J.** Functional motor microdomains of the outer hair cell lateral membrane. *Pflügers Arch* 445: 331–336, 2002.
288. **Santos-Sacchi J.** Determination of cell capacitance using the exact empirical solution of partial differential Y/partial differential Cm and its phase angle. *Biophys J* 87: 714–727, 2004.
289. **Santos-Sacchi J.** Asymmetry in voltage-dependent movements of isolated outer hair cells from the organ of Corti. *J Neurosci* 9: 2954–2962, 1989.
290. **Santos-Sacchi J.** Reversible inhibition of voltage-dependent outer hair cell motility and capacitance. *J Neurosci* 11: 3096–3110, 1991.
291. **Santos-Sacchi J.** On the frequency limit and phase of outer hair cell motility: effects of the membrane filter. *J Neurosci* 12: 1906–1916, 1992.
292. **Santos-Sacchi J.** Harmonics of outer hair cell motility. *Biophys J* 65: 2217–2227, 1993.
293. **Santos-Sacchi J, Dilger JP.** Whole cell currents and mechanical responses of isolated outer hair cells. *Hear Res* 35: 143–150, 1988.
294. **Santos-Sacchi J, Huang G.** Temperature dependence of outer hair cell nonlinear capacitance. *Hear Res* 116: 99–106, 1998.
295. **Santos-Sacchi J, Kakehata S, Kikuchi T, Katori Y, Takasaka T.** Density of motility-related charge in the outer hair cell of the guinea pig is inversely related to best frequency. *Neurosci Lett* 256: 155–158, 1998.
296. **Santos-Sacchi J, Kakehata S, Takahashi S.** Effects of membrane potential on the voltage dependence of motility-related charge in outer hair cells of the guinea-pig. *J Physiol* 510: 225–235, 1998.
297. **Santos-Sacchi J, Navarrete E.** Voltage-dependent changes in specific membrane capacitance caused by prestin, the outer hair cell lateral membrane motor. *Pflügers Arch* 444: 99–106, 2002.
298. **Santos-Sacchi J, Rybalchenko V, Bai JP, Song L, Navaratnam D.** On the temperature and tension dependence of the outer hair cell lateral membrane conductance G (metL) and its relation to prestin. *Pflügers Arch* 452: 283–289, 2006.
299. **Santos-Sacchi J, Shen W, Zheng J, Dallos P.** Effects of membrane potential and tension on prestin, the outer hair cell lateral membrane motor protein. *J Physiol* 531: 661–666, 2001.
300. **Santos-Sacchi J, Song L, Zheng J, Nuttall AL.** Control of mammalian cochlear amplification by chloride anions. *J Neurosci* 26: 3992–3998, 2006.
301. **Santos-Sacchi J, Wu M.** Protein- and lipid-reactive agents alter outer hair cell lateral membrane motor charge movement. *J Membr Biol* 200: 83–92, 2004.
302. **Santos-Sacchi J, Wu M, Kakehata S.** Furosemide alters nonlinear capacitance in isolated outer hair cells. *Hear Res* 159: 69–73, 2001.
303. **Schaechinger TJ, Oliver D.** Nonmammalian orthologs of prestin (SLC26A5) are electrogenic divalent/chloride anion exchangers. *Proc Natl Acad Sci USA* 104: 7693–7698, 2007.
304. **Scherer MP, Gummer AW.** Vibration pattern of the organ of Corti up to 50 kHz: evidence for resonant electromechanical force. *Proc Natl Acad Sci USA* 101: 17652–17657, 2004.
305. **Scherer MP, Gummer AW.** How many states can the motor molecule, prestin, assume in an electric field? *Biophys J* 88: L27–L29, 2005.
306. **Schulte BA.** Immunohistochemical localization of intracellular Ca-ATPase in outer hair cells, neurons and fibrocytes in the adult and developing inner ear. *Hear Res* 65: 262–273, 1993.
307. **Sellick PM, Patuzzi R, Johnstone BM.** Measurement of basilar membrane motion in the guinea pig using the Mossbauer technique. *J Acoust Soc Am* 72: 131–141, 1982.
308. **Sheetz MP, Singer SJ.** Equilibrium and kinetic effects of drugs on the shapes of human erythrocytes. *J Cell Biol* 70: 247–251, 1976.
309. **Shehata WE, Brownell WE, Dieler R.** Effects of salicylate on shape, electromotility and membrane characteristics of isolated outer hair cells from guinea pig cochlea. *Acta Otolaryngol* 111: 707–718, 1991.
310. **Sigg D, Bezanilla F, Stefani E.** Fast gating in the *Shaker* K^+ channel and the energy landscape of activation. *Proc Natl Acad Sci USA* 100: 7611–7615, 2003.
311. **Simmons DD.** Development of the inner ear efferent system across vertebrate species. *J Neurobiol* 53: 228–250, 2002.
312. **Slepecky N, Ulfendahl M.** Glutaraldehyde induces cell shape changes in isolated outer hair cells from the inner ear. *J Submicrosc Cytol Pathol* 20: 37–45, 1988.
313. **Slepecky N, Ulfendahl M, Flock A.** Effects of caffeine and tetracaine on outer hair cell shortening suggest intracellular calcium involvement. *Hear Res* 32: 11–21, 1988.
314. **Slepecky NB.** Structure of the mammailian cochlea. In: *The Cochlea*, edited by Dallos P, Fay RR, Popper AN. New York: Springer, 1996, p. 44–129.

315. **Smith CA, Sjostrand FS.** Structure of the nerve endings on the external hair cells of the guinea pig cochlea as studied by serial sections. *J Ultrastruct Res* 5: 523–556, 1961.
316. **Song L, Seeger A, Santos-Sacchi J.** On membrane motor activity and chloride flux in the outer hair cell: lessons learned from the environmental toxin tributyltin. *Biophys J* 88: 2350–2362, 2005.
317. **Souter M, Nevill G, Forge A.** Postnatal development of membrane specialisations of gerbil outer hair cells. *Hear Res* 91: 43–62, 1995.
318. **Souter M, Nevill G, Forge A.** Postnatal maturation of the organ of Corti in gerbils: morphology and physiological responses. *J Comp Neurol* 386: 635–651, 1997.
319. **Spector AA, Brownell WE, Popel AS.** Elastic properties of the composite outer hair cell wall. *Ann Biomed Eng* 26: 157–165, 1998.
320. **Spector AA, Brownell WE, Popel AS.** Effect of outer hair cell piezoelectricity on high-frequency receptor potentials. *J Acoust Soc Am* 113: 453–461, 2003.
321. **Spector AA, Brownell WE, Popel AS.** Elastic properties of the composite outer hair cell wall. *Ann Biomed Eng* 26: 157–165, 1998.
322. **Spector AA, Brownell WE, Popel AS.** Estimation of elastic moduli and bending stiffness of the anisotropic outer hair cell wall. *J Acoust Soc Am* 103: 1007–1011, 1998.
323. **Spector AA, Jean RP.** Modes and balance of energy in the piezoelectric cochlear outer hair cell wall. *J Biomech Eng* 126: 17–25, 2004.
324. **Sturm AK, Rajagopalan L, Yoo D, Brownell WE, Pereira FA.** Functional expression and microdomain localization of prestin in cultured cells. *Otolaryngol Head Neck Surg* 136: 434–439, 2007.
325. **Sziklai I, Dallos P.** Acetylcholine controls the gain of the voltage-to-movement converter in isolated outer hair cells. *Acta Otolaryngol* 113: 326–329, 1993.
326. **Sziklai I, He DZ, Dallos P.** Effect of acetylcholine and GABA on the transfer function of electromotility in isolated outer hair cells. *Hear Res* 95: 87–99, 1996.
327. **Sziklai I, Szonyi M, Dallos P.** Phosphorylation mediates the influence of acetylcholine upon outer hair cell electromotility. *Acta Otolaryngol* 121: 153–156, 2001.
328. **Szonyi M, He DZ, Ribari O, Sziklai I, Dallos P.** Intracellular calcium and outer hair cell electromotility. *Brain Res* 922: 65–70, 2001.
329. **Terakawa S.** Potential-dependent variations of the intracellular pressure in the intracellularly perfused squid giant axon. *J Physiol* 369: 229–248, 1985.
330. **Tolomeo JA, Steele CR.** Orthotropic piezoelectric properties of the cochlear outer hair cell wall. *J Acoust Soc Am* 97: 3006–3011, 1995.
331. **Tolomeo JA, Steele CR.** A dynamic model of outer hair cell motility including intracellular and extracellular fluid viscosity. *J Acoust Soc Am* 103: 524–534, 1998.
332. **Tunstall MJ, Gale JE, Ashmore JF.** Action of salicylate on membrane capacitance of outer hair cells from the guinea-pig cochlea. *J Physiol* 485: 739–752, 1995.
333. **Van den AT, Tran Ba HP, Teulon J.** A calcium-activated nonselective cationic channel in the basolateral membrane of outer hair cells of the guinea-pig cochlea. *Pflügers Arch* 427: 56–63, 1994.
335. **Weber T, Gopfert MC, Winter H, Zimmermann U, Kohler H, Meier A, Hendrich O, Rohbock K, Robert D, Knipper M.** Expression of prestin-homologous solute carrier (SLC26) in auditory organs of nonmammalian vertebrates and insects. *Proc Natl Acad Sci USA* 100: 7690–7695, 2003.
336. **Weber T, Zimmermann U, Winter H, Mack A, Kopschall I, Rohbock K, Zenner HP, Knipper M.** Thyroid hormone is a critical determinant for the regulation of the cochlear motor protein prestin. *Proc Natl Acad Sci USA* 99: 2901–2906, 2002.
337. **Wersall J, Flock A, Lundquist PG.** Structural basis for directional sensitivity in cochlear and vestibular sensory receptors. *Cold Spring Harb Symp Quant Biol* 30: 115–132, 1965.
338. **Wier CC, Pasanen EG, McFadden D.** Partial dissociation of spontaneous otoacoustic emissions and distortion products during aspirin use in humans. *J Acoust Soc Am* 84: 230–237, 1988.
339. **Wilson JP.** Cochlear mechanics In: *Advances in the Biosciences: Auditory Physiology and Perception*, edited by Cazals Y, Demeny L, Horner K. Oxford, UK: Pergamon, 1992, vol. 38, p. 71–84.
340. **Winter H, Braig C, Zimmermann U, Geisler HS, Franzer JT, Weber T, Ley M, Engel J, Knirsch M, Bauer K, Christ S, Walsh EJ, McGee J, Kopschall I, Rohbock K, Knipper M.** Thyroid hormone receptors TRalpha1 and TRbeta differentially regulate gene expression of Kcnq4 and prestin during final differentiation of outer hair cells. *J Cell Sci* 119: 2975–2984, 2006.
341. **Wu X, Currall B, Yamashita T, Parker LL, Hallworth R, Zuo J.** Prestin-prestin and prestin-GLUT5 interactions in HEK293T cells. *Dev Neurobiol* 67: 483–497, 2007.
342. **Yau KW, Lamb TD, Baylor DA.** Light-induced fluctuations in membrane current of single toad rod outer segments. *Nature* 269: 78–80, 1977.
343. **Yu N, Zhu ML, Zhao HB.** Prestin is expressed on the whole outer hair cell basolateral surface. *Brain Res* 1095: 51–58, 2006.
344. **Zajic G, Schacht J.** Shape changes in isolated outer hair cells: measurements with attached microspheres. *Hear Res* 52: 407–410, 1991.
345. **Zenner HP.** K^+-induced motility and depolarization of cochlear hair cells. Direct evidence for a new pathophysiological mechanism in Meniere's disease. *Arch Otorhinolaryngol* 243: 108–111, 1986.
346. **Zenner HP.** Motile responses in outer hair cells. *Hear Res* 22: 83–90, 1986.
347. **Zenner HP, Zimmermann R, Gitter AH.** Active movements of the cuticular plate induce sensory hair motion in mammalian outer hair cells. *Hear Res* 34: 233–239, 1988.
348. **Zenner HP, Zimmermann U, Gitter AH.** Fast motility of isolated mammalian auditory sensory cells. *Biochem Biophys Res Commun* 149: 304–308, 1987.
349. **Zhang PC, Keleshian AM, Sachs F.** Voltage-induced membrane movement. *Nature* 413: 428–432, 2001.
350. **Zhang R, Qian F, Rajagopalan L, Pereira FA, Brownell WE, Anvari B.** Prestin modulates mechanics and electromechanical force of the plasma membrane. *Biophys J* 2007.
351. **Zhao HB, Santos-Sacchi J.** Auditory collusion and a coupled couple of outer hair cells. *Nature* 399: 359–362, 1999.
352. **Zheng J, Du GG, Anderson CT, Keller JP, Orem A, Dallos P, Cheatham M.** Analysis of the oligomeric structure of the motor protein prestin. *J Biol Chem* 281: 19916–19924, 2006.
353. **Zheng J, Du GG, Matsuda K, Orem A, Aguinaga S, Deak L, Navarrete E, Madison LD, Dallos P.** The C-terminus of prestin influences nonlinear capacitance and plasma membrane targeting. *J Cell Sci* 118: 2987–2996, 2005.
354. **Zheng J, Long KB, Shen W, Madison LD, Dallos P.** Prestin topology: localization of protein epitopes in relation to the plasma membrane. *Neuroreport* 12: 1929–1935, 2001.
355. **Zheng J, Shen W, He DZ, Long KB, Madison LD, Dallos P.** Prestin is the motor protein of cochlear outer hair cells. *Nature* 405: 149–155, 2000.
356. **Zwislocki JJ.** Theory of the acoustical action of the cochlea. *J Acoust Soc Am* 22: 778, 1950.
357. **Zwislocki JJ.** Five decades of research on cochlear mechanics. *J Acoust Soc Am* 67: 1679–1685, 1980.

Cochlear Outer Hair Cell Motility

Jonathan Ashmore

Physiol Rev 88:173-210, 2008. doi:10.1152/physrev.00044.2006